

ADA 056373

AFML-TR-77-193

DEVELOPMENT OF A CRACK GROWTH RATE TEST FOR QUALITY CONTROL

*DEL WEST ASSOCIATES, INC.
6324 VARIEL AVENUE
WOODLAND HILLS, CALIFORNIA 91367*

NOVEMBER 1977

TECHNICAL REPORT AFML-TR-77-193
Final Report — April 1975 - June 1977

Approved for public release; distribution unlimited.


AIR FORCE MATERIALS LABORATORY
AIR FORCE WRIGHT AERONAUTICAL LABORATORIES
AIR FORCE SYSTEMS COMMAND
WRIGHT-PATTERSON AIR FORCE BASE, OHIO 45433

20080819 218

NOTICE

When Government drawings, specifications, or other data are used for any purpose other than in connection with a definitely related Government procurement operation, the United States Government thereby incurs no responsibility nor any obligation whatsoever, and the fact that the government may have formulated, furnished, or in any way supplied the said drawings, specifications, or other data, is not to be regarded by implication or otherwise as in any manner licensing the holder or any other person or corporation, or conveying any rights or permission to manufacture, use, or sell any patented invention that may in any way be related thereto.

This technical report has been reviewed and is approved for publication.



ALLAN W. GUNDERSON
Engineering & Design Data
Materials Integrity Branch



CLAYTON L. HARMSWORTH
Technical Manager
Engineering & Design Data
Materials Integrity Branch

FOR THE COMMANDER



THOMAS D. COOPER
Chief, Materials Integrity Branch
Systems Support Division

"If your address has changed, if you wish to be removed from our mailing list, or if the addressee is no longer employed by your organization please notify AFML/MXA, W-P AFB, OH 45433 to help us maintain a current mailing list".

Copies of this report should not be returned unless return is required by security considerations, contractual obligations, or notice on a specific document.

REPORT DOCUMENTATION PAGE		READ INSTRUCTIONS BEFORE COMPLETING FORM
1. REPORT NUMBER AFML-TR-77-193	2. GOVT ACCESSION NO.	3. RECIPIENT'S CATALOG NUMBER
4. TITLE (and Subtitle) DEVELOPMENT OF A CRACK GROWTH RATE TEST FOR QUALITY CONTROL		5. TYPE OF REPORT & PERIOD COVERED FINAL TECHNICAL REPORT April, 1975-June, 1977
		6. PERFORMING ORG. REPORT NUMBER DW9-30
7. AUTHOR(s) M. Creager and A. W. Sommer		8. CONTRACT OR GRANT NUMBER(s) F33615-75-C-5106
9. PERFORMING ORGANIZATION NAME AND ADDRESS Del West Associates, Inc. 6324 Variel Avenue Woodland Hills, Ca 91367		10. PROGRAM ELEMENT, PROJECT, TASK AREA & WORK UNIT NUMBERS
11. CONTROLLING OFFICE NAME AND ADDRESS Air Force Materials Laboratory (AFML/ MXA) Air Force Wright Aeronautical Laboratories Wright-Patterson Air Force Base, Ohio 45433		12. REPORT DATE November, 1977
		13. NUMBER OF PAGES
14. MONITORING AGENCY NAME & ADDRESS (if different from Controlling Office)		15. SECURITY CLASS. (of this report) Unclassified
		15a. DECLASSIFICATION/DOWNGRADING SCHEDULE NA
16. DISTRIBUTION STATEMENT (of this Report)		
17. DISTRIBUTION STATEMENT (of the abstract entered in Block 20, if different from Report)		
18. SUPPLEMENTARY NOTES		
19. KEY WORDS (Continue on reverse side if necessary and identify by block number) Fatigue Crack Growth Rates; Quality Control Tests; Constant ΔK Testing; Aluminum, Titanium, Steel, K_{Isc} ; da/dt ; Crack Growth Retardation		
20. ABSTRACT (Continue on reverse side if necessary and identify by block number) A test method has been developed which reliably and inexpensively provides the fatigue crack growth rate of a material sample at any given stress intensity level. The method employs a notched three point bend bar, typically 4 1/4" x 1/2" x 1/4", in a con- trolled displacement amplitude test mode. The specimen/test system is configured such that a constant stress intensity ampli- tude exists over the central region of the test specimen.		

UNCLASSIFIED

SECURITY CLASSIFICATION OF THIS PAGE(When Data Entered)

Due to the unique attributes of a displacement controlled constant K test specimen, no visual or COD measurements of crack length are required for the crack growth rate measurement. An autographic record of load amplitude versus cycles exhibits a straight line portion, the slope of which provides a measurement of the central region crack growth rate. The test is simple enough so that a well trained quality control laboratory technician can perform it employing about one hour of his time to set it up, run the test and analyze the result.

Capability of our newly developed test method to perform as required has been demonstrated by comparing the results of 137 tests using the newly developed method with crack growth rate data generated employing compact tension geometry samples. This comparison was conducted on 15 heat/lots of aerospace metals, ranging from 7000 series aluminum to 6Al-4V Ti to Ph 13-8Mo steel. These results showed that both techniques produced identical results in both lab air and salt water.

In addition to its service as a quality control test, the newly developed test method also has been demonstrated to have a potential use for stress corrosion cracking measurements and overload crack growth retardation determinations as well as several other important crack growth material properties.

SECURITY CLASSIFICATION OF THIS PAGE(When Data Entered)

AD A056373

PREFACE

This report was prepared by Del West Associates, Inc., Woodland Hills, Ca under USAF Contract No. F33651-75-C-5106. The contract work was administered under the Air Force Material Laboratory, Air Force Systems Command, Wright-Patterson AFB, Ohio with Mr. Allan Gunderson as Project Engineer.

Dr. M. Creager served as Program Manager for Del West Associates, Inc., and directed all activities. Dr. A. W. Sommer of Del West served as Principal Investigator. The reporting periods extend from April, 1975 to June, 1977.

The authors wish to acknowledge the efforts of their co-worker, Mr. W. Renslen, both for his initial suggestion of the viability of a spring modified constant displacement fatigue crack growth test as well as his extremely helpful efforts involved in bringing this method to experimental fruition. Additionally, we wish to thank Mr. W. Kerwin for assisting in formulating the electronics required to make the required load measurements and for running many of the tests in the Program. Mrs. Mary Rhodes is also due thanks for her patience with the authors and for the typing of this final report.

TABLE OF CONTENTS

SECTION	PAGE
I INTRODUCTION	1
II THE G-RATE TEST	5
A. Basic Description	5
B. Test Procedure Summary	23
C. Test Equipment Used	27
III CORRELATION OF FATIGUE CRACK GROWTH RATES AS DETERMINED BY CONSTANT LOAD AMPLITUDE AND G-RATE TESTS	30
IV OTHER APPLICATIONS OF THE G-RATE TEST ...	60
V SUMMARY	79
APPENDICES	
APPENDIX A: ANALYSIS OF A REMOTE DIPLACEMENT CONTROLLED CONSTANT K SPECIMEN	80
APPENDIX B: PROGRAM MATERIAL SELECTION PHILOSOPHY	95
APPENDIX C: CONSIDERATION OF CANDIDATE QUALITY CONTROL TEST SPECIMENS/PROCEDURES	105

LIST OF TABLES

TABLE		PAGE
I	VARIATION IN STRESS INTENSITY FACTOR.....	9
II	ALUMINUM ALLOY TEST PROGRAM.....	31
III	TI ALLOY TEST PROGRAM	32
IV	STEEL ALLOY TEST PROGRAM	32
V	7075/7475 CONSTANT ΔK DATA	40
VI	7075-T651 PLATE A CONSTANT ΔK DATA ENVIRONMENT - 3.5% NaCl IN H ₂ O.....	42
VII	6Al-4V TI CONSTANT ΔK DATA	54
VIII	PH 13-8MO STEEL CONSTANT ΔK DATA	56
IX	MATERIAL DESCRIPTION OF A/F 1410	63
A-I	ANALYSIS OF REMOTE DISPLACEMENT CONTROLLED THREE POINT BEND SPECIMEN, S/W = 8	83
A-II	ANALYSIS OF REMOTE DISPLACEMENT CONTROLLED THREE POINT BEND SPECIMEN, S/W = 4	87
A-III	CONSTANTS FOR EVALUATING CRACK GROWTH RATE	93
A-IV	CONSTANTS USED IN TEST PROGRAM	94
B-I	ALUMINUM ALLOY LOT DESCRIPTION	97
B-II	ALLOY CHEMISTRY OF 7475	98
B-III	CHEMICAL ANALYSIS AND HEAT TREATMENT PROCESSING OF TITANIUM HEATS	100
B-IV	TENSILE PROPERTIES OF TI ALLOY HEATS	101
B-V	CHEMICAL ANALYSIS AND PROCESSING OF PH 13-8MO STEEL FORGINGS	103
B-VI	MECHANICAL PROPERTIES OF PH 13-8MO STEEL FORGINGS	104

LIST OF ILLUSTRATIONS

FIGURE		PAGE
1	G-RATE TEST FIGURE CONFIGURATION	6
2	STRESS INTENSITY FACTORS FOR THREE POINT BEND SPECIMEN	6
3	FATIGUE CRACK GROWTH DATA RECORD	15
4	TYPICAL FATIGUE CRACK GROWTH RATE TEST RECORD (60% REDUCTION)	17
5	COMPACT VS CONSTANT ΔK DATA FOR 7075-T6 IN SALT WATER	18
6	LOAD VERSUS CYCLES - ONE PRECRACKING STAGE..	21
7	LOAD VERSUS CYCLES - TWO PRECRACKING STAGES.	21
8	STRESS INTENSITY EVALUATION CONSTANT	26
9	CRACK GROWTH RATE CONSTANT	26
10	OFFSET CAM DISPLACEMENT CONTROL SYSTEM	28
11	LAB AIR FATIGUE CRACK GROWTH ALUMINUM HEAT/LOT A	34
12	LAB AIR FATIGUE CRACK GROWTH ALUMINUM HEAT/LOT B	35
13	LAB AIR FATIGUE CRACK GROWTH ALUMINUM HEAT/LOT C	36
14	LAB AIR FATIGUE CRACK GROWTH ALUMINUM HEAT/LOT D	37
15	LAB AIR FATIGUE CRACK GROWTH ALUMINUM HEAT/LOT E	38
16	COMPACT VS CONSTANT ΔK DATA FOR 7075-T6 IN SALT WATER	39
17	LAB AIR FATIGUE CRACK GROWTH TITANIUM HEAT/LOT F	44

LIST OF ILLUSTRATIONS

FIGURE		PAGE
18	LAB AIR FATIGUE CRACK GROWTH TITANIUM HEAT/LOT G	45
19	LAB AIR FATIGUE CRACK GROWTH TITANIUM HEAT/LOT H	46
20	LAB AIR FATIGUE CRACK GROWTH TITANIUM HEAT/LOT J	47
21	LAB AIR FATIGUE CRACK GROWTH TITANIUM HEAT/LOT K	48
22	LAB AIR FATIGUE CRACK GROWTH STEEL HEAT/LOT L.....	49
23	LAB AIR FATIGUE CRACK GROWTH STEEL HEAT/LOT M	50
24	LAB AIR FATIGUE CRACK GROWTH STEEL HEAT/LOT N	51
25	LAB AIR FATIGUE CRACK GROWTH STEEL HEAT/LOT O	52
26	LAB AIR FATIGUE CRACK GROWTH STEEL HEAT/LOT P	53
27	EQUIVALENCES OF LOAD VERSUS TIME AND CRACK LENGTH VERSUS TIME	65
28	STRESS CORROSION CRACKING - A/F 1410 IN NACL SOLUTION	66
29	CRACK GROWTH RATE OF A/F 1410 in 3.5% NACL VERSUS DISTANCE GROWN	67
30	CRACK GROWTH RATE OF A/F 1410 IN 3.5% NACL VERSUS TIME	68
31	STRESS CORROSION OF A/F 1410 WITH STEP LOADING	71
32	FATIGUE CRACK GROWTH RETARDATION LOAD RECORD...	73

LIST OF ILLUSTRATIONS

FIGURE		PAGE
33	EQUIVALENT CRACK LENGTH - CYCLE INTERPRE- TATION OF RETARDATION DATA	74
34	LOW FREQUENCY CRACK GROWTH RATE TEST	75
A-1	STRESS INTENSITY EVALUATION CONSTANT (S/W = 8)	90

SECTION I

INTRODUCTION

The objective of this Program was to develop a low cost fatigue crack growth rate correlation test which can easily discriminate between material lots whose fatigue crack propagation rates differ by more than 20%. A test has been developed which more than meets the latter requirement. Furthermore, employing our newly developed test method in a production support mode, one can easily obtain the desired fatigue crack propagation rate data at a total cost of less than the equivalent of two man hours. The test developed is simple enough so that a quality control laboratory technician can perform it using approximately one hour of his time to set it up, run the test and analyze the result. Moreover, the specimen fabrication costs are low, material usage is small and a relatively inexpensive test machine is used.

The test result is the crack growth rate associated with a specific stress intensity factor. The crack growth rate and the stress intensity factor are measured independently and a permanent test record is produced from which the crack growth rate can be documented at any time. At no time during the test is a crack length measurement made. Typically only two measurements

are ever made; one is a load measurement and the other is the slope of a straight line.

Although the primary emphasis in this Program was the development of a quality control test method to assess fatigue crack propagation rates, a number of additional potential uses of the test developed have been identified. Some of these may prove to be equally (or more) significant uses of the test. Additional uses that have been identified include:

- generation of low frequency/low crack growth rate engineering data;
- the investigation of the effects of variables other than ΔK (e.g., stress ratio, alloy chemistry, environment, test frequency, temperature, etc.);
- investigations of fatigue crack growth retardation;
- investigations of static stress corrosion;
- the development of fatigue crack growth rate statistical information.

The Program contained two distinct phases of work. In Phase I test configuration/procedures were conceived, analyzed and evaluated. In Phase II the test configuration and test procedure which emerged as being clearly superior to all the others considered was tested and evaluated in depth. Additionally, other

applications for our newly developed test method were considered and in some cases explored experimentally.

The total sum of results obtained during this Program are partitioned by subject matter into subsections. In Chapter II we describe our recommended quality control fatigue crack growth rate test method in detail. Included in this Chapter is a basic description of the test, a step by step summary of the test procedure and a description of the equipment and instrumentation used. Details of the analytical basis for the simple data reduction relations used are given in Appendix A.

Chapter III reports the results of fatigue crack propagation tests which were conducted on five heat/lots each of 6Al-4V Ti plate, 7075/7475 aluminum alloy plate and Ph 13-8Mo steel forgings. Two compact specimens were used to generate the fatigue crack growth rate data for each heat/lot. Three heat/lots from each alloy system were then chosen to be used to evaluate the quality control test procedure. The salt water corrosion fatigue crack growth rate was established for one heat/lot of 7075 to be used as an additional means of evaluation. Twelve quality control tests for each of the ten material/environment conditions selected were conducted and the results compared to the baseline compact specimen fatigue crack growth rate results. The resulting correlation has demonstrated the accuracy and

reliability of the G-Rate Test. Appendix B presents a detailed metallurgical description of each of the 15 heats of metal employed in this verification test Program.

Chapter IV sketches other applications of the basic G-Rate Test. Experimental evidence that the basic test method approach can provide other types of fracture mechanics engineering data is also presented.

In order to arrive at the G-Rate Test method outlined in Chapter II, it was necessary to define a set of criteria for the success of such a test and then evaluate myriad test sample geometries/test procedures within the framework of that criteria. A description of the effort expended in performing this task is presented in Appendix C.

SECTION II

THE G-RATE TEST

A) Basic Description

The quality control fatigue crack propagation test developed is a displacement controlled constant stress intensity (K) test. This constant K test accounts for and in fact takes advantage of the test system compliance (or springiness). A sketch of the test set up which shows the three point bend specimen used is shown in Figure 1. The spring in that Figure represents the overall test system's compliance. Note that the displacement is not controlled at the specimen but at a remote point in the test system. This is done primarily since it is far easier to control a displacement away from the test specimen. For example, the use of an offset cam to achieve this is a very inexpensive and convenient technique. One of our motivations for using a displacement controlled test was the fact that this type of test machine is inexpensive. In our initial work on test development another important reason for controlling the displacement remotely was that it allowed us to maintain a constant stress intensity as the crack grew for a variety of three point bend specimen geometries. That is K could be made independent of crack length (a). As will be shown in subsequent analysis the S/W = 8 three point bend specimen finally adopted has a constant K region, even under direct displacement control. The way in which the compliance of the test machine can

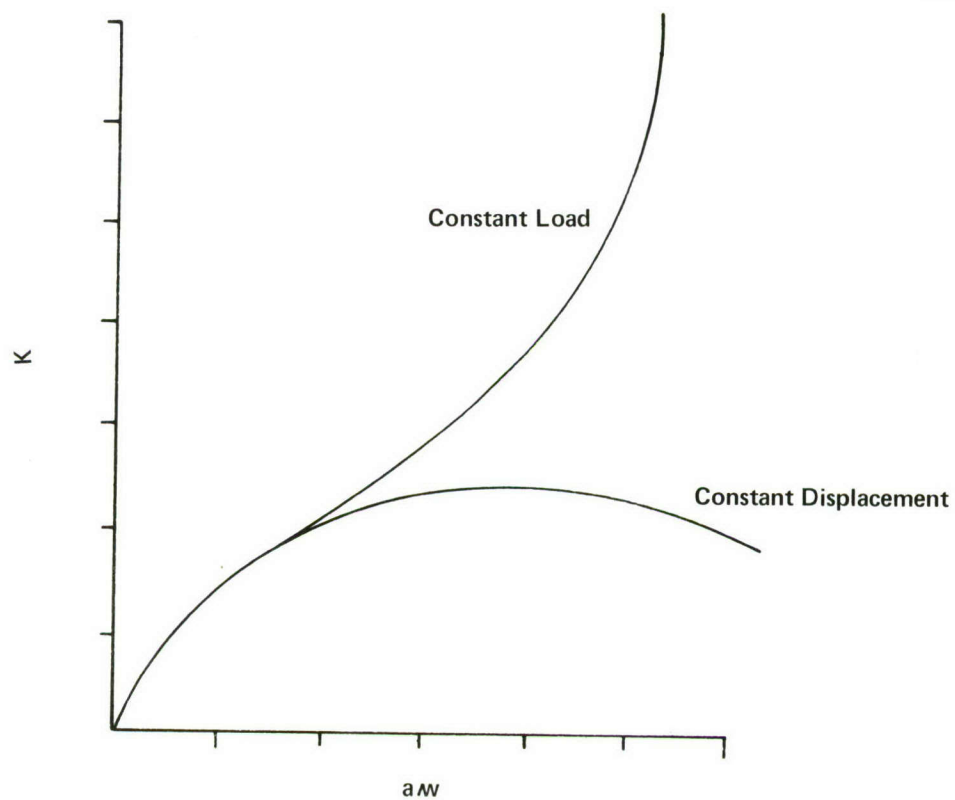
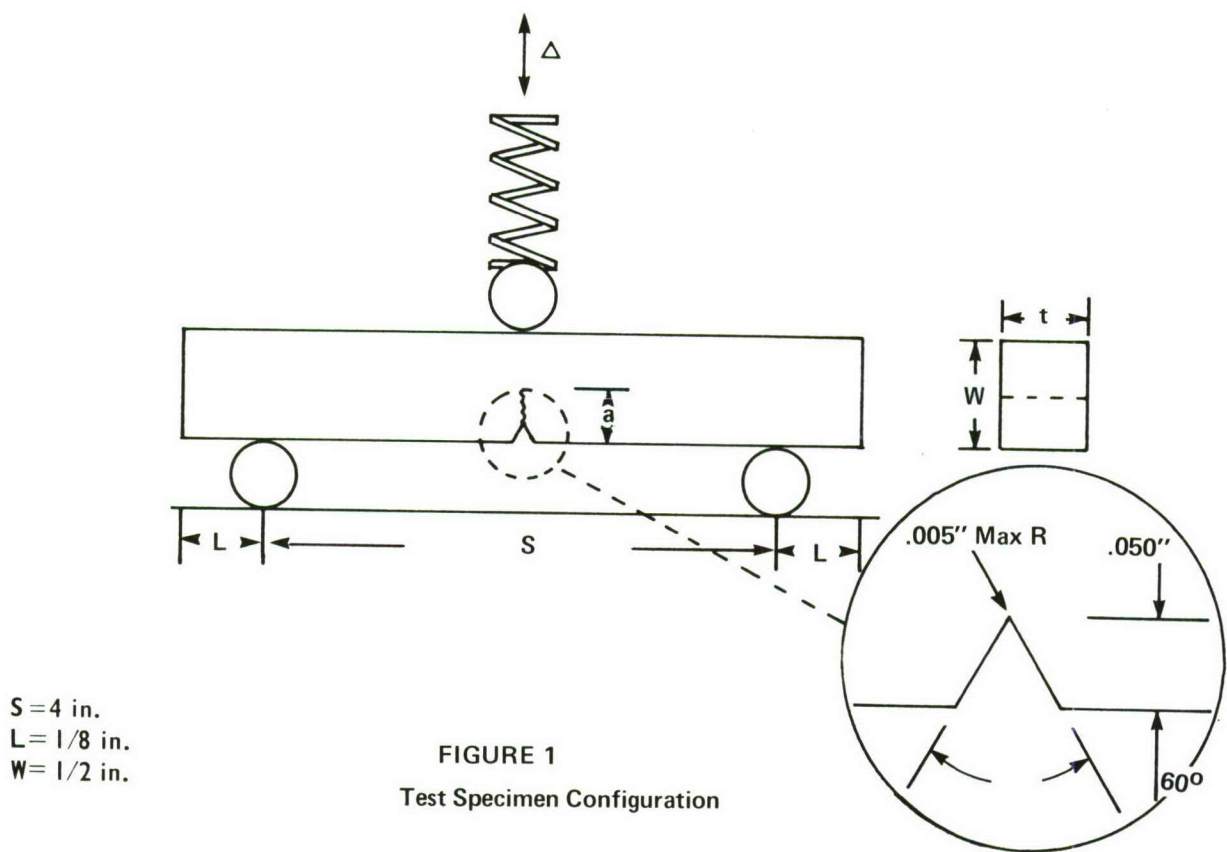


FIGURE 2
Stress intensity Factors For Three Point Bend Specimen

aid us in obtaining a constant K region is easily seen by considering Figure 2. In that Figure the stress intensity versus crack length for a three point bend specimen is presented for two loading conditions. One is constant load and the other constant displacement at the specimen (Reference 1). Note that under load control as the crack grows, the resistance to bending diminishes and the stress intensity rises. Under pure displacement control, at short crack lengths, changes in crack length do not affect the specimen compliance and therefore the load remains essentially constant and the K versus " a " curve initially follows the constant load specimen curve. Eventually changes in crack length affect the specimen compliance significantly and the load begins to drop. As the crack continues to grow a point is reached where the load drop off is sufficiently fast to cause the stress intensity to decrease with increasing crack length.

If one could control the rate of load drop off one could maintain a constant K within a significant domain of the test specimen. By inserting an appropriately sized spring in between a displacement control device and the test specimen the rate of load drop off can be controlled. Note that the extreme cases of a rigid spring and an infinitely flexible spring correspond to pure displacement control and pure load control respectively. Thus by choosing various spring stiffnesses one can generate a series of K versus " a " specimen configurations between those presented in Figure 2.

Detailed analyses for a wide range of spring stiffnesses are presented in Appendix A for both the $S/W = 8$, $W = 1/2$ inch, three point bend specimen selected as the G-Rate Test specimen and for an $S/W = 4$ specimen that was at one time considered. From these analyses we were able to ascertain the ranges of spring compliances that would optimize the constancy in K . Pertinent ranges for the $S/W = 8$ configuration are presented in Table I. In the Table the spring compliances have all been normalized by the product of the specimen's Young's modulus and thickness. One notes in Table I that the crack depth " a " associated with the highest K point in the "constant K " section of the sample (a_{\max}) is a function of CEt . The K variation within the "constant K " region is also a function of CEt (see Table I). For the compliance range used in this Program (25 to 75), the maximum K point was always near the specimen center as shown in Table I. At one point in time we planned on using a very stiff test machine and controlling the spring stiffness by inserting a matched spring (perhaps a beam of the same material as the test specimen) into the load train. However, after some initial compliance measurements were made (see Appendix A), it became apparent that the stiffness of test machine we were initially using was in the right range. The slight gain to be obtained by stiffening the test machine and optimizing the spring stiffness did not warrant the cost or effort. Therefore, we simply used our test machine as a compliant element and accounted for variations in relative specimen stiffness (as specimens with different moduli were tested) in our analysis and data reduction.

TABLE I

VARIATION IN STRESS INTENSITY FACTOR

(S/W = 8, W = .5 Remote Displacement Controlled Specimen)

Relative Machine Compliance (CEt)	K Variation in Region Adjacent to a_{max} (± 0.050 " on either side of a_{max})	a_{max} (inches)
400	$\pm 5.5\%$.355
300	$\pm 4.3\%$.345
200	$\pm 3.4\%$.330
100	$\pm 2.1\%$.300
75	$\pm 1.8\%$.290
50	$\pm 1.5\%$.275
25	$\pm 1.3\%$.255
10	$\pm 1.3\%$.235
0	$\pm 1.3\%$.225

C = Test Machine Compliance

E = Specimen Modulus

t = Specimen Thickness

a_{max} = Location of Peak Stress Intensity Factor

Thus the basic test procedure is:

- use a notched three point beam (see Figure 1) as a test specimen;
- cyclically load the specimen under remote (not at the specimen) displacement control allowing the crack to initiate and grow across the specimen.

This results in attaining a constant ΔK and concomitantly a constant crack growth rate across the central region of the specimen. It should be noted here that the attainment of a constant K (e.g., crack length invariant) region is quite desirable. The constant K approach removes the experimental error in K determination due to errors in crack length measurement whenever tests are run where gradients in K exist.

For this displacement controlled constant ΔK specimen the method for establishing ΔK is straightforward. Note that we are controlling a displacement and that the value of the stress intensity at any point in the test sample is determined by and is proportional to the value of the applied displacement. Similarly the applied displacement also determines and is proportional to the magnitude of the resulting initial load. Although the load varies (decreases)

throughout the test, a unique linear relationship exists between the initially applied load and the magnitude of the stress intensity attained in the constant K region because the applied displacement remains a constant throughout the test. Thus, ΔK is simply determined by measuring the initial load range (ΔP_o) and using the following equation

$$\Delta K = D_1 \Delta P_o \quad (1)$$

The analysis which determines D_1 is presented in Appendix A. D_1 varies slightly with test specimen/machine stiffness. For our test machine (stiffness = 1.05×10^{-5} in/lb) and a .25 inch thick specimen, D_1 is $65 \text{ in}^{-3/2}$ for aluminum, $68.5 \text{ in}^{-3/2}$ for titanium and $74 \text{ in}^{-3/2}$ for steel. The stress ratio is simply the initially set stress ratio, R given by

$$R = \frac{P_o \text{ min}}{P_o \text{ max}} \quad (2)$$

Although we maintain a constant displacement amplitude during the fatigue crack propagation test we set the magnitude of that displacement by setting the initial loads. These loads are chosen, of course, by choosing the values of ΔK and R desired and using equations 1 and 2 to determine the initial loads. The setting and determination of the applied stress intensity factor in this manner takes advantage of the facts that displacements are easy to control but difficult to measure accurately and that although loads are difficult (expensive) to control they are relatively easy to measure with high accuracy.

It is possible to measure crack growth rates visually as the crack traverses the center of the specimen. However, the displacement controlled constant K specimen has certain attributes which makes a much more advantageous method of obtaining the crack growth rate available.

Since we are controlling the displacement remotely, we may consider the three point bend specimen and the entire test machine as our "test specimen" and that when the crack is in the central region of the three point bend specimen our "test specimen" is a displacement controlled constant stress intensity specimen. Consider such a specimen where the displacement, Δ , and the load, P, are related by

$$\Delta = CP \quad (3)$$

$$k = 1/C \quad (4)$$

where C (the compliance) and k (the stiffness) are functions of the crack length a.

It is well known that the strain energy release rate \mathcal{G} is related to the stress intensity factor and the compliance by the relations (Reference 1):

$$\mathcal{G} = \begin{cases} (1 - \nu^2) \frac{K^2}{E}, & \text{plane strain} \\ \frac{K^2}{E}, & \text{plane stress} \end{cases} \quad (5)$$

$$\mathcal{G} = \frac{P^2}{2t} \frac{\partial C}{\partial a} \quad (6)$$

where E is the specimen modulus, ν is the specimen Poissons

1. Tada, H. "The Stress Analysis of Cracks Handbook,"
Del Research Corporation, 1973.

ratio and t is the crack front length which in our case is the three point bend specimen thickness.

Substitution of equations (3) and (4) into equation (6) yields

$$\mathcal{G} = -\frac{\Delta^2}{2t} \frac{\partial k}{\partial a} \quad (7)$$

Since Δ , t and \mathcal{G} are constant, $\partial k/\partial a$ is constant and negative. Thus for a displacement controlled constant K specimen the load decreases linearly with crack length. Here again the load magnitude at any crack length is proportional to the initial load setting, P_0 , due to the constancy of the applied displacement and therefore in the constant K region of the sample

$$-dP/da = P_0/D_2 \quad (8)$$

where the proportionality constant, D_2 , is independent of crack length. This load:crack length linearity provides a very convenient method for determining da/dN . Since da/dN is a constant (by virtue of the constancy of ΔK) and dP/da is constant,

$$-\frac{da}{dN} = \frac{D_2}{P_0} \frac{dP}{dN} \quad (9)$$

Thus, when P versus N is recorded autographically, da/dN is easily determined by measuring dP/dN which is the slope of a straight line. One does not have the difficulties often associated with generating fatigue crack growth rate data (via conventional compliance or optical methods) by determining the first derivative

of a curved line at a series of points along that line.

Although the G-Rate Test specimen is not a constant K specimen throughout its width, all the steps leading to equation (9) are valid and equation (9) can be used to easily evaluate da/dN for the remote displacement controlled three point bend specimen in the constant K region. All that is required is a record of peak load versus cycles as shown schematically in Figure 3. The slope dP/dN is simply $-\tan\theta$. Note that since a load term is in both the numerator and denominator of equation (9), the ordinate of Figure 3 need not be calibrated, it need only be proportional to the load. In Appendix A we show that the constant D_2 is virtually independent of specimen stiffness and is equal to $.30 \text{ (in)}^{-1/2}$.

Although the autographic load versus cycles line generated is typically quite straight, we have adopted the procedure of measuring the steepest slope on the load cycle plot; this removes any variability that would be found from operator to operator if a visual averaging procedure was used.

The availability of this permanent test record is invaluable. It affords the opportunity of checking the data at future points in

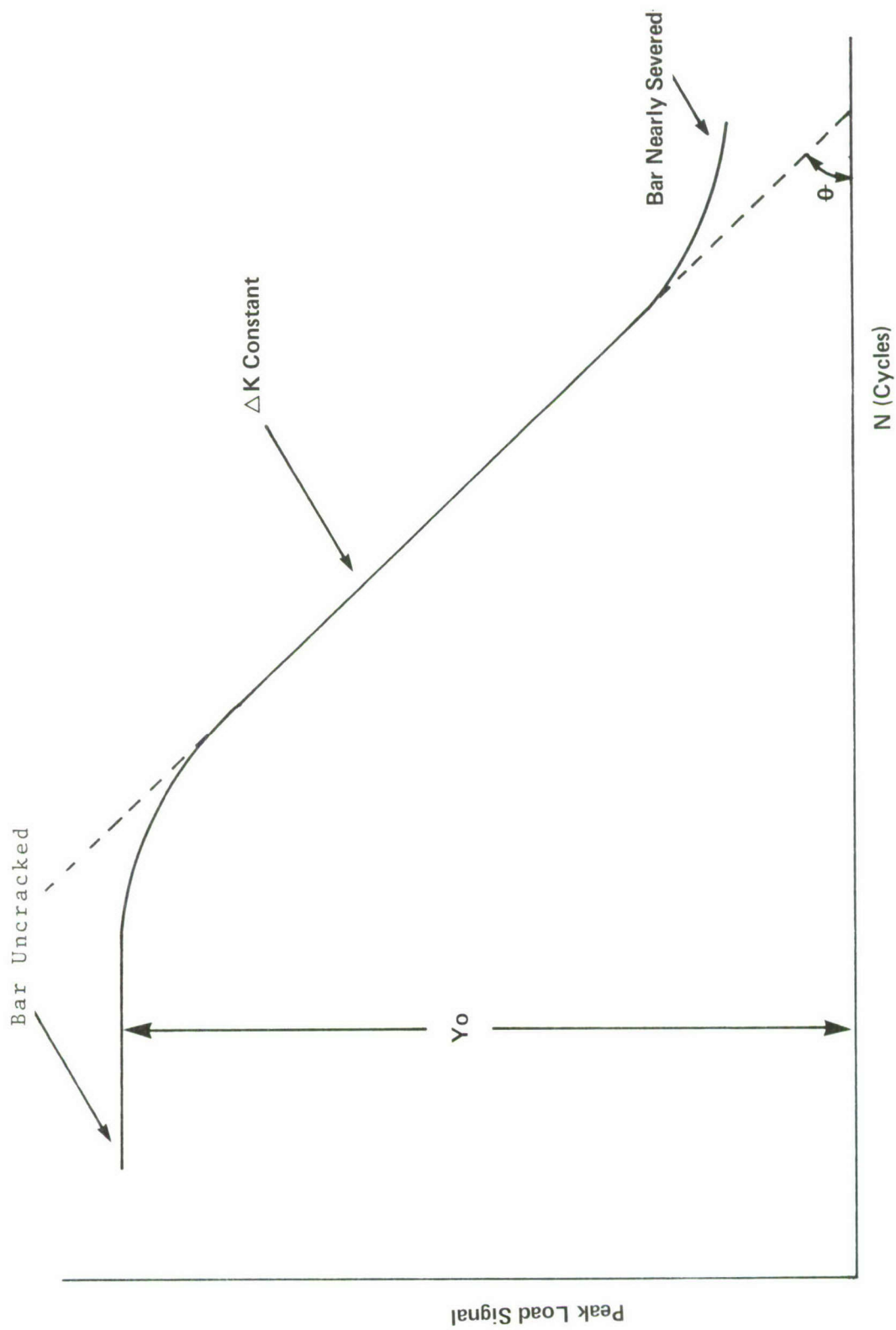


FIGURE 3
Fatigue Crack Growth Data Record

time. Additionally it allows bad tests to be screened out since any variability in the linear portion of the test record or unusual behavior during precracking stages are permanently recorded.

In our tests using the displacement controlled constant K specimen, the peak load versus cycles plot is produced by conditioning the alternating load signal using an analog circuit which outputs a voltage proportional to the peak load and inputting this signal onto the Y axis of a strip chart recorder moving at constant speed. Various chart speed settings are used to maintain the angle of the straight line portion of the record to as close to 45° as possible. In terms of the physical quantities available during a test, equation (9) becomes

$$\frac{da}{dN} = \frac{D_2(\text{C.S.})}{Y_0 \text{ freq.}} \tan \theta \quad (10)$$

where Y_0 is the initial value of the ordinate setting (in.) on the strip chart (recall that $Y_0 \sim P_0$), C.S. is the chart speed (in/min.) and freq. is the loading frequency (cycles/min.)

An example of a typical test record and data reduction is given in Figure 4. The straightness of the record is an indication of the constancy of ΔK and the accuracy of the slope (rate) measurement. As a comparison to compact specimen data, we have shown in Figure 5 twelve constant K test results superimposed

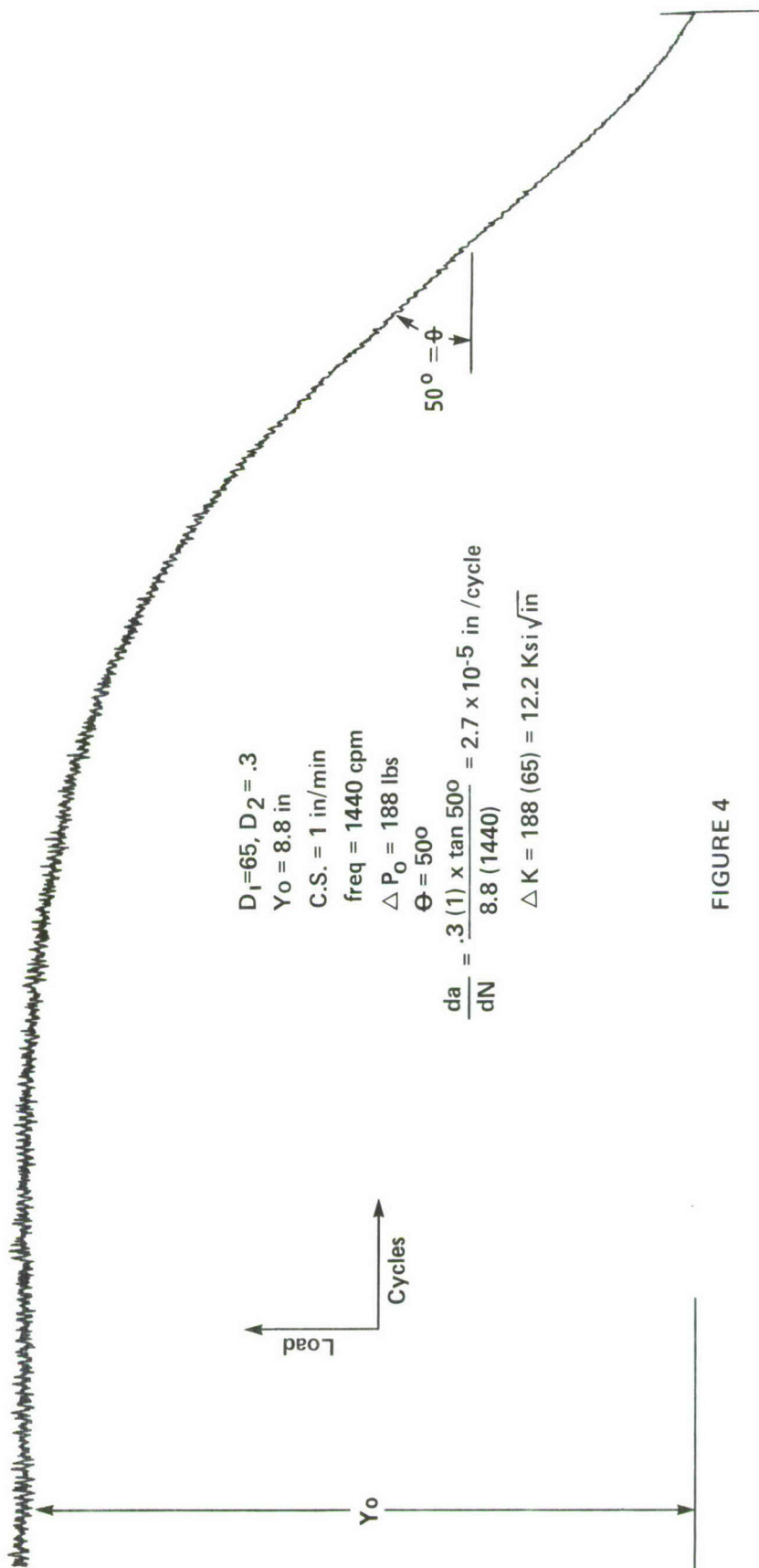


FIGURE 4

Typical Fatigue Crack Growth Rate Test Record
(60% Reduction)

COMPACT VS CONSTANT DELTA-K DATA FOR 7075-T6 IN SALT WATER

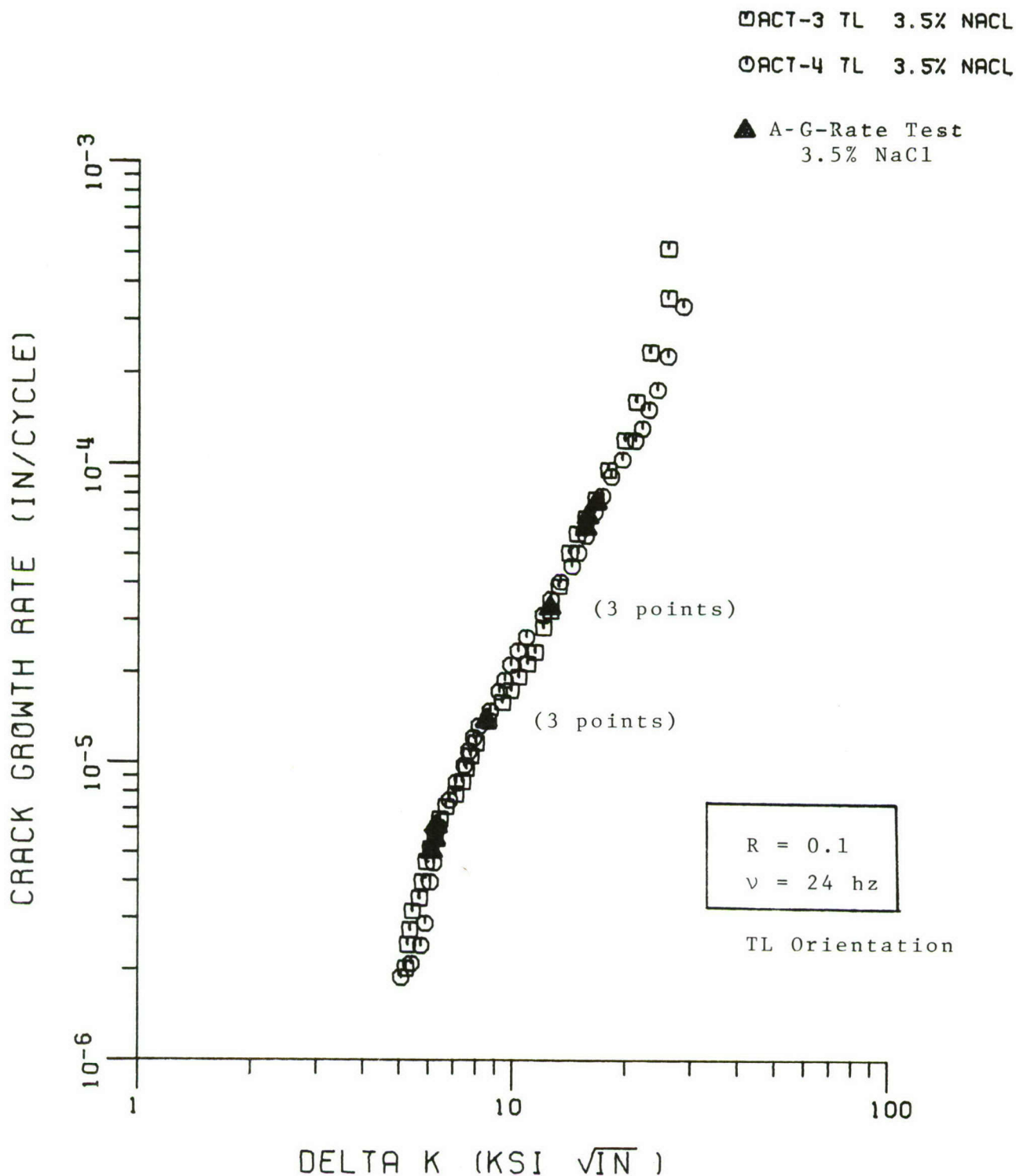


Figure 5

on data from two compact specimens. These data are discussed more fully in Chapter III, but it suffices here to point out that as one would expect the agreement is quite good.

Precracking

In the discussion so far we have presumed that the precracking of the notched bar and the fatigue crack propagation test itself were done at the same applied displacement amplitude. While this is possible in most cases, in some cases where the ΔK to be tested is low the precracking would take too long or crack initiation would not occur if a single displacement amplitude were used. The simple expedient of using higher precracking displacements works quite well. Once the crack advances significantly (load drop $\sim 5-10\%$) the displacement is reduced. The new initial load level is usually chosen so that the overload factor due to the higher final precracking load, is on the order of 1.5 and never greater than 1.8. For very low fatigue crack propagation rate tests ($\sim 10^{-7}$ in/cycle) we have reduced the load in two steps. Schematics of two test records, one with a single precracking stage and one with two precracking stages are shown in Figures 6 and 7. For test records such as these, equations (1) and (10) can still be used to determine ΔK and da/dN employing values of Y_0 and ΔP_0 corresponding to those that would have existed for the uncracked sample had the actual test displacement amplitude been imposed on the sample at that time. This back extrapolation is straight forward and the appropriate equations are given in the Figures. Note that the scale of the load voltage need not be the same for precracking and testing stages. The initial precracking load is set by choosing the ΔK to be tested, the allowable overload ratio (O.L.) and using equation (11)

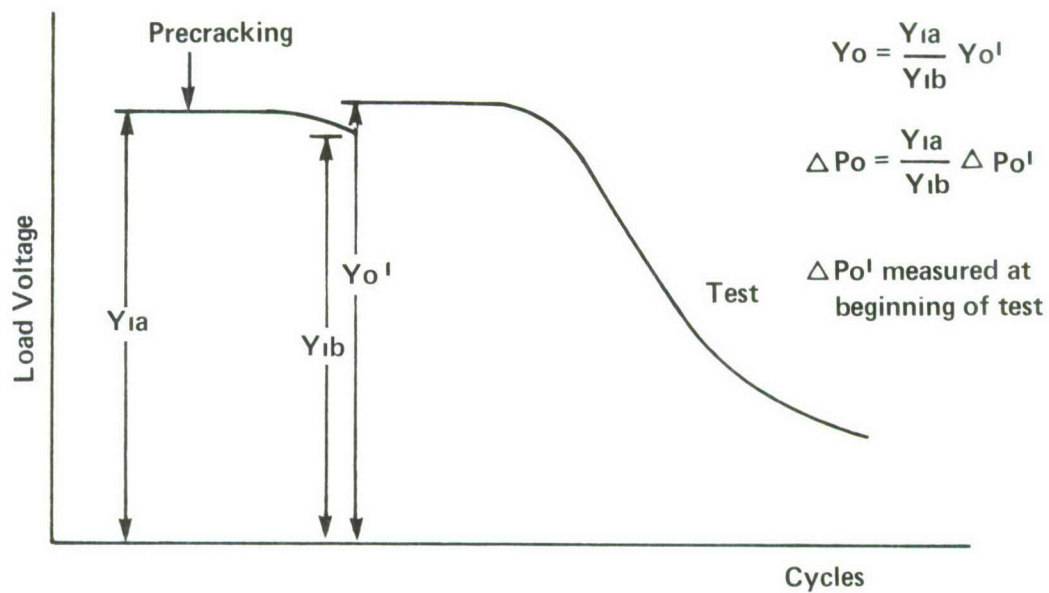


FIGURE 6
Load Versus Cycles - One Precracking Stage

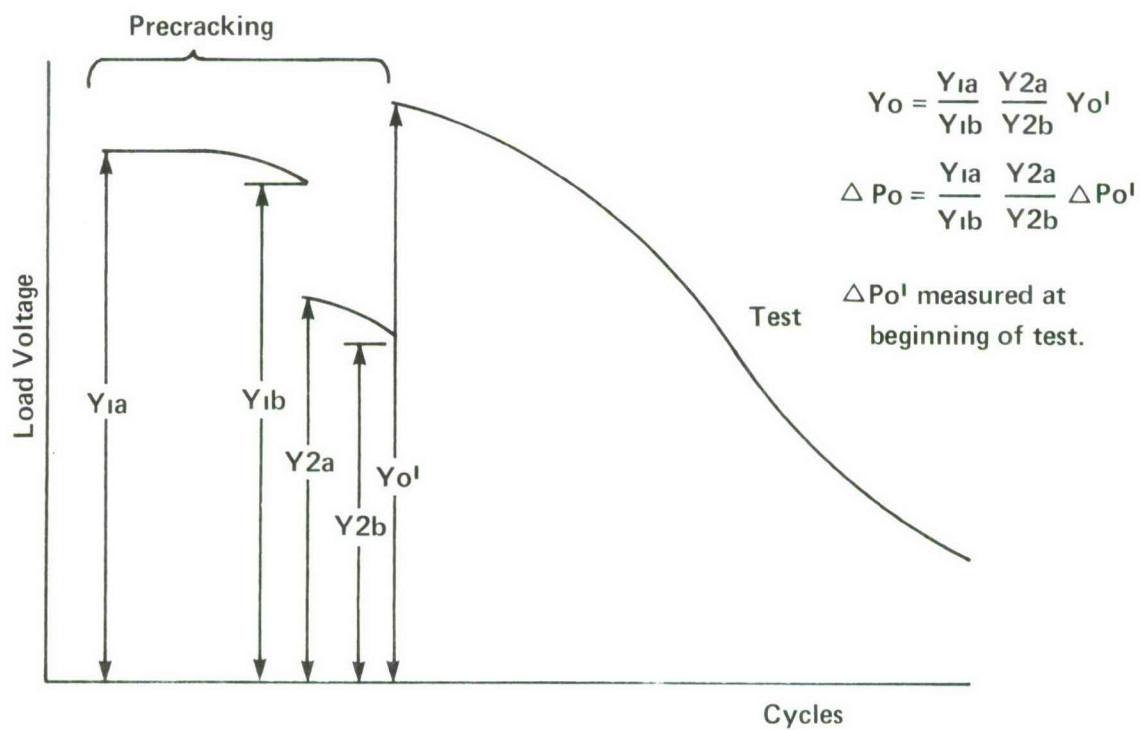


FIGURE 7
Load Versus Cycles - Two Precracking Stages

$$\Delta P_{\text{fatigue}} = \begin{cases} \frac{O.L.}{D_1} \Delta K, & \text{one precracking stage} \\ \frac{(O.L.)^2}{D_1} \Delta K, & \text{two precracking stages} \end{cases} \quad (11)$$

Whether one or two precracking stages are required must be determined by experience with the material/load ranges being tested. For high stress ratio testing, the precracking stress ratio would not be kept the same but would be reduced.

A check that the fatigue crack growth rate test is out of the precracking overload region is available in this test. The straightness of the load-cycle record serves as an excellent check. As shown in Chapter IV overload affects are readily apparent.

B) Test Procedure Summary

The following four pages include a step by step description of the test procedure, for tests with and without precracking, and charts to determine the data reduction constants D_1 and D_2 . The generation of these charts is described fully in Appendix A.

The test procedures described presume that the test machine being used is a machine in which a cyclic displacement amplitude is held constant and that the compliance of the test system is known. A simple method of determining the test system compliance is to:

- a) Place a relatively rigid spacer between the test system loading fixtures.
- b) Set a typical displacement amplitude on test machine.
- c) Record the load amplitude ΔP .
- d) Remove the rigid spacer.
- e) Measure the cyclic displacement amplitude of the loading fixture $\Delta disp$.
- f) The compliance of the test system is given with sufficient accuracy for use with Figures 8 and 9 by

$$C = \frac{\Delta disp}{\Delta P}$$

TEST PROCEDURE - NO PRECRACKING

1. Check and record specimen dimensions.
2. Set and record test frequency (freq).
3. Using knowledge of specimen thickness, specimen modulus and test machine compliance use Figures 8 and 9 to determine D_1 and D_2 .
4. Set and record ΔP_o and R $\Delta P_o = \Delta K/D_1$
5. Set and record chart speed (C.S.) (Choose C.S. as close as possible to paper width x freq/ D_2 x expected da/dN.
6. Adjust load voltage scale to start at approximately full scale.
7. Start test
8. At completion of test measure θ and Y_o (See Figure 3).
9. Reduce data.

$$\Delta K = D_1 \Delta P_o$$

$$\frac{da}{dN} = \frac{D_2}{Y_o} \frac{C.S.}{freq} \tan \theta$$

TEST PROCEDURE - PRECRACKING

1. Check specimen dimensions.
2. Set test frequency (freq).
3. Using knowledge of specimen thickness, specimen modulus and test machine compliance use Figures 8 and 9 to determine D_1 and D_2 .
4. a) Set precracking loads
$$\Delta P_{\text{precracking}} = (O.L.)^n \Delta K / D_1$$
where n is the number of precracking steps and $O.L.$ is the allowable overload factor ($O.L. \sim 1.5 - 1.8$)
b) Begin precracking
c) Reduce loads by $O.L.$ factor as crack growth (5 - 10% drop in load) is detected.
5. Set chart speed (C.S.) - choose C.S. as close as possible to (paper width) $\times (O.L.)^n \times \text{freq} / D_2 \times \text{expected } da/dN$.
6. Adjust load voltage scale to start at approximately full scale.
7. Start test.
8. At completion of test measure Y'_o , Y_{1a} , Y_{1b} , etc. (See Figures 6 and 7).
9. Reduce data.

$$\Delta P_o = \frac{Y_{1a}}{Y_{1b}} \Delta P'_o \quad \text{or} \quad \Delta P_o = \frac{Y_{1a}}{Y_{1b}} \frac{Y_{2a}}{Y_{2b}} \Delta P'_o$$
$$Y_o = \frac{Y_{1a}}{Y_{1b}} Y'_o \quad \text{or} \quad Y_o = \frac{Y_{1a}}{Y_{1b}} \frac{Y_{2a}}{Y_{2b}} Y'_o$$

$$\Delta K = D_1 \Delta P_o$$

$$\frac{da}{dN} = \frac{D_2}{Y_o} \frac{C.S.}{\text{freq}} \tan \theta$$

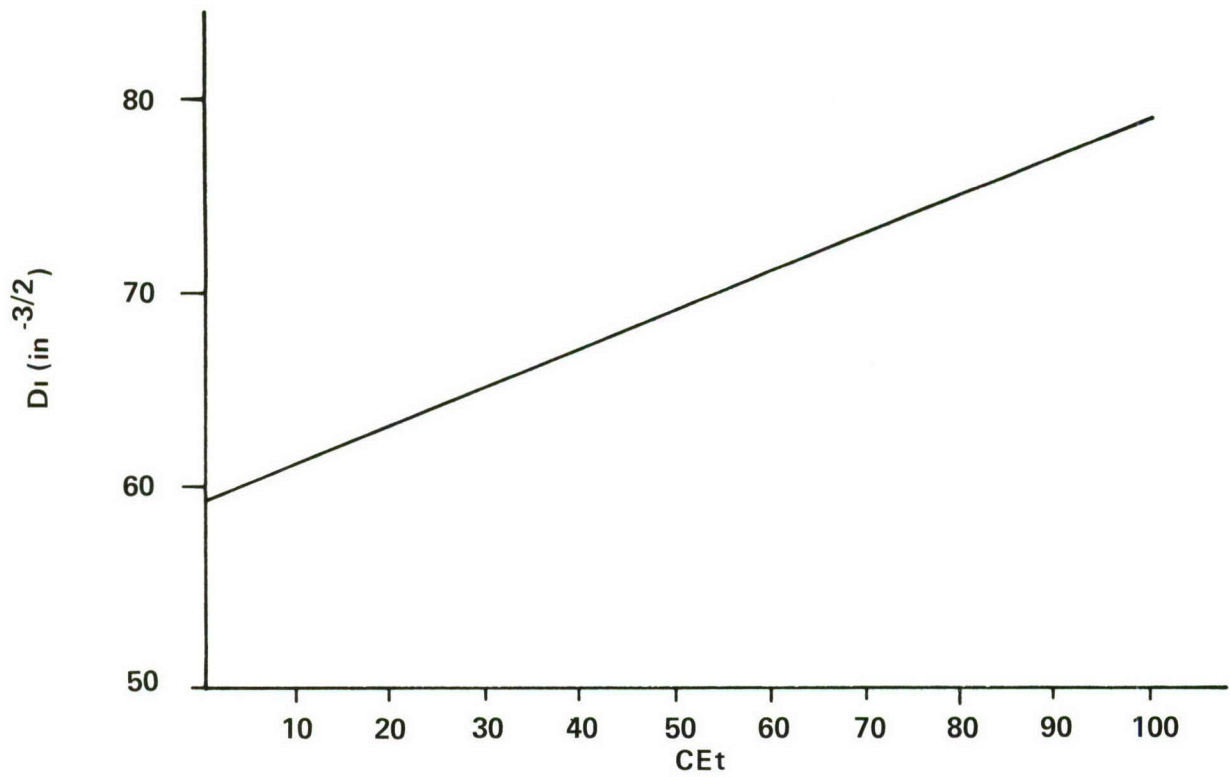


FIGURE 8 Stress Intensity Evaluation Constant
(s/w = 8, w=.5, t = .25 specimen)

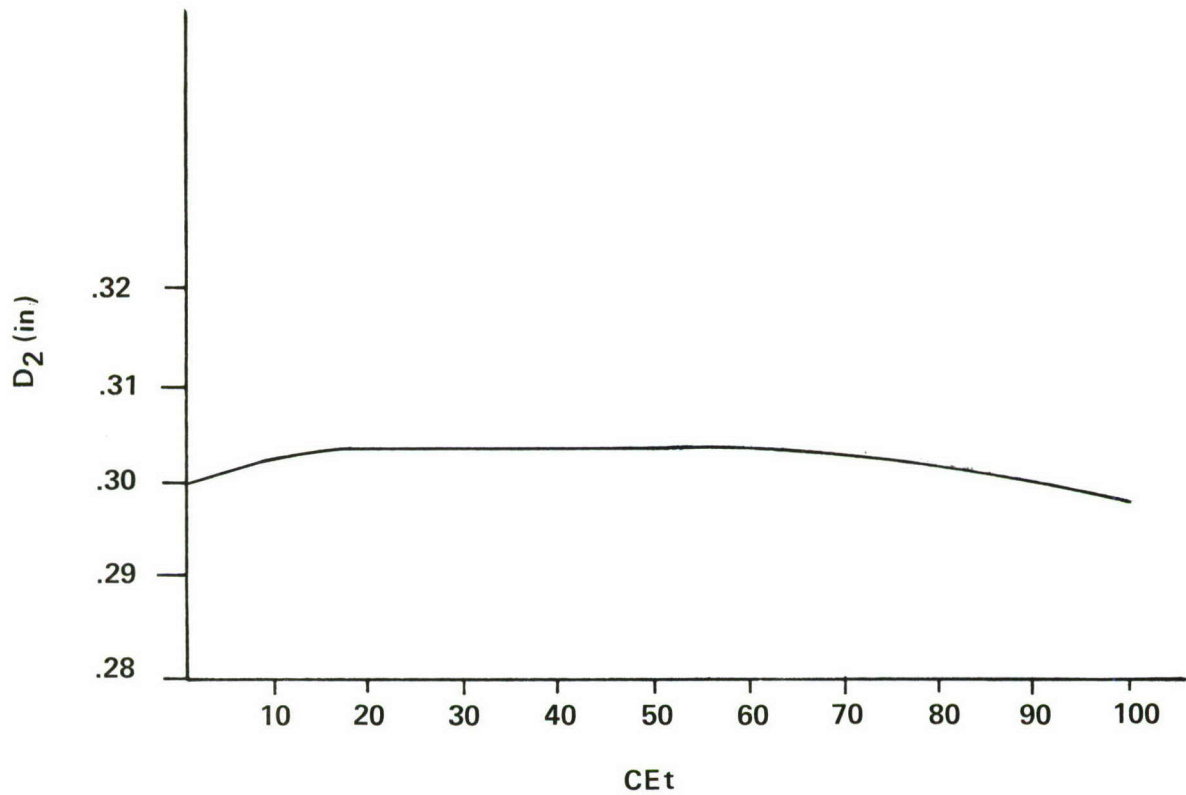


FIGURE 9 Crack Growth Rate Constant
(s/w = 8) w=.5, t=.25 specimen)

C) Test Equipment Used

For initial studies during Phase I an MTS servo controlled electro-hydraulic test machine under stroke control was used. However, all the "quality control" testing during Phase II and much of the Phase I testing was conducted using a simple offset cam displacement control test machine. This test machine was initially designed and used for other purposes at Del West, simple minor modifications made it acceptable for use in this Program. These modifications included the addition of a load cell and minor changes in the loading frame. A photograph of the load frame portion of the test system is shown in Figure 10. The displacement amplitude was adjusted by rotation of an offset cam which in turn drives the front vertical linkage shown in Figure 10. Displacement mean is set by adjusting the length of the vertical linkage arm. The output signal from the load cell alternates with the frequency of loading which was 24 Hz for most of this Program. This is too high a frequency to run directly to the strip chart recorder. Therefore, this alternating load signal was conditioned by an analog circuit to produce a constant d.c. voltage proportional to the load voltage peak. This signal is fed into the 11 inch strip chart recorder. The strip chart recorder is run at a constant chart speed (C.S.). In an alternate operating mode we drove the chart paper by using a signal from the load cell. In that

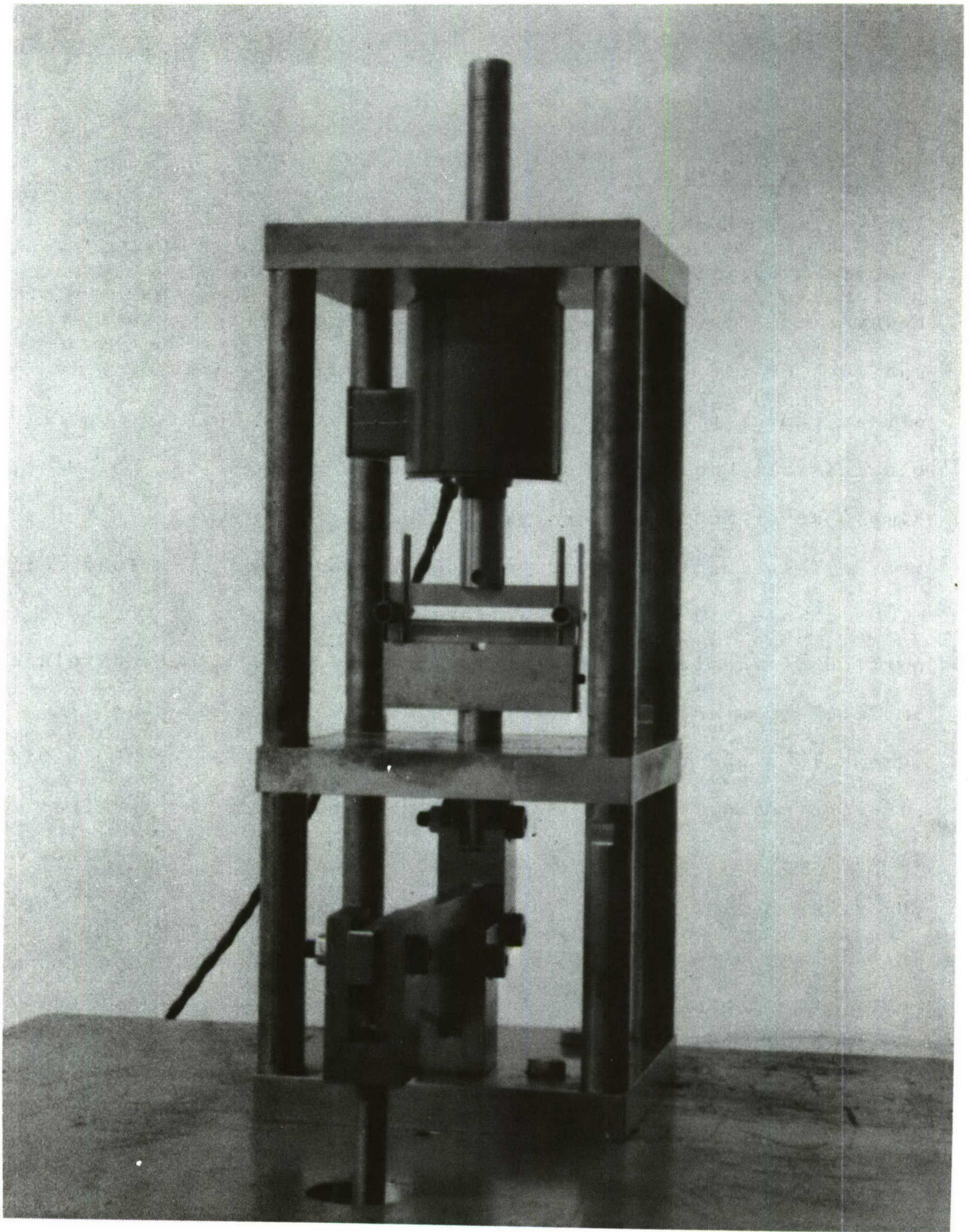


FIGURE 10
Offset Cam Displacement Control System

mode the chart paper advanced a specific distance each time the load was cycled; thus the chart speed would always be proportional to frequency. This mode was abandoned when we were beset by electronics problems, however, it is probably a desirable testing procedure to be used in the future. When this latter mode is used the data reduction equation is

$$\frac{da}{dN} = \frac{D_1(ADV) \tan \theta}{Y_o} \quad (12)$$

where ADV is the distance the chart paper advances with each cycle.

SECTION III
CORRELATION OF FATIGUE CRACK GROWTH
RATES AS DETERMINED BY CONSTANT LOAD
AMPLITUDE AND G-RATE TESTS

The constant load amplitude fatigue crack growth rate test employing a compact tension sample geometry has become the standard engineering test employed by the aerospace community for material evaluation and design data generation. In order to verify that our newly developed constant ΔK test provides as reliable a measure of fatigue crack growth rate as does its conventional constant amplitude counterpart, we formulated and conducted a comprehensive fatigue crack growth rate test program. The test program employed five heats of metal from each of the following alloy systems:

(1) Aluminum

Heats A, B, and C; 7075-T651 Plate (3 heats)

Heat D; 7475-T7651 Plate (1 heat)

Heat E; 7475-T7351 Plate (1 heat)

(2) Titanium

Heats F, G, H, J, and K; 6Al-4V Ti (5 heats)

(3) Steel

Heats L, M, N, O, and P; Ph 13-8Mo (5 heats)

The logic governing the specific alloy selections employed here and a detailed metallurgical description of each of the selected materials heat lots can be found in Appendix B.

A test program sample matrix for the aluminum alloys is given in Table II. Similar test sample matrices for the titanium and steel alloy heats tested here are given in Tables III and IV respectively. All tests conducted under the condition of constant load amplitude during this Program employed a compact tension specimen geometry ($B = 1/4"$, $W = 5"$). All of these constant load amplitude tests were conducted and the data reduced in accord with the recommendations for such tests as found in Reference 2. During this evaluation Phase (Phase II) the constant ΔK or G-Rate Test universally employed the $1/4"$ thick bend bar geometry shown in Figure 1.

TABLE II
ALUMINUM ALLOY TEST PROGRAM
SAMPLE MATRIX
($R = 0.1$, $\nu = 24$ cps)

Material	Alloy Heat Designation	Test Orientation (per ASTM E-399)	Test Type	Chemical Environment	No. of Samples
7075-T651	A	LT	Constant Load Amplitude	lab air	2
7075-T651	B	LT	" "	lab air	2
7075-T651	C	LT	" "	lab air	2
7075-T651	A	TL	" "	3.5%NaCl in H_2O	2
7075-T7651	D	LT	" "	lab air	2
7075-T7351	E	LT	" "	lab air	2
7075-T651	A	LT	Cons't ΔK	lab air	12
7075-T651	B	LT	" "	lab air	21
7075-T651	D	LT	" "	lab air	4
7475-T7351	E	LT	" "	lab air	14
7075-T651	A	TL	" "	3.5%NaCl in H_2O	13

2. Hudak, S. J., R. J. Bucci, "Development of Standard Methods of Testing and Analyzing Fatigue Crack Growth Rate Data," Air Force Materials Laboratory Contract F33615-75-C-5064.

TABLE III
TI ALLOY TEST PROGRAM
SAMPLE MATRIX

(R = 0.1, v = 24 cps, LT Orientation, lab air)

Material	Alloy Heat Designation	Test Type	No. of Samples Tested
6Al-4V Ti	F	Constant Load Amplitude	2
6Al-4V Ti	G	Constant Load Amplitude	2
6Al-4V Ti	H	Constant Load Amplitude	2
6Al-4V Ti	J	Constant Load Amplitude	2
6Al-4V Ti	K	Constant Load Amplitude	2
6Al-4V Ti	F	Constant ΔK	10
6Al-4V Ti	H	Constant ΔK	13
6Al-4V Ti	J	Constant ΔK	11

TABLE IV
STEEL ALLOY TEST PROGRAM
SAMPLE MATRIX

(R = 0.1; v = 24 cps; LT Orientation; lab air)

Material	Alloy Heat Designation	Test Type	No. of Samples Tested
Ph 13-8Mo	L	Constant Load Amplitude	2
Ph 13-8Mo	M	Constant Load Amplitude	2
Ph 13-8Mo	N	Constant Load Amplitude	2
Ph 13-8Mo	O	Constant Load Amplitude	2
Ph 13-8Mo	P	Constant Load Amplitude	2
Ph 13-8Mo	L	Constant ΔK	13
Ph 13-8Mo	M	Constant ΔK	13
Ph 13-8Mo	P	Constant ΔK	13

Turning to the aluminum portion of the Program, one notes both constant load amplitude and G-Rate Tests were conducted on four of the five heats. Additionally, in the case of Heat A, both test types were also employed to generate similar fatigue crack growth rate information in a highly saline chemical environment. The results of the aluminum alloy tests conducted in accord with Table II are presented graphically in Figures 11 through 16. Additionally, Tables V and VI enumerate the specific aluminum constant ΔK results obtained during this effort. As one can note in examining Tables V and VI several constant ΔK results are labelled as improper test or data. The reasons for this labelling derive from irregularities noted in the load drop:cycle records obtained during the course of running these specific tests. A large majority, if not all, of these test record irregularities are traceable to mechanical difficulties with the test apparatus*. Whenever the notation "improper test or data" appears in the Tables, the result quoted there is not presented graphically in Figures 11 - 16.

Examination of the constant load amplitude (labelled Heat No. -CT-1 or 2) and constant ΔK (labelled G-Rate Test) test data shown in Figures 11-16 demonstrate that the two test methods provide identical results over the da/dN range from 2×10^{-7} inches/cycle to 1×10^{-4} inches/cycle in both lab air and 3.5% NaCl in H_2O .

*Chronologically, the G-Rate Test portion of the aluminum test matrix (Table II) was run in large part prior to its titanium and steel counterparts. As such, one could say that we learned about the vagaries of our experimental test set up during the running of these samples and thus account for the high sample attrition rate (~20% of the total tested population) experienced here.

LAB AIR FATIGUE CRACK GROWTH

ALUMINUM HEAT/LOT A

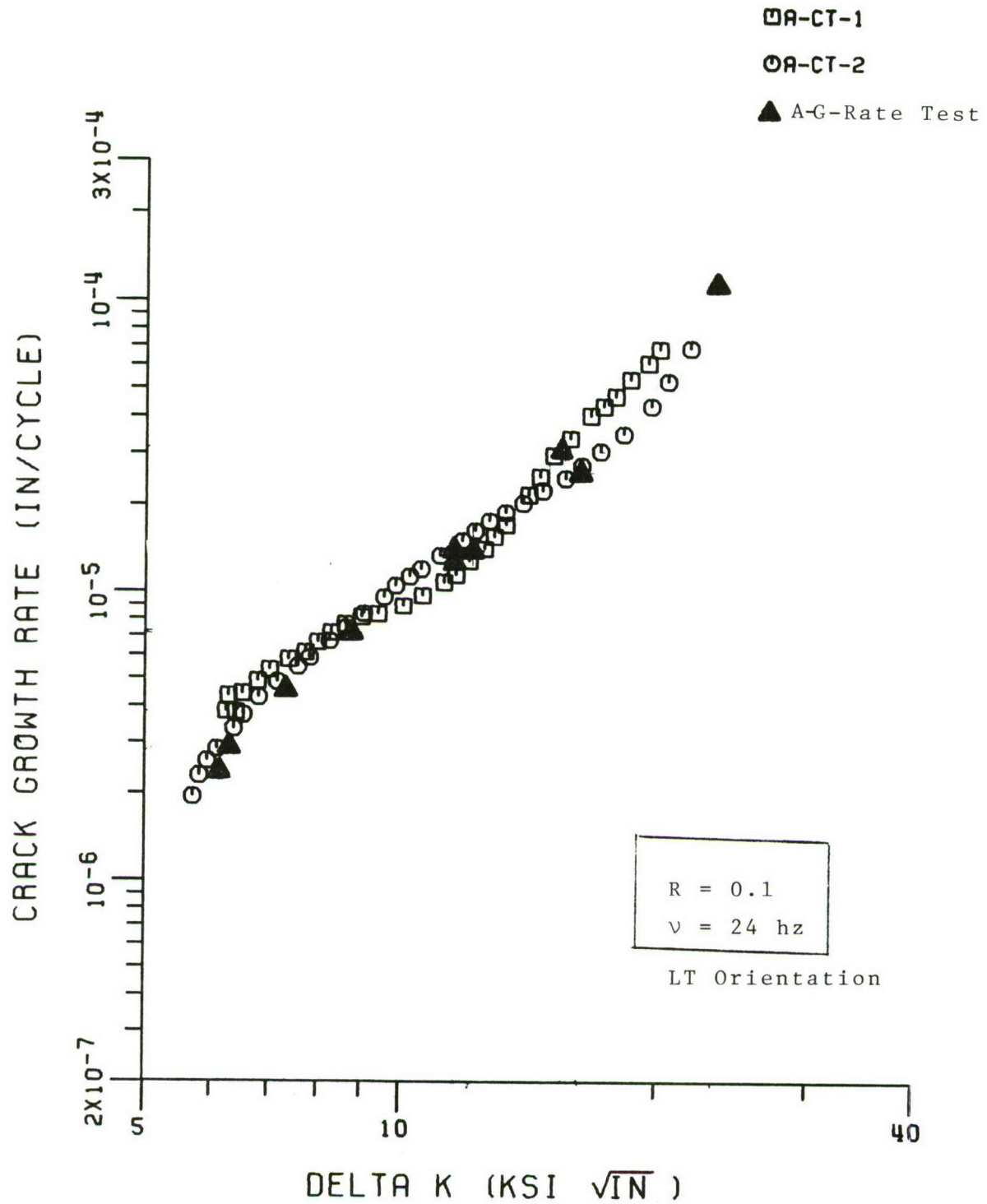


Figure 11

LAB AIR FATIGUE CRACK GROWTH

ALUMINUM HEAT/LOT B

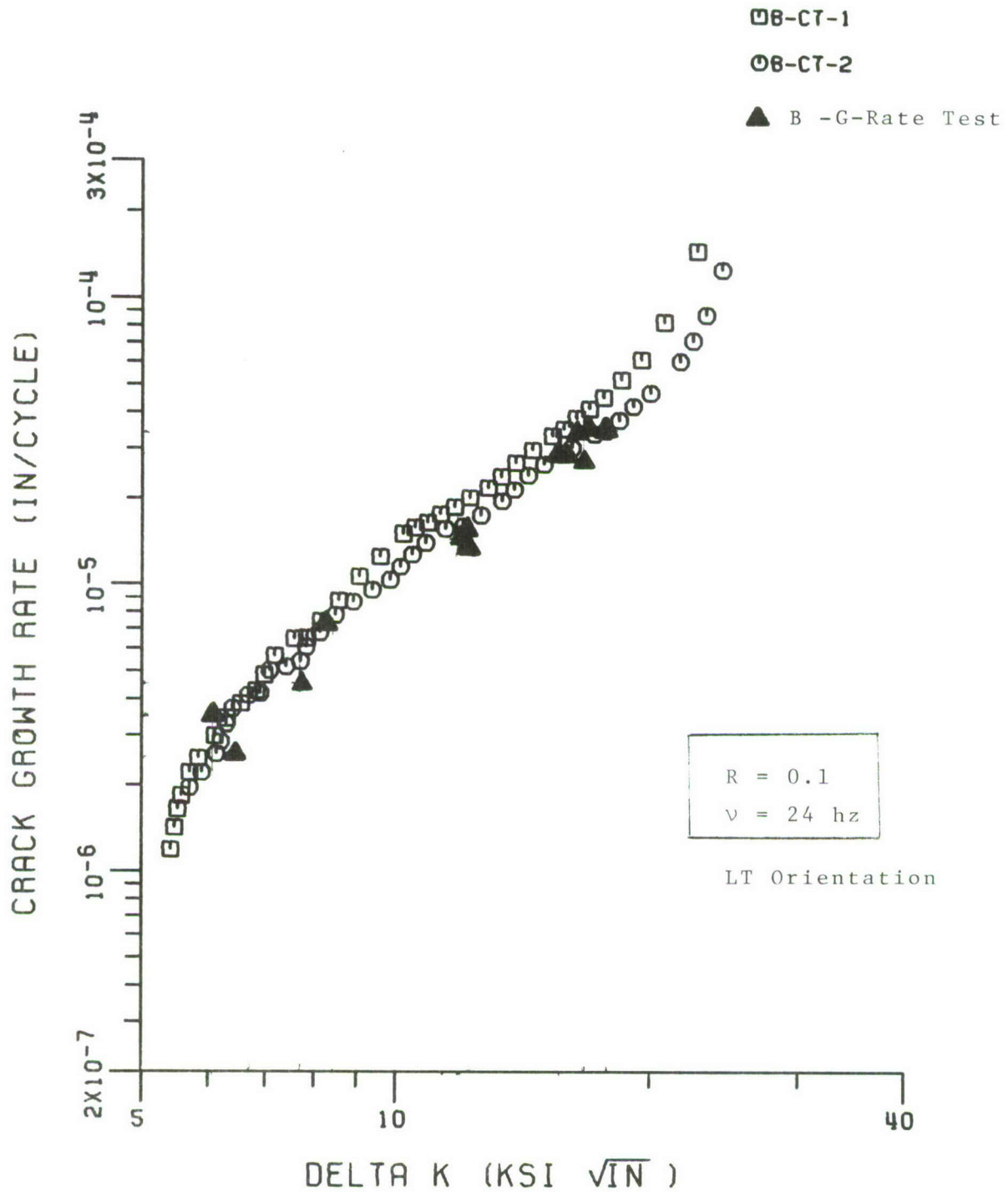


Figure 12

LAB AIR FATIGUE CRACK GROWTH
ALUMINUM HEAT/LOT C

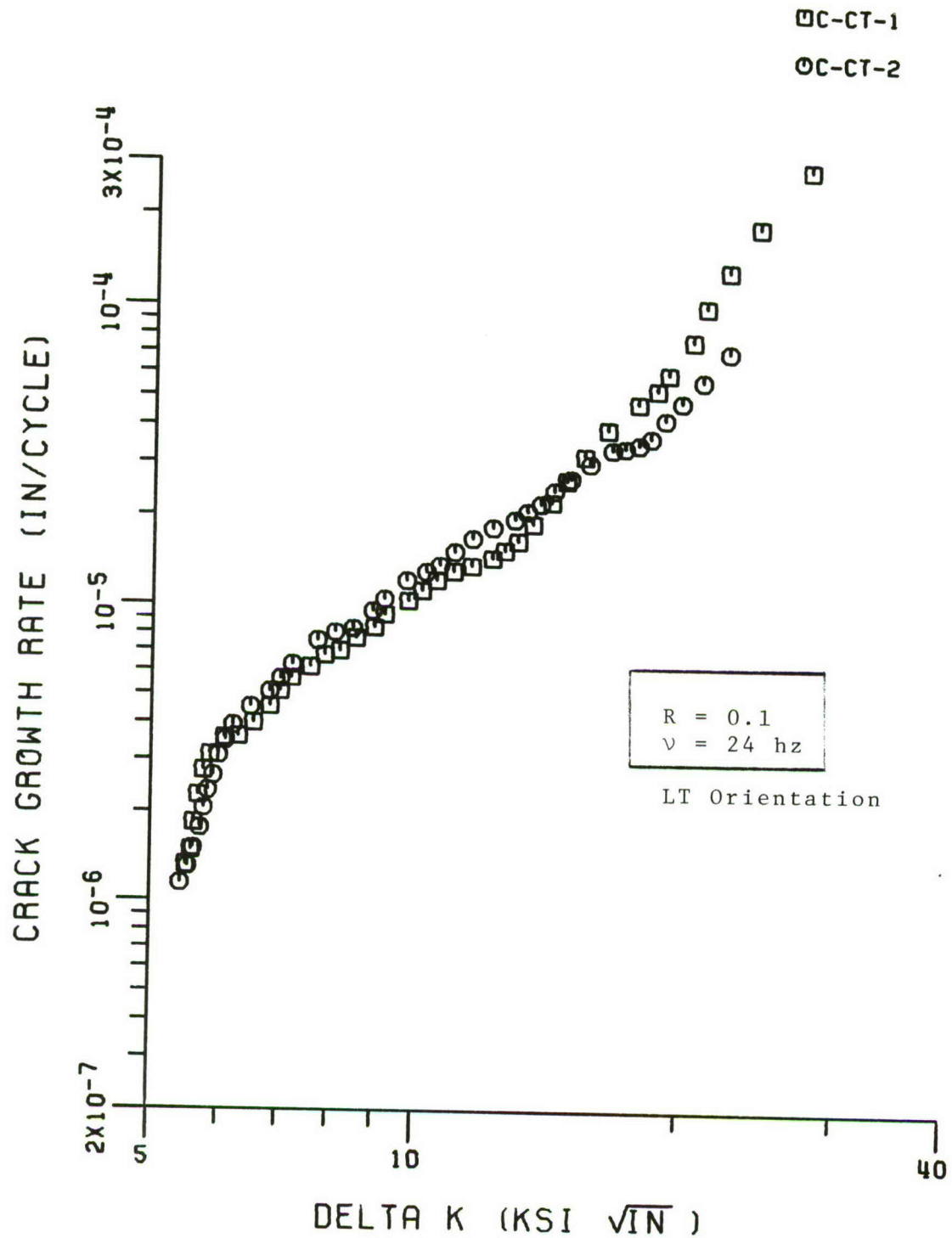


Figure 13

LAB AIR FATIGUE CRACK GROWTH

ALUMINUM HEAT/LOT D

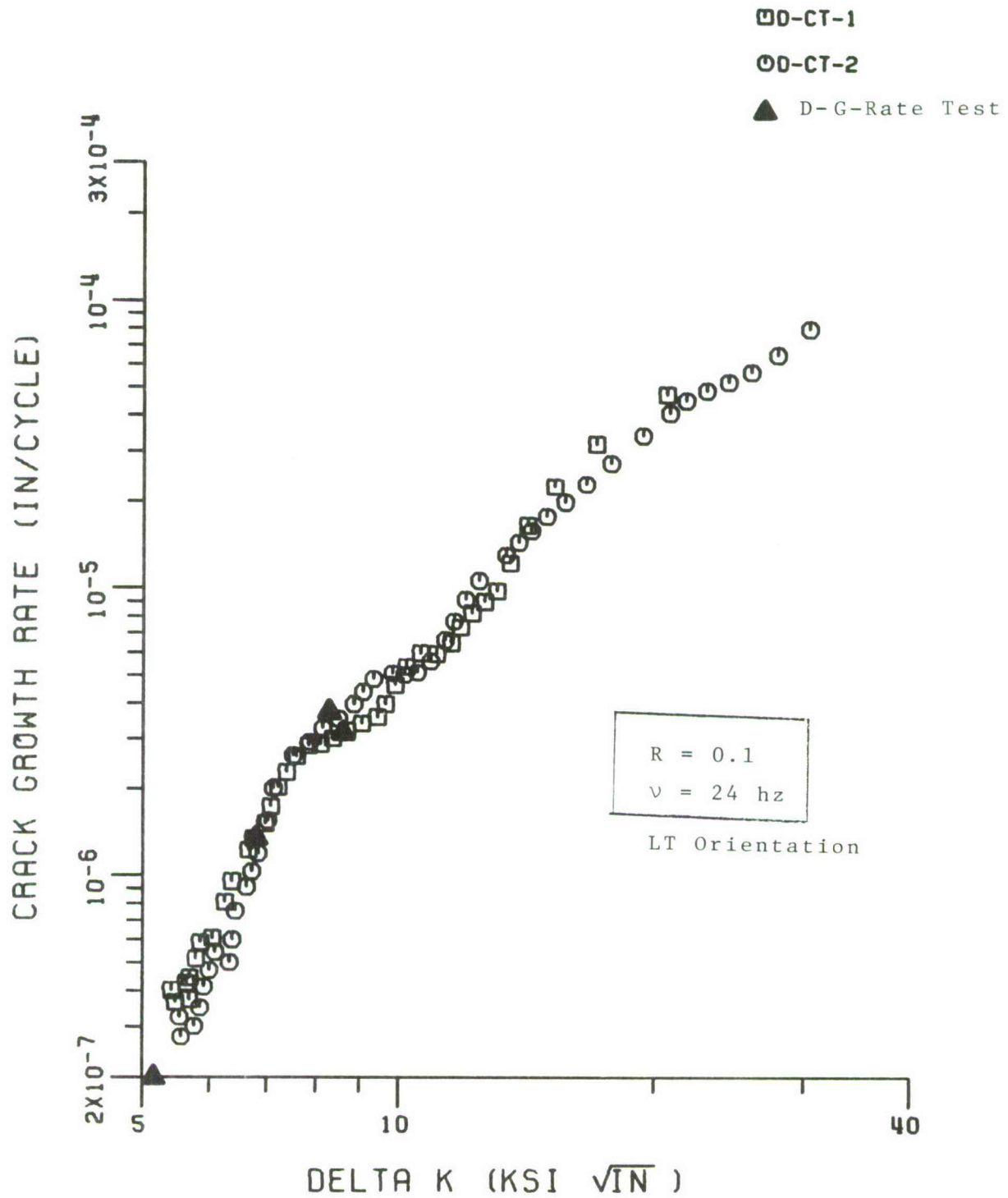


Figure 14

LAB AIR FATIGUE CRACK GROWTH

ALUMINUM HEAT/LOT E

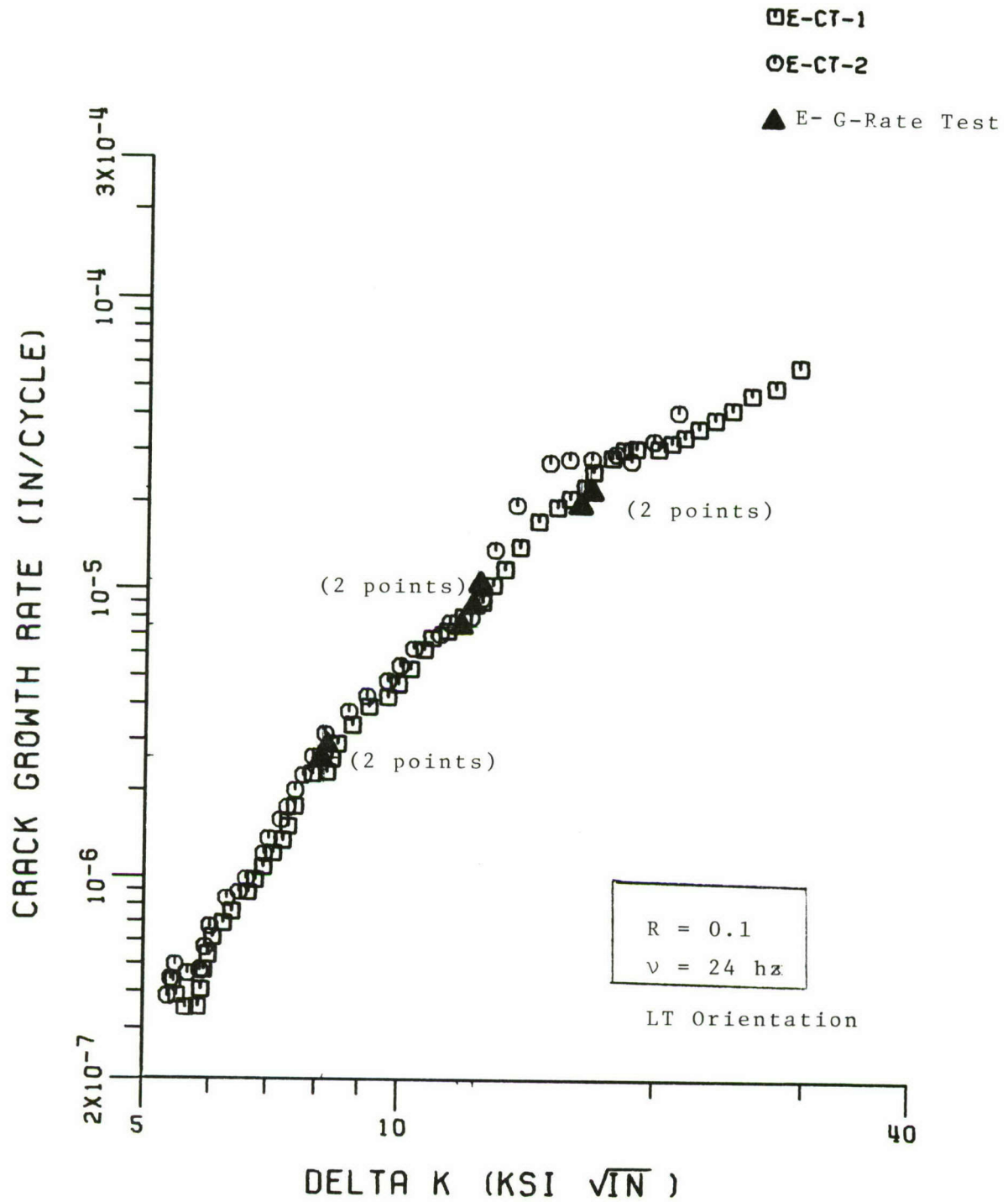


Figure 15

COMPACT VS CONSTANT DELTA-K DATA FOR 7075-T6 IN SALT WATER

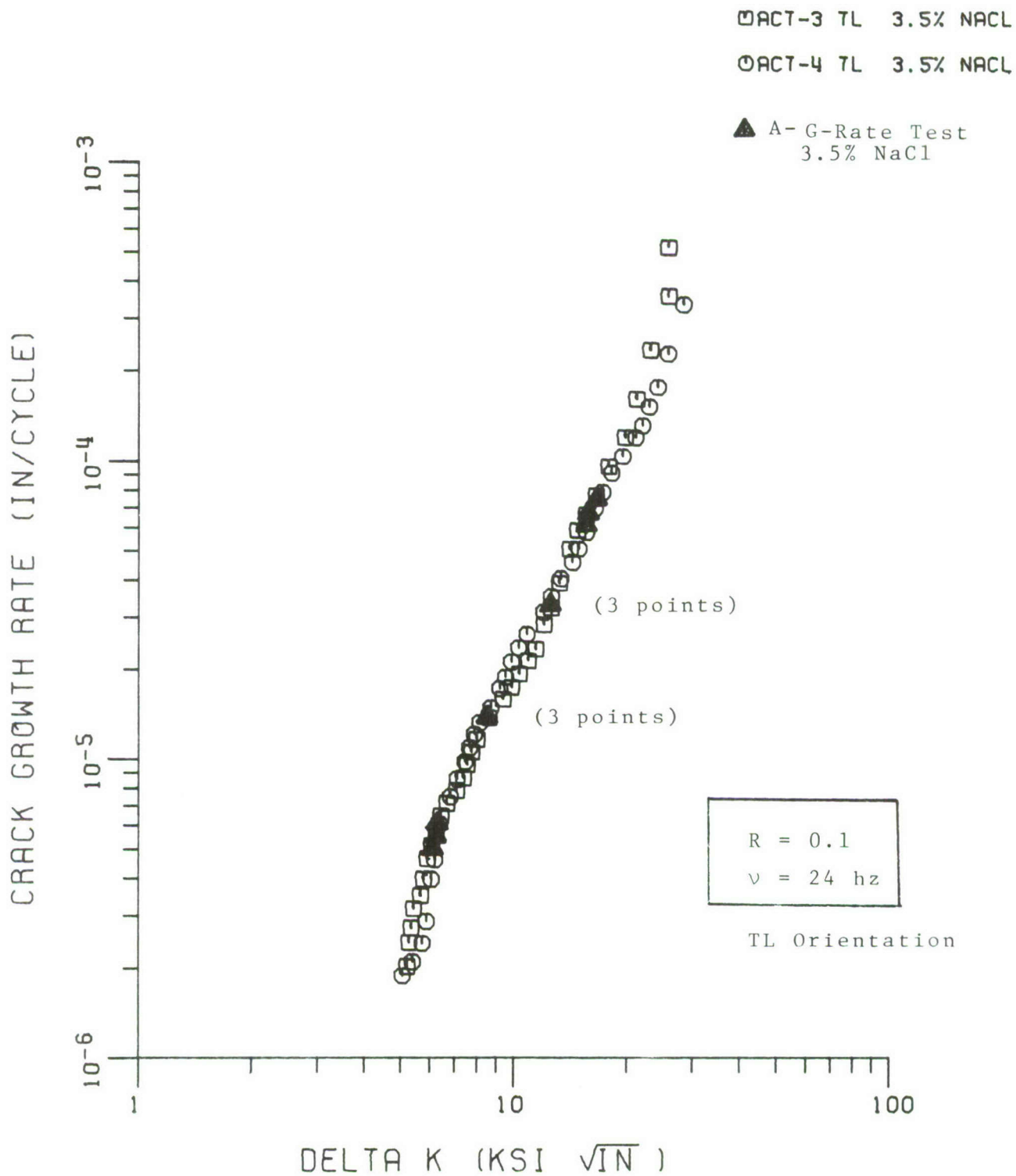


Figure 16

TABLE V
7075/7475 CONS'T ΔK DATA
Environment: Lab Air; R Factor = 0.1
LT Orientation

<u>Sample No.*</u>	$\frac{da}{dN}$ $\times 10^{-6}$ inches/cycle	ΔK Ksi $\sqrt{\text{in.}}$	<u>Remarks</u>
<u>Heat A*</u>			
4-A-30	4.72	7.3	
4-A-31	2.46	6.1	
4-A-33	2.78	6.25	
4-A-34	7.11	8.77	
4-A-36	13.0	12.0	
4-A-36	31.1	15.7	
4-A-20	150.	23.53	
4-A-11	25.7	16.1	
4-A-10	13.4	12.1	
4-A-12	13.6	11.6	
4-A-14	10.0	15.2	Improper Data
4-A-27	4.66	8.77	Improper Data
<u>Heat B*</u>			
4-B-44	3.47	6.04	
4-B-43	7.13	8.39	
4-B-41	13.5	12.5	
4-B-42	34.0	17.7	
4-B-40	29.3	15.3	
4-B-12	25.6	16.6	
4-B-14	32.1	16.4	
4-B-13	23.8	16.5	
4-B-15	29.8	16.3	
4-B-16	33.1	16.7	
4-B-37	11.0	11.2	
4-B-26	13.0	11.8	

*For a metallurgical definition of the various aluminum heats employed here, see Tables B-I and B-II.

TABLE V
(Cont)

<u>Sample No</u>	$\frac{da}{dN}$ $\times 10^{-6}$ Inches/Cycle	$\frac{\Delta K}{\text{Ksi}\sqrt{\text{in.}}}$	<u>Remarks</u>
4-B-18	13.0	11.8	
4-B-17	14.1	12.1	
4-B-36	4.41	7.67	
4-B-24	10.5	7.93	Improper Test
4-B-31	25.2	8.02	Improper Test
4-B-39	2.40	6.58	
4-B-38	2.86	6.62	Improper Test
4-B-32	1.62	6.07	Improper Test
4-B-33	3.83	7.04	Improper Test
<u>Heat E</u>			
4-E-34	19.5	16.1	
4-E-33	22.0	16.3	
4-E-32	22.0	16.4	
4-E-10	10.3	11.9	
4-E-37	9.3	12.2	
4-E-31B	2.66	8.3	
4-E-21	10.5	12.2	
4-E-30	7.4	11.7	
4-E-31A	0.73	6.4	
4-E-38	2.6	8.2	
4-E-35	3.1	8.4	Improper Test
4-E-20	12.0	11.5	Improper Test
4-E-36	1.12	6.3	Improper Test
4-E-39	2.0	6.1	Improper Test
<u>Heat D</u>			
4-D-1	0.2	5.2	
4-D-2	1.3	6.8	
4-D-3	3.6	7.9	
4-D-4	3.2	8.1	

TABLE VI
7075 - T651 PLATE A CONS'T ΔK DATA
Environment - 3.5% NaCl in H₂O, R Factor = 0.1
Test Frequency - 24 cps; TL Orientation

Sample No.	$\frac{da}{dN}$ ($\times 10^{-6}$ inches/cy)	ΔK (Ksi $\sqrt{\text{in}}$)	Remarks
4-A-TL-12	12.0	8.30	
4-A-TL-13	3.9	5.70	
4-A-TL-10	4.3	6.10	
4-A-TL-11	4.5	6.07	
4-A-TL-8	12.5	7.80	
4-A-TL-7	12.0	7.90	
4-A-TL-6	31.0	12.2	
4-A-TL-4	32.0	12.0	
4-A-TL-2	27.0	12.2	
4-A-TL-3	64.0	15.9	
4-A-TL-1	72.0	15.8	
4-A-TL-5	60.5	16.2	
4-A-TL-9	-	-	Improper Test

Comparisons of the two test methods abilities' to measure lab air fatigue crack growth rates in 6Al-4V Ti and Ph 13-8Mo steel are shown graphically in Figures 17-26. Here again, we have additionally tabulated our constant ΔK results in Tables VII and VIII for titanium and steel respectively*. As one can note in Figures 17 through 26 both test techniques once again provide identical results. Thus, one can conclude that the constant ΔK test method provides a quantitative measure of da/dN at any ΔK with the same accuracy and precision as can be gained employing the conventional constant load amplitude approach.

Let us now consider an occasion during the above test Program where the G-Rate Test technique was employed to distinguish one heat of 6Al-4V Ti from another in a situation where either the metal's producer or Del West receiving inspection exchanged the marking designation on a pair of forged plates. Crucible Materials Research Center shipped each of the Ti heats as a series of small plate segments. This multiplicity of plate segments/heat and their complex plate/heat numbering system permitted one of us to interchange one each of the J and K Heat plates. This interchange was first suspected when the constant load amplitude da/dN data for pairs of CT samples taken from Heats "J" and "K" turned out to be identical. In Appendix B, one notes that Heat J was processed

*The sample attrition% in Tables VII and VIII is only 4% reflecting our growing familiarity with our experimental apparatus. Recent measurements of aluminum alloy fatigue crack growth rates for NASA-AMES (NAS 2-9672) show less than 1% attrition due to equipment malfunctions.

LAB AIR FATIGUE CRACK GROWTH

TITANIUM HEAT/LOT F

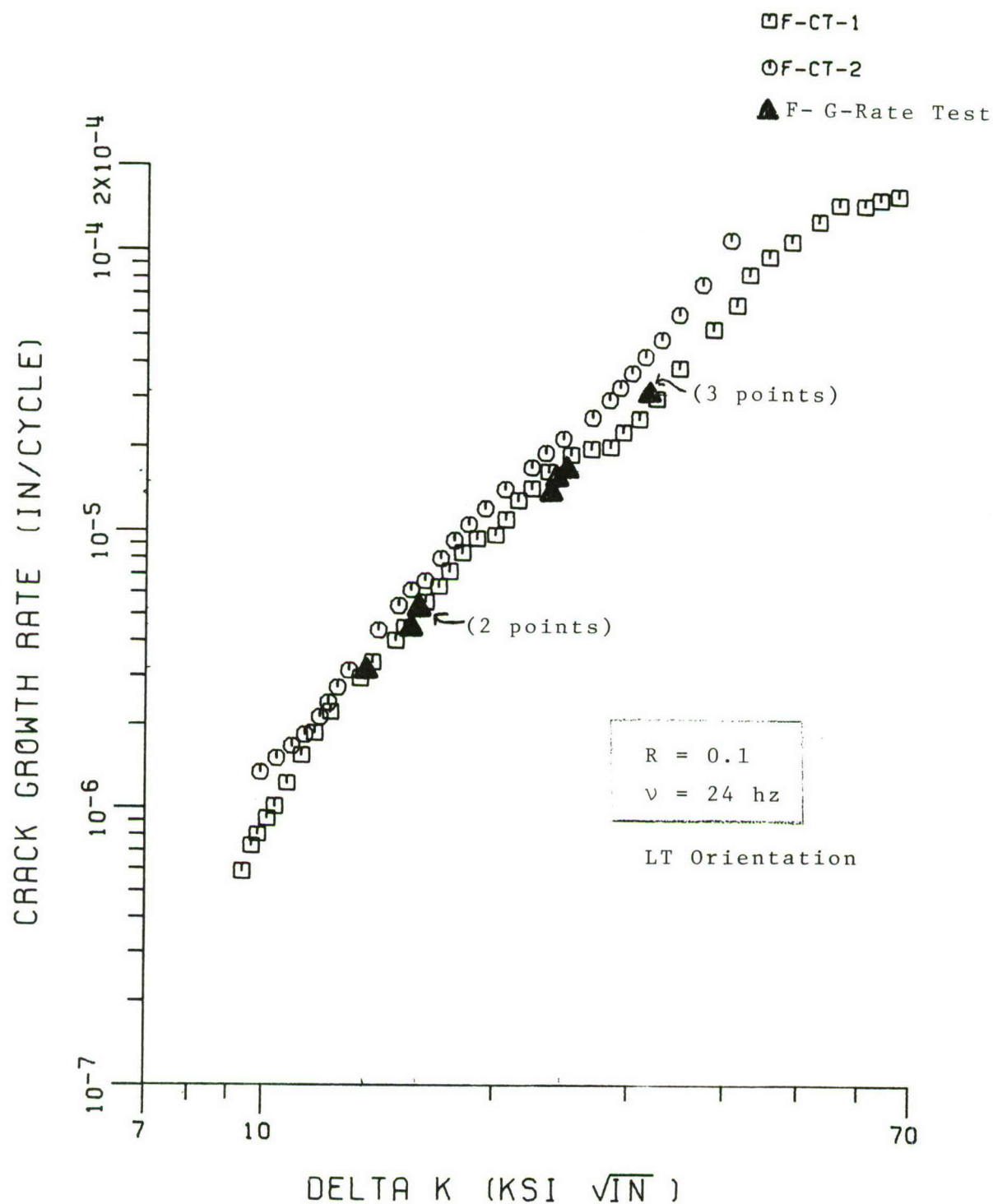


Figure 17

LAB AIR FATIGUE CRACK GROWTH

TITANIUM HEAT/LOT G

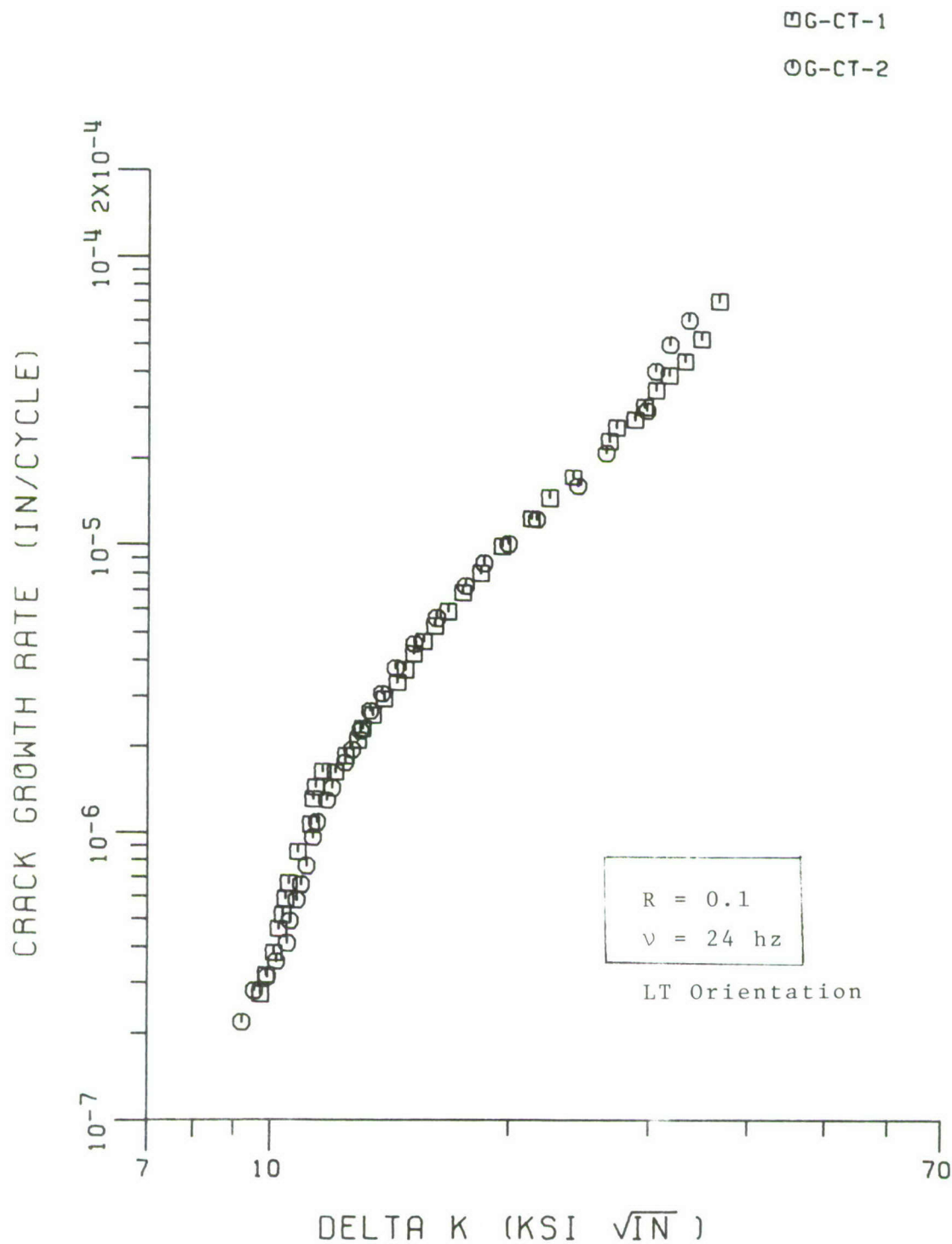


Figure 18

LAB AIR FATIGUE CRACK GROWTH

TITANIUM HEAT/LOT H

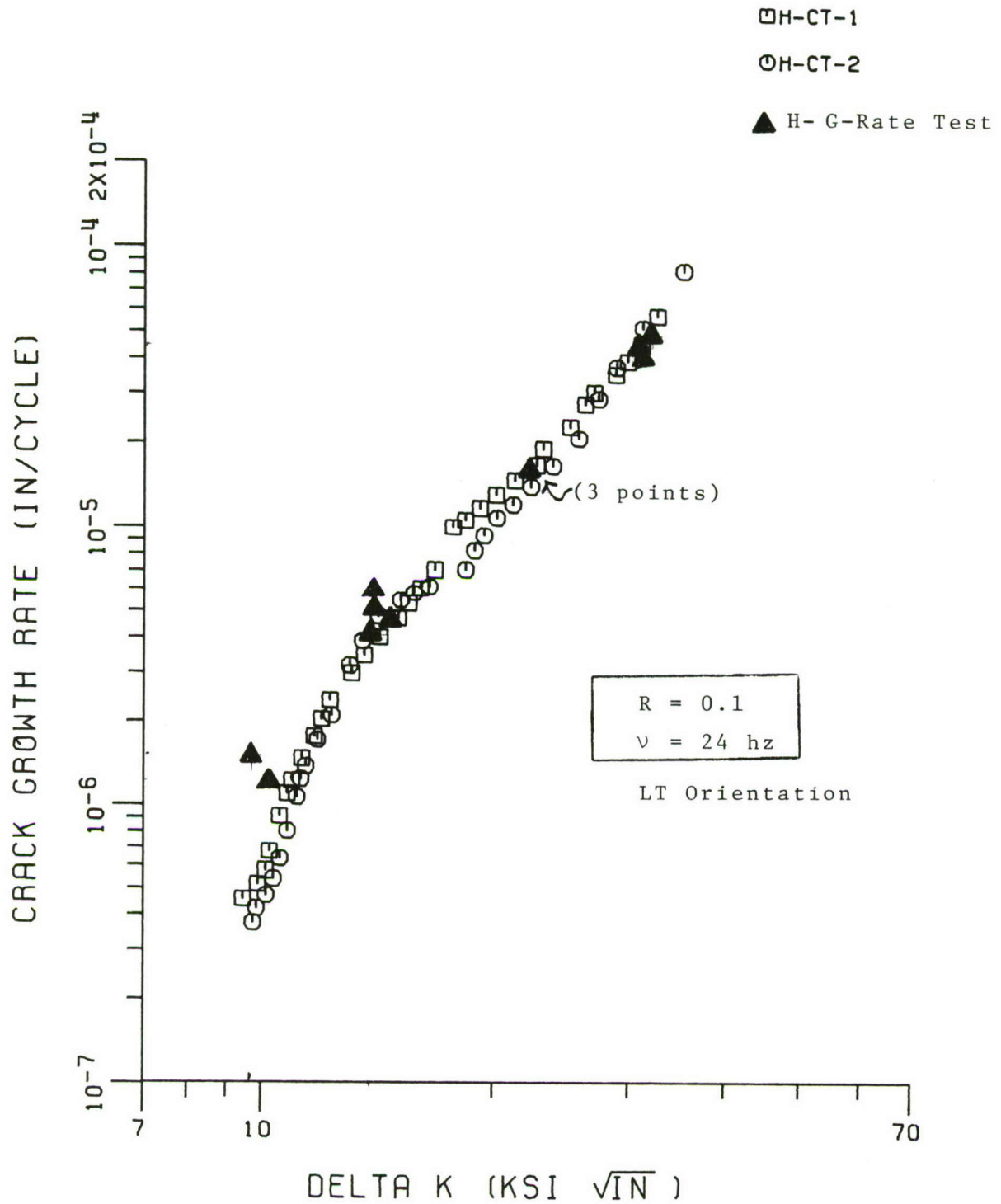


Figure 19

LAB AIR FATIGUE CRACK GROWTH

TITANIUM HEAT/LOT J

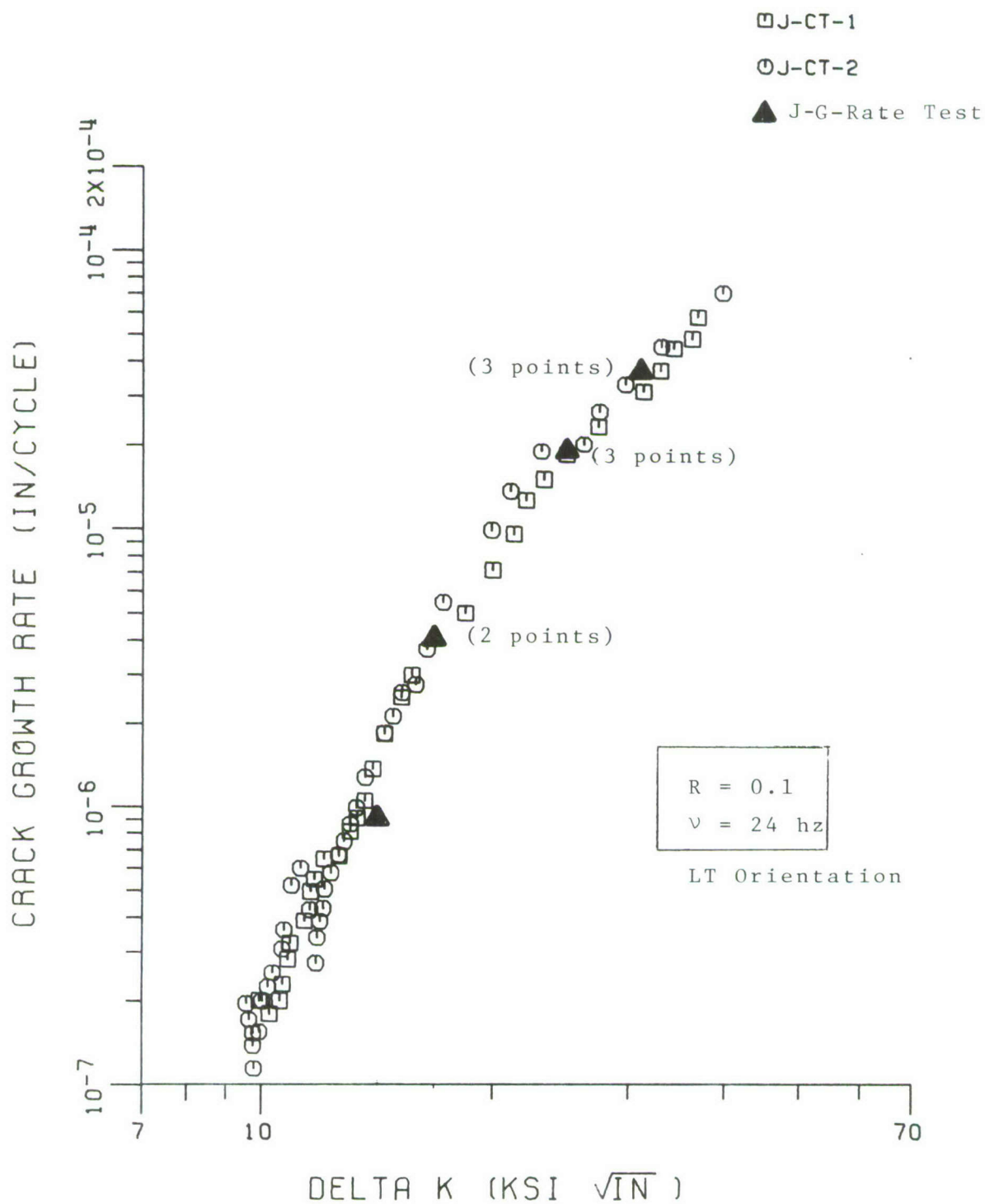


Figure 20

LAB AIR FATIGUE CRACK GROWTH

TITANIUM HEAT/LOT K

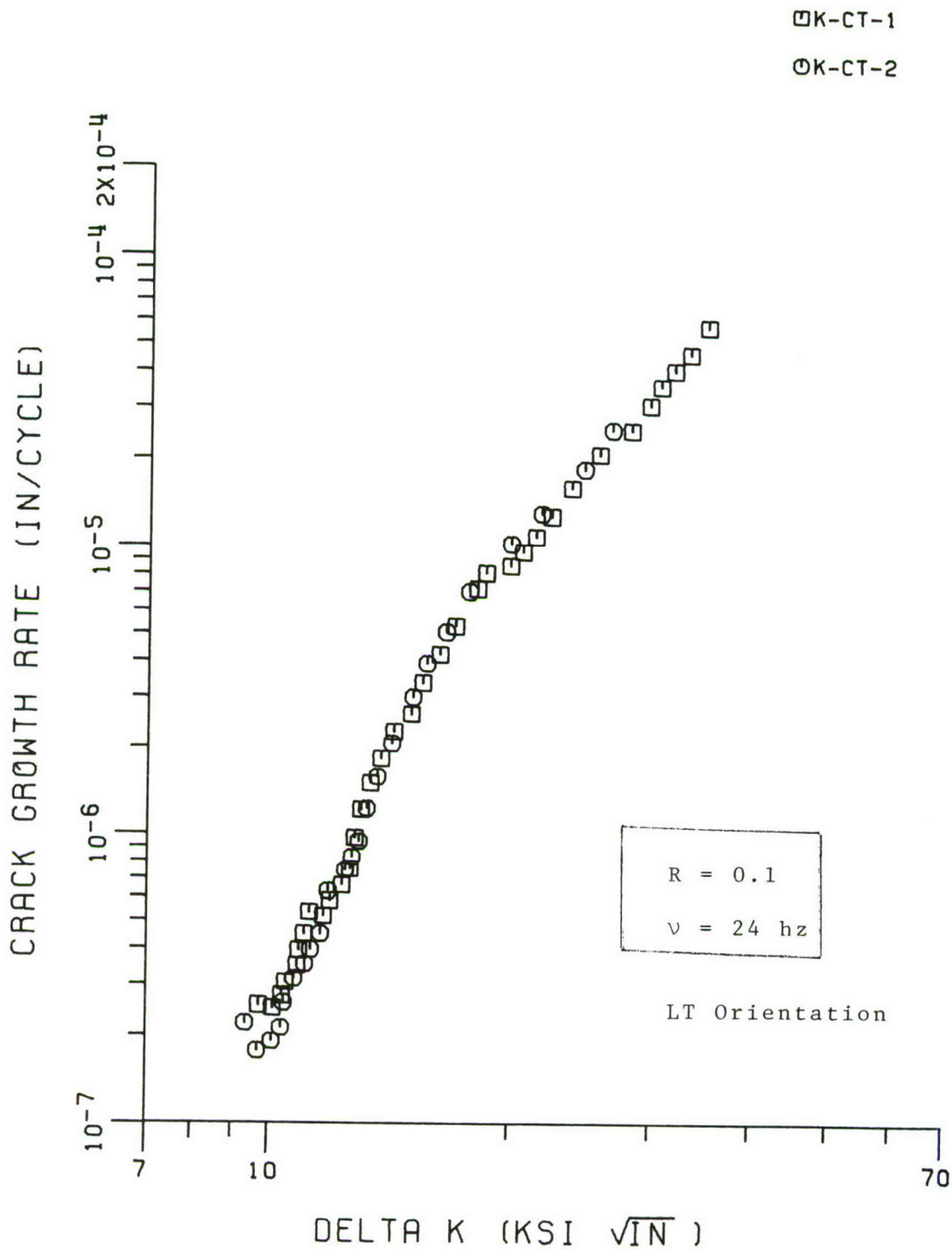


Figure 21

LAB AIR FATIGUE CRACK GROWTH

STEEL HEAT/LOT L

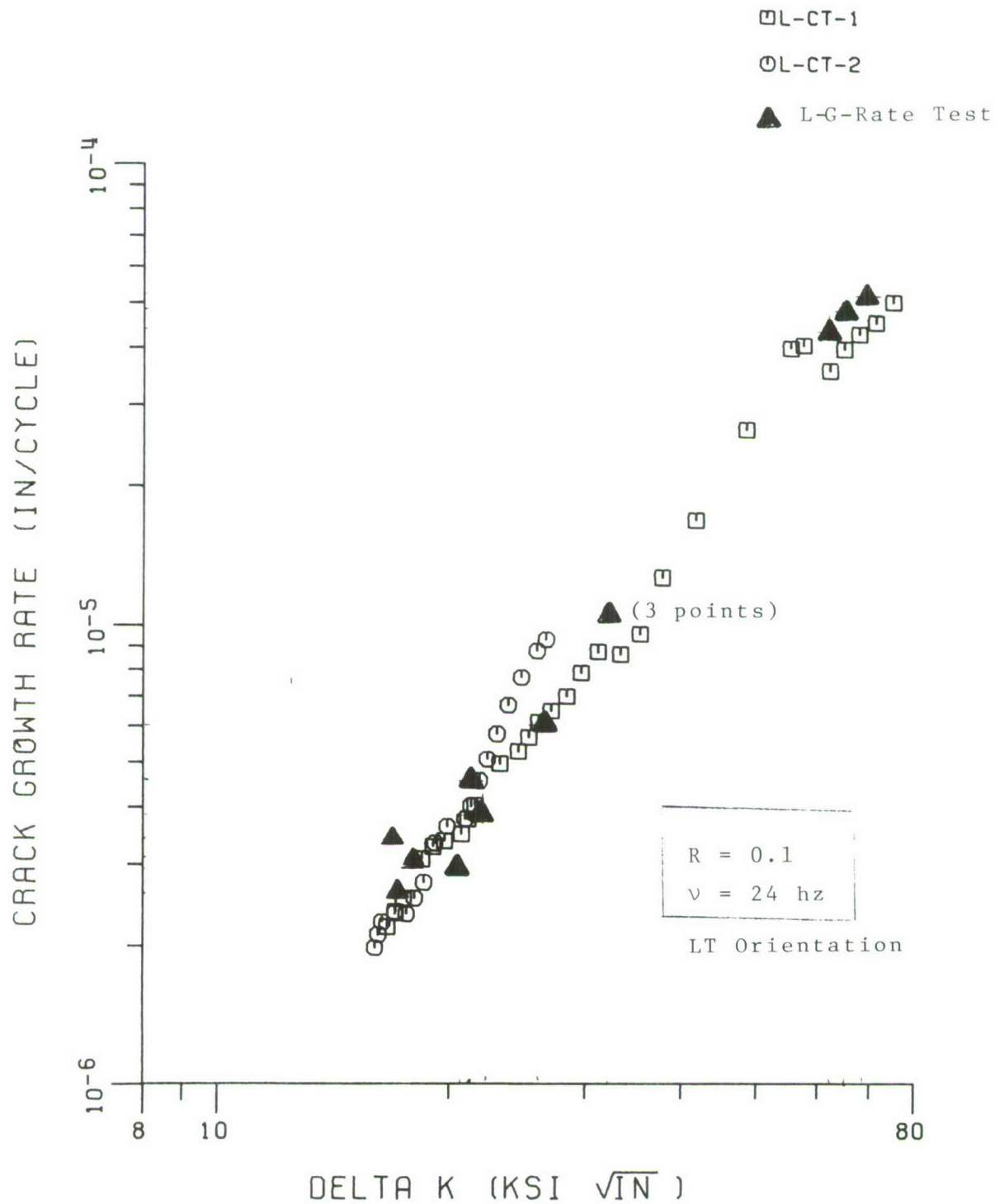


Figure 22

LAB AIR FATIGUE CRACK GROWTH

STEEL HEAT/L0T M

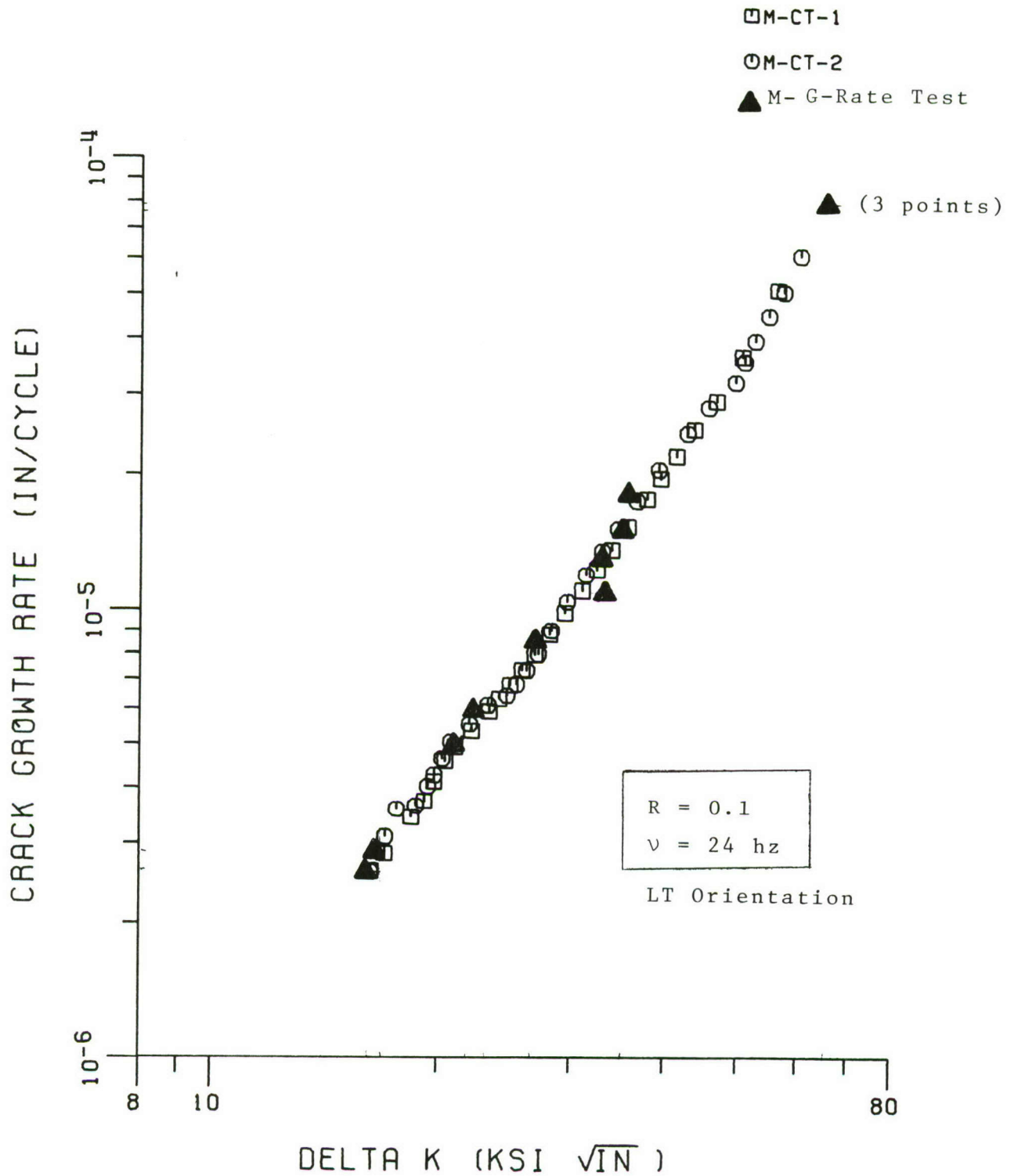


Figure 23

LAB AIR FATIGUE CRACK GROWTH

STEEL HEAT/LOT N

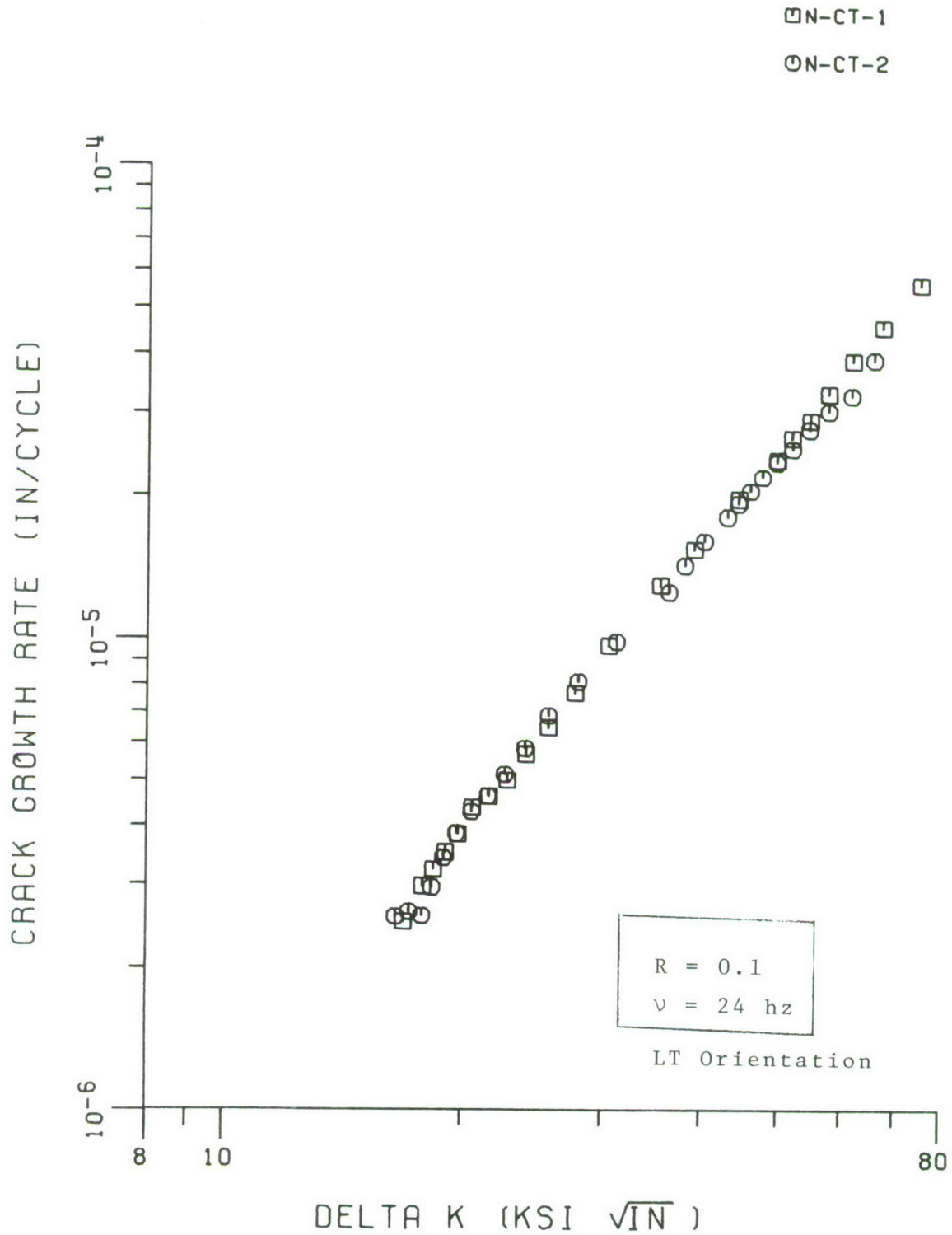


Figure 24

LAB AIR FATIGUE CRACK GROWTH

STEEL HEAT/LOT 0

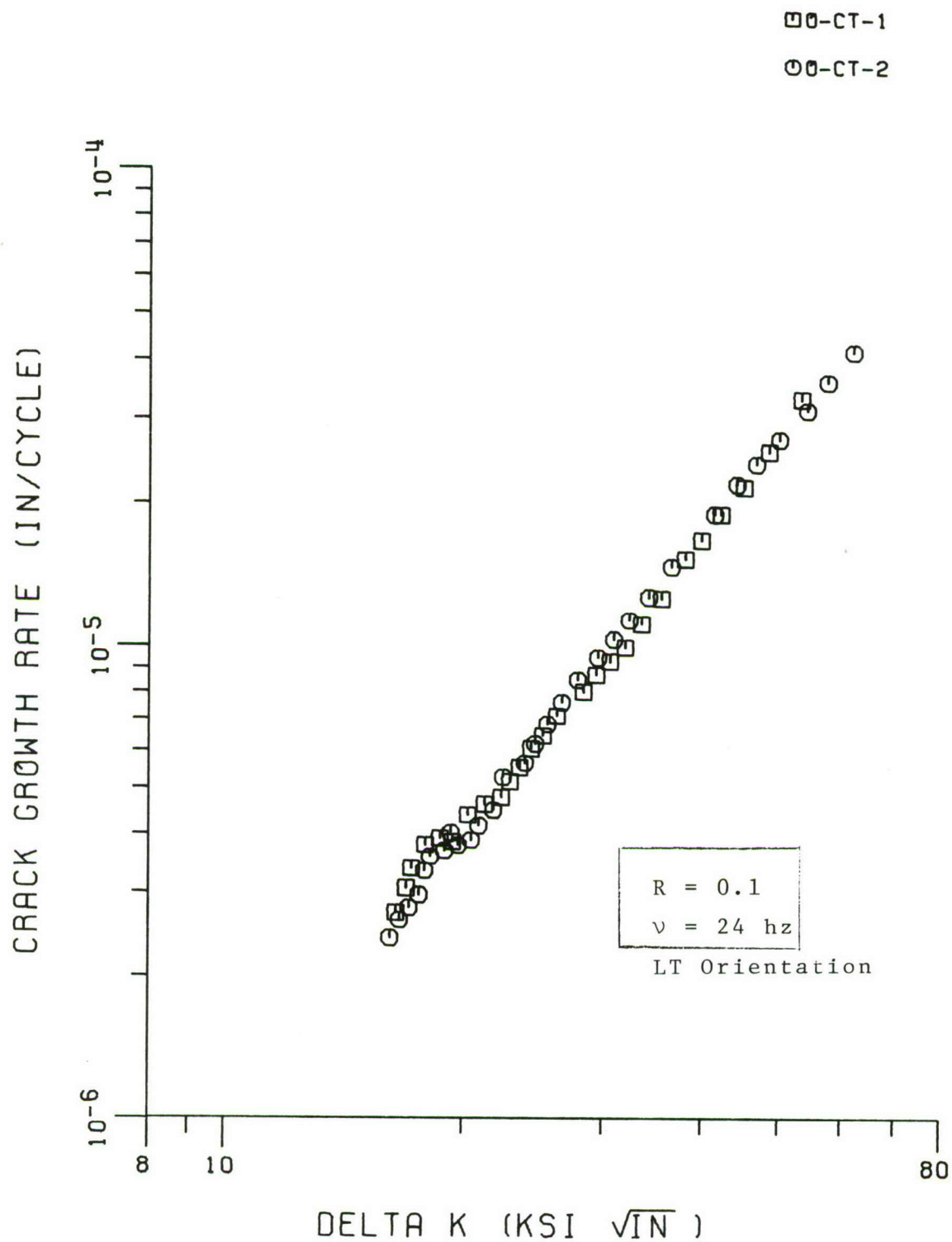


Figure 25

LAB AIR FATIGUE CRACK GROWTH

STEEL HEAT/L0T P

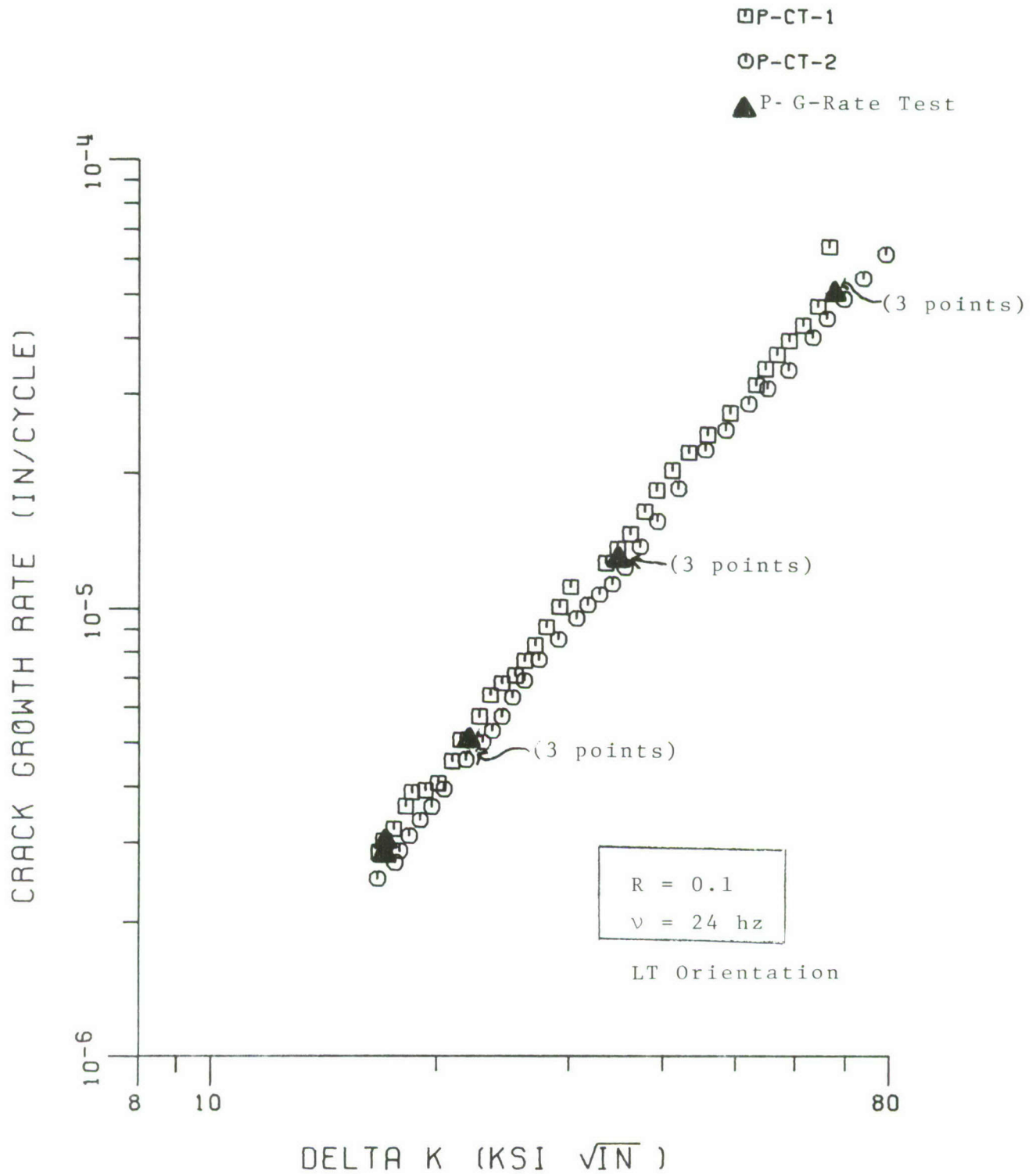


Figure 26

TABLE VII

6Al-4V TI CONS'T ΔK DATAEnvironment: Lab Air; R Factor = .1LT Orientation

<u>Sample No.</u>	$\frac{da}{dN}$ $\times 10^{-6}$ inches/cycle	$\frac{\Delta K}{Ksi\sqrt{in.}}$	<u>Remarks</u>
<u>Heat F*</u>			
4-F-9	5.2	16.2	
4-F-8	14	24.15	
4-F-12	31	32.15	
4-F-10	4.5	15.9	
4-F-13	16	25.0	
4-F-14	15.3	24.15	
4-F-1	30	31.74	
4-F-5	32	31.6	
4-F-11	5	15.4	
4-F-6	3.15	13.45	
<u>Heat H*</u>			
4-H-3	42.7	30.1	
4-H-6	40.4	31.05	
4-H-5	46	32.0	
4-H-1	18.7	24.7	
4-H-2	16.7	24.5	
4-H-9	16.4	23.8	
4-H-4	4.5	13.7	
4-H-7	6.0	13.4	
4-H-8	4.6	15.3	
4-H-11	1.2	10.2	
4-H-13	1.08	8.8	Improper Test
4-H-12	1.53	9.7	
4-H-14	4.1	13.8	

TABLE VII
(Cont)

<u>Sample No.</u>	$\frac{da}{dN}$ $\times 10^{-6}$ inches/cycle	$\frac{\Delta K}{Ksi\sqrt{in.}}$	<u>Remarks</u>
<u>Heat J*</u>			
4-J-1	36.4	31.0	
4-J-3	37.2	30.8	
4-J-5	33.1	32.08	
4-J-2	18.7	25.0	
4-J-6	17.7	24.6	
4-J-4	17.9	25.4	
4-J-7	4.0	17.25	
4-J-11	3.8	17.55	
4-J-13	2.0	9.86	Improper Test
4-J-14	1.8	13.8	Improper Test
4-J-15	0.91	14.0	

*For Metallurgical Definition of Heats F, H, and J
See Table B-III and B-IV

TABLE VIII

PH 13-8 MO STEEL CONS'T ΔK DATAEnvironment: Lab Air; R Factor = .1LT Orientation

<u>Sample No.</u>	<u>da/dN</u> inches/cycle	<u>ΔK</u> (Ksi $\sqrt{\text{in}}$)
<u>Heat P*</u>		
4-P-5	2.75×10^{-6}	17.1
4-P-6	2.99×10^{-6}	17.3
4-P-7	$5.02 \times 10^{-6}^{**}$	16.8**
4-P-2	4.7×10^{-6}	21.1
4-P-3	5.03×10^{-6}	21.1
4-P-4	5.00×10^{-6}	21.1
4-P-8	1.15×10^{-5}	34.3
4-P-11	1.20×10^{-5}	33.3
4-P-12	1.09×10^{-5}	32.8
4-P-1	5.05×10^{-5}	61.0
4-P-9	4.94×10^{-5}	64.2
4-P-10	5.55×10^{-5}	65.0
<u>Heat M*</u>		
4-M-7	2.84×10^{-6}	16.3
4-M-14	2.57×10^{-6}	16.8
4-M-4	5.37×10^{-6}	22.2
4-M-5	4.72×10^{-6}	21.1
4-M-13	4.69×10^{-6}	21.2
4-M-3	8.33×10^{-6}	26.2
4-M-8	2×10^{-5}	35.3
4-M-2	1.77×10^{-5}	34.6
4-M-6	1.38×10^{-5}	33.6
4-M-10	1.02×10^{-5}	33.6
4-M-1	7.58×10^{-5}	65.5
4-M-11	7.52×10^{-5}	68.5
4-M-12	7.74×10^{-5}	67.9

TABLE VIII
(Cont)

<u>Sample No.</u>	<u>da/dN</u> inches/cycle	<u>ΔK</u> (Ksi√in)
<u>Heat L*</u>		
4-L-12	3.14×10^{-6}	17.5
4-L-13	2.6×10^{-6}	17.0
4-L-14	3.27×10^{-6}	16.7
4-L-2	3.82×10^{-6}	22.3
4-L-10	2.91×10^{-6}	21.8
4-L-11	4.5×10^{-6}	21.0
4-L-3	1.05×10^{-5}	32.4
4-L-4	1.07×10^{-5}	32.2
4-L-9	1.00×10^{-5}	31.6
4-L-1	4.79×10^{-5}	63.7
4-L-7	4.34×10^{-5}	61.7
4-L-8	5.16×10^{-5}	68.8
4-L-5	6.04×10^{-6}	26.0

*For Metallurgical Definitions of Heats P, M, and L
See Tables B-V and B-VI.

** Improper Test

by beta annealing in order that it exhibit a large prior beta grain size acicular microstructure whereas Heat K was strictly $\alpha + \beta$ processed and mill annealed to exhibit an equiaxed microstructure. Moreover, it is now generally accepted that lab air da/dN rates at low ΔK and low stress ratio will be significantly lower in materials processed as was Heat J than they would be in metal processed in the manner of Heat K (Ref. 3 & 4). Inspection of the fracture surfaces and microstructure of the compact tension samples labelled Heats J and K provided additional evidence that all four CT samples were from the only beta annealed heat of the five Ti heats employed here. Thus we never did measure the fatigue crack growth rate resistance of Heat K under constant load amplitude conditions.

The Crucible Material Research numbering system was such that there was only one of the Heat J plates that could have actually been K material and mismarked. To check on the true identification of this possibly discrepantly marked plate, a constant ΔK test ($R = 0.1$, LT, $\nu = 24$ cps, lab air) was run with the sample marked as 4-"J"-12. Our G-Rate Test result here was $da/dN = 1.3 \times 10^{-6}$ inches/cycle at $\Delta K = 9.25 \text{ Ksi}\sqrt{\text{in}}$. By contrast, Heat J did not exhibit this crack growth rate until a ΔK of $15.0 \text{ Ksi}\sqrt{\text{in}}$ was attained employing either test technique. The fracture face of 4-"J"-12 was so finely faceted

3. Harrigan, M., M. Kaplan and A. W. Sommer, "Fracture Prevention and Control Symposium," D. Hoepfner, Editor, ASM, Metals Park, Ohio, 1974
4. Yoder, G. R., L. A. Cooley and T.W. Crooker; "A Transition to Enhanced Fatigue Crack Propagation Resistance in a β -annealed Ti 6Al-4V Alloy of Commercial Purity," Boston, Mass; Aug, 1976.

so as to preclude this sample's having been beta annealed. Thus, the G-Rate Test method can be employed to separate rapidly cracking heats from those whose crack growth rate is significantly lower at a common ΔK .

SECTION IV
OTHER APPLICATIONS OF THE
G-RATE TEST

The test sample configuration and procedure developed for fatigue crack propagation quality control purposes also offers advantages for a number of other applications (with appropriate minor modifications). Its attributes include:

- The test provides a quantitative measure of crack growth rate at any stress intensity level.
- The test sample is simple, small and inexpensive.
- The test need not be attended.
- A permanent test record is available.
- The stress intensity and crack growth rate determinations are independent. (Neither depend on a crack length measurement).
- The test is simple to run and the resultant data is easily reduced.
- The test results are highly reproducible.

A number of additional uses have been considered by Del West and some experimentation has been done. In the following

paragraphs we will discuss these applications and cite experimental results where available.

Stress Corrosion Cracking

The most common fracture mechanics test for stress corrosion cracking is some form of the K_{Isc} test. Rate data are sometimes developed, but the difficulty of observing the crack, the need to monitor the crack for long periods of time and the inconsistency of much of the results have mitigated against the generation of rate data. The G-Rate Test eliminates many of the problems associated with stress corrosion cracking rate determination and may prove to be a quite useful tool for examining this complex phenomenon as well.

The general test procedures would be to: precrack the specimen to the constant K region, apply a constant static displacement to the test system, and autographically monitor load versus time. The slope of the load versus time record will yield the crack growth rate.

$$da/dt = \frac{D_2 (C.S.)}{Y_o} \tan \theta \quad (13)$$

$$K = D_1 P_o$$

Y_0 and P_0 are calculated in a manner similar to that for the precracked fatigue crack growth test. If the crack growth rate is transient, θ will vary with time and we will not be measuring the slope of a straight line. This causes some loss in precision, but obviously even direct measurements of the crack length would have the same problem. The ability to monitor the crack growth automatically, the fact that the average crack growth across the whole specimen (not simply the surface) is measured and, of course, the fact that K is constant make the measurement of the crack growth rate, whether constant or transient reasonably convenient and meaningful.

As an example of the utility of the G-Rate Test for stress corrosion cracking, we have conducted a series of tests on A/F 1410 steel. The material used for this brief study was supplied by Rockwell International B-1 Division and is described in Table IX. The test program has provided crack growth rate data as a function of stress intensity level and time for A/F 1410 in 3.5% NaCl solution.

The stress corrosion cracking test procedure followed is listed below:

1. Choose a particular stress intensity K for each specimen.
2. Precrack the specimen in 3.5% NaCl at $K_{\max} = K$, stress ratio = .1.
3. Apply and maintain the appropriate static displacement

TABLE IX

MATERIAL DESCRIPTION OF A/F 1410

Product - 2" thick rolled plate

Producer - Universal Cyclops Corp.

Heat No. - L 3550K20

Heat Treat Condition

- (1) Austenitize 1650°F/1 hr. + W. Q.
- (2) Austenitize 1500°F/1 hr. + W. Q.
- (3) Age 950°F/5 hrs/a.c.

	σ_{yield} (Ksi)	σ_{ultimate} (Ksi)	R/A %	E %	K_{Ic} (Ksi $\sqrt{\text{in}}$)
Long	228	248	70	16	131.3 - 147.8
Transverse	228	248	70	16	131.4 - 141.9

to cause the stress intensity K to be applied to the specimen.

4. Monitor (i.e., permanently record) load versus time.
5. Break the specimen and observe the fracture faces.
6. Measure the crack length change (Δa) and check that the load implied total Δa is the same.
7. Reduce the load versus time data to crack length and crack growth rate versus time.

Since dP/da is a constant, the resultant load versus time plot is, except for a scale factor and an inversion, a plot of crack length versus time at constant K . This is shown schematically in Figure 27. Since test times and chart paper used were extensive, actual data outputs of load versus time are not presented here. Instead in Figure 28, we have presented a plot of indicated change in crack length versus time for results of tests at 4 intensity levels. This, as shown in Figure 27, is equivalent to an inverted, compressed version of the actual load versus time plots. In Figures 29 and 30 we have shown the crack growth rate as a function of total crack growth and time since growth began.

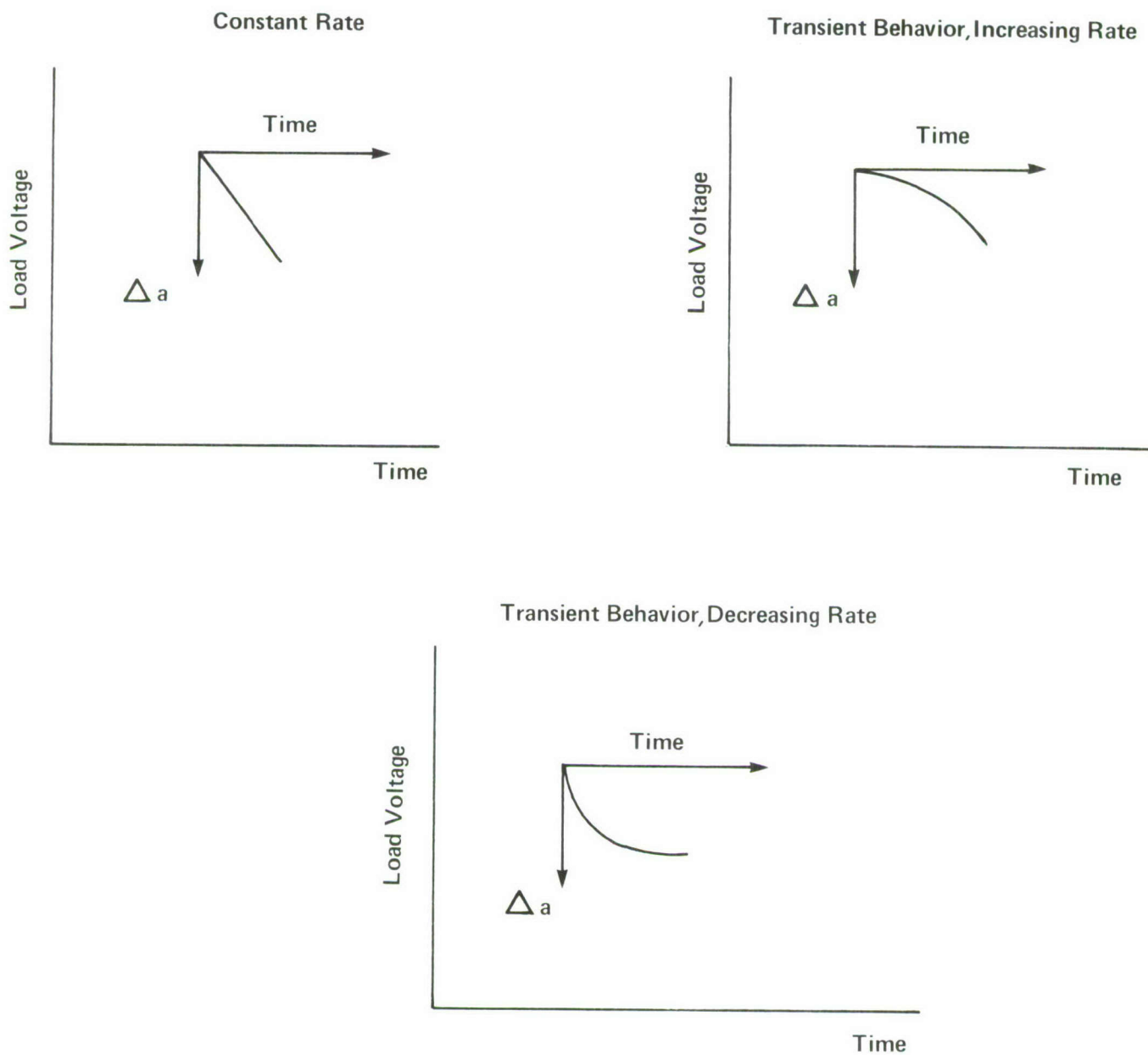


FIGURE 27
Equivalence Of Load Versus Time And Crack Length Versus Time

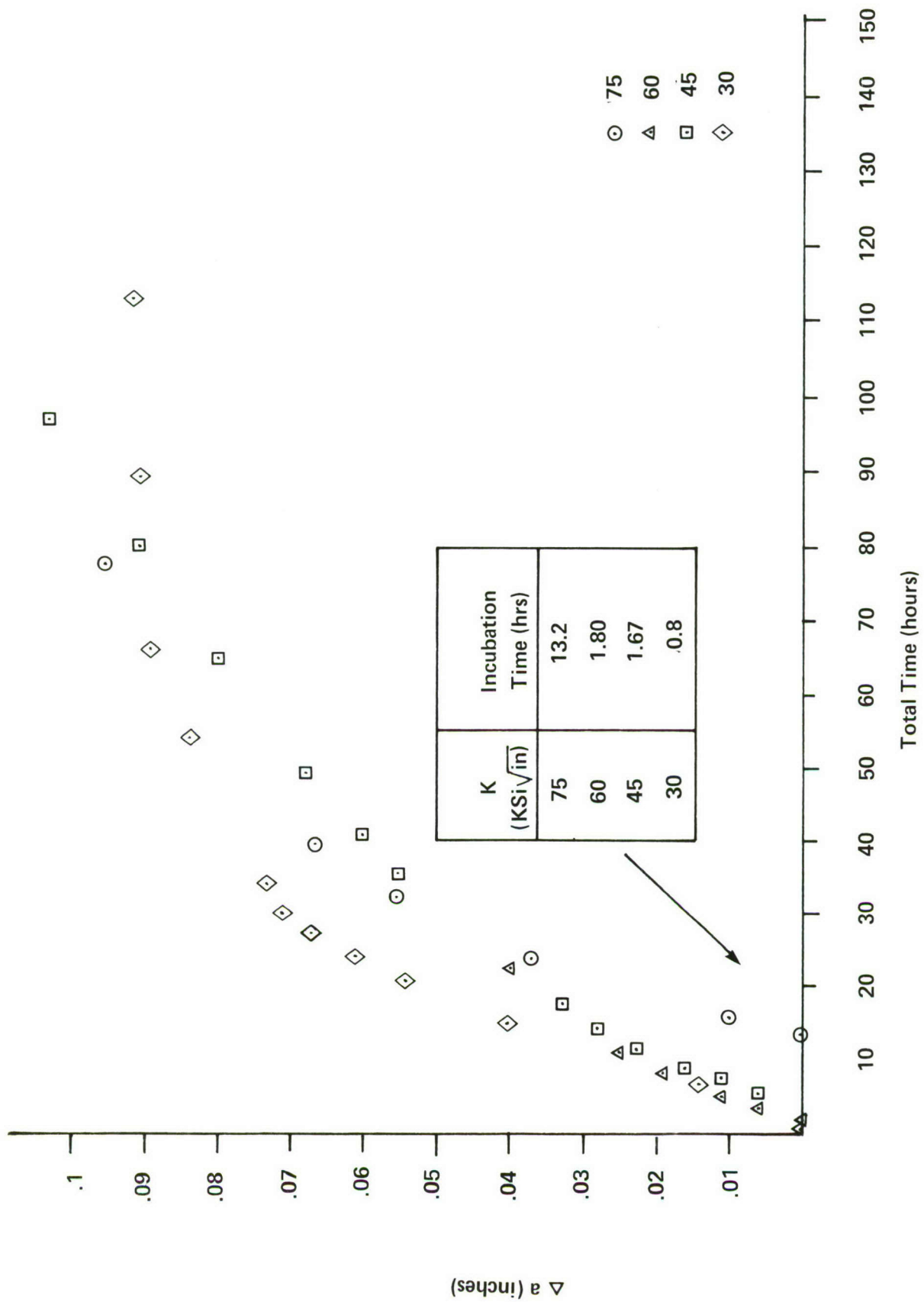


FIGURE 28
Stress Corrosion Cracking – AF1410 in NaCl solution

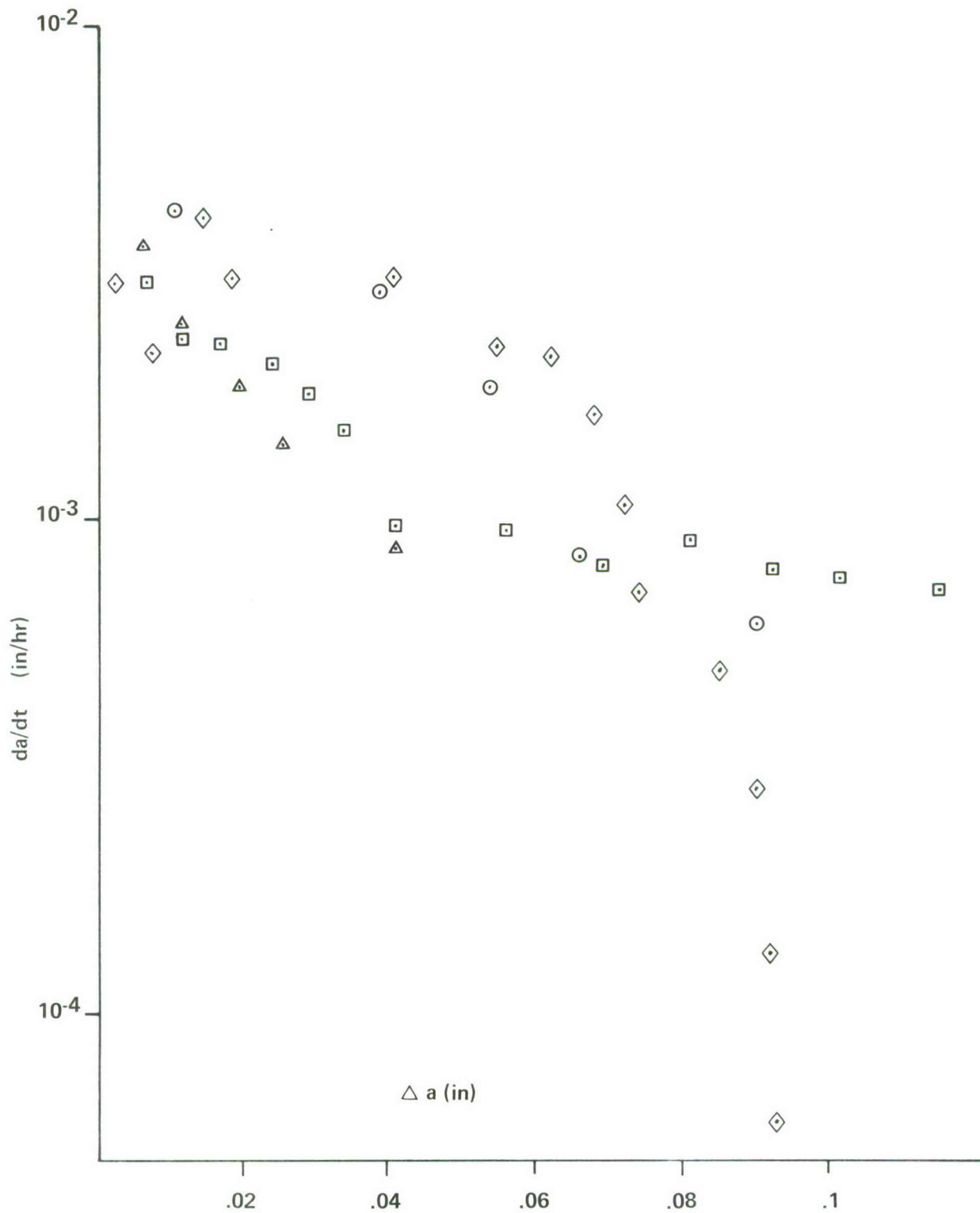


FIGURE 29

Crack Growth Rate of AF1410 in 3.5% NaCl Versus Distance Grown

Constant K Level

△ K=60

○ K=75

□ K=45

◇ K=30

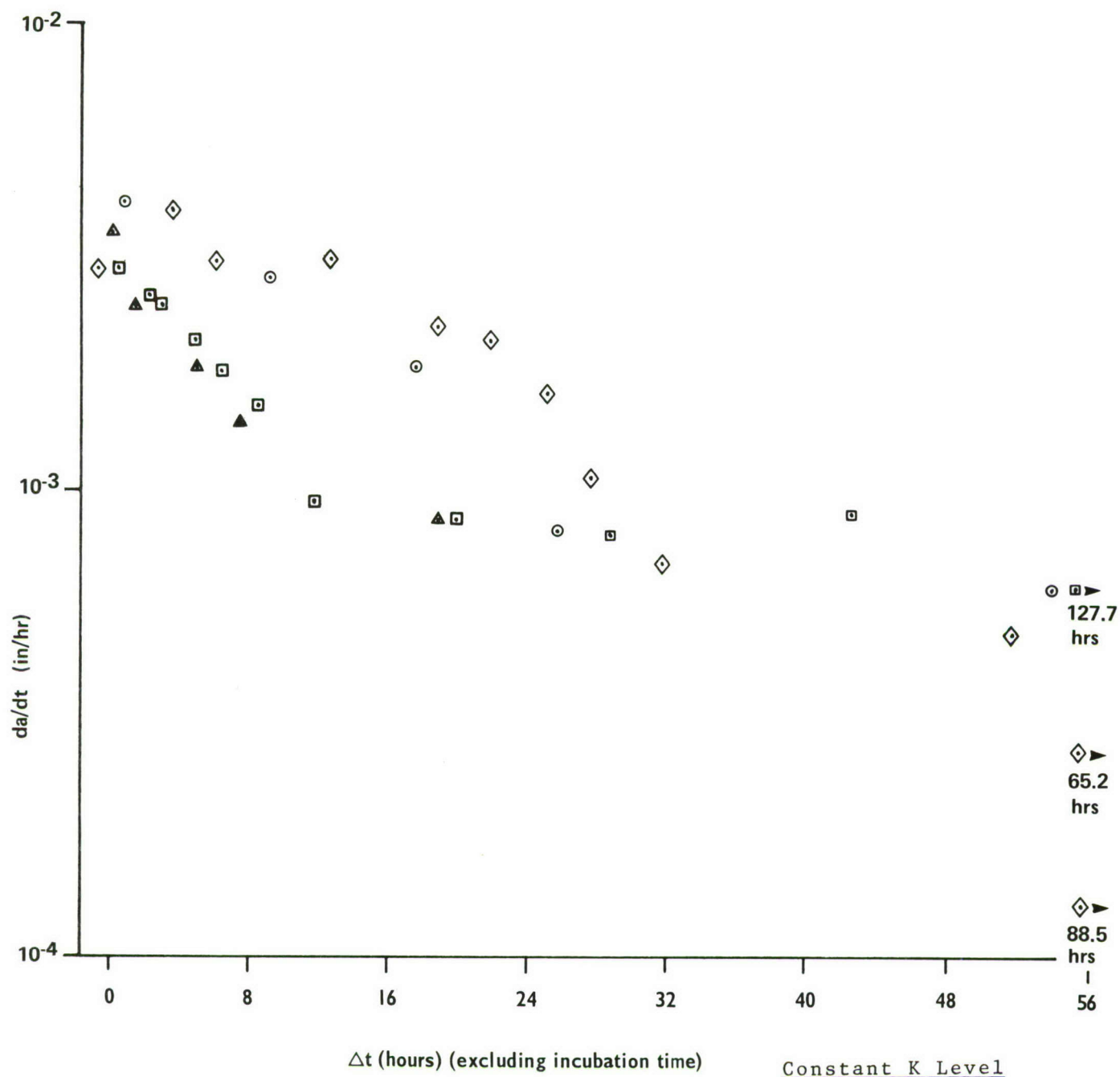


FIGURE 30
Crack Growth Rate of AF1410 in 3.5% NaCl Versus Time

- K=75
- ▲ K=60
- K=45
- ◇ K=30

The Table inserted in Figure 28 shows the values of the intersection of each curve with the abscissa. A number of interesting observations can be made from the AF 1410 steel data displayed in these Figures.

- a) The incubation time (i.e., the time it takes for growth to begin after the static load application) increases with increasing K.
- b) In all cases tested (i.e., K from 30 to 75) the crack growth jumps discontinuously from 0 to a high rate and then decreases.
- c) For K from 45 to 75 the crack growth rate does not continue to decrease unceasingly but stabilizes and appears to reach a steady state.
- d) The steady state crack growth rate for K from 45 to 75 is independent of K and approximately equal to 6×10^{-4} in/hr.
- e) At a K of 30 the crack growth rate continues to decrease with time. There is no indication of attaining a steady state rate other than zero. The minimum crack growth rate measured was 6×10^{-5} in/hr after 120 hours.
- f) The total damage accumulated for each specimen after 20 to 70 hours was roughly equal for all K levels tested (30 to 75 Ksi $\sqrt{\text{in.}}$.)
- g) The damage accumulated for time periods after 70 hours would be the same for K from 45 to 75 but would be negligible for a K of 30.

- h) For time periods less than 20 hours, incubation times play an important role and because of this an applied K of 30 could cause significantly more damage accumulation than a K of 75 in this time range.

In Figure 31 we have plotted the results of one additional experiment. Here we have taken a specimen loaded at a K of 45 for 140 hours and suddenly increased the load to a K of 60. We note that:

- a) The incubation time is reduced compared to the original K = 60 test.
- b) Similarly the transient behavior is less pronounced.
- c) The same steady state rate as in the original K = 60 test is reached.

The above description of a limited test program shows that the G - Rate Test can be used effectively to extract a great deal of information about the stress corrosion cracking process that is not available from a conventional K_{Iscc} test.

Fatigue Crack Growth Rate Retardation Studies

The G-Rate Test, primarily because it is a constant K test, may prove quite useful for retardation studies. The facts that measurement of load reduction is more accurate than crack length measurement and the average crack growth (not simply the surface growth) is monitored, make the G-Rate Test attractive for

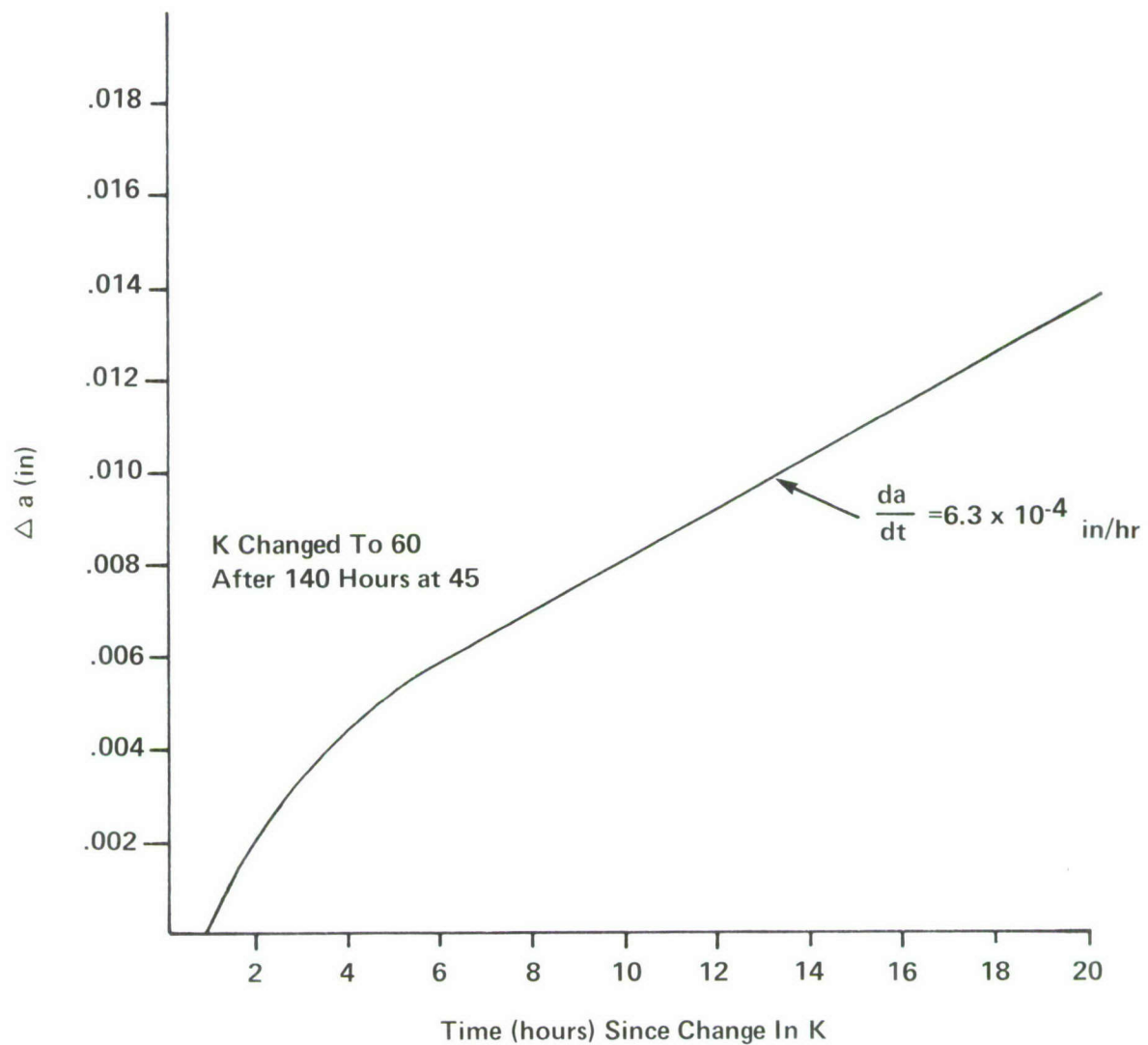


FIGURE 31
Stress Corrosion of AF1410 With Step Loading

this purpose. As a simple example of the potential offered by this approach, we present a result obtained with a 7000 series aluminum alloy in Figures 32 and 33. Figure 32 shows the actual load versus cycle plot generated before and after 1.8 factor overload in 7475-T7351. Figure 33 is simply an inversion and scaling of Figure 32 and is a plot of crack length versus cycles. The constancy in K and the ease of the crack length (via the load) measurement make crack details after the overload readily apparent.

Low Frequency/Low Crack Growth Rate Studies

The inexpensive test machine used and the fact that the test may be monitored autographically make the G-Rate Test ideal for long time fatigue crack growth studies. For low frequency tests it is not necessary to modify the cyclic load signal; the signal can be fed directly into a strip chart recorder. Del West has not conducted low frequency low rate studies using this method but we have conducted low frequency (.2Hz) moderate rate tests in Ti-6Al-4V in 3.5% NaCl. A typical test record is shown in Figure 34. As can be seen the slope of the peak load versus cycles plot has an extensive constant region which is readily established.

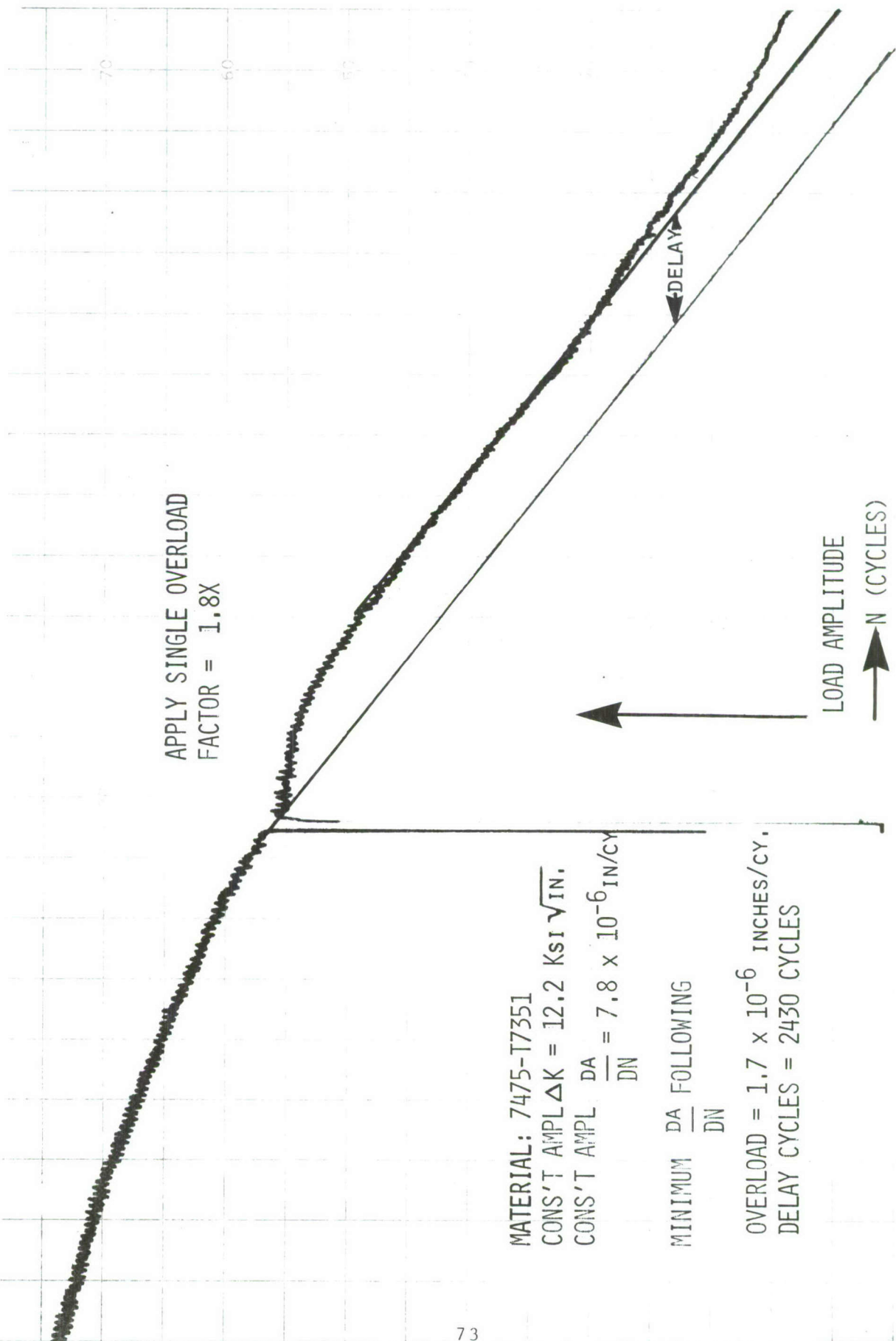


FIGURE 32
Fatigue Crack Growth Retardation Load Record

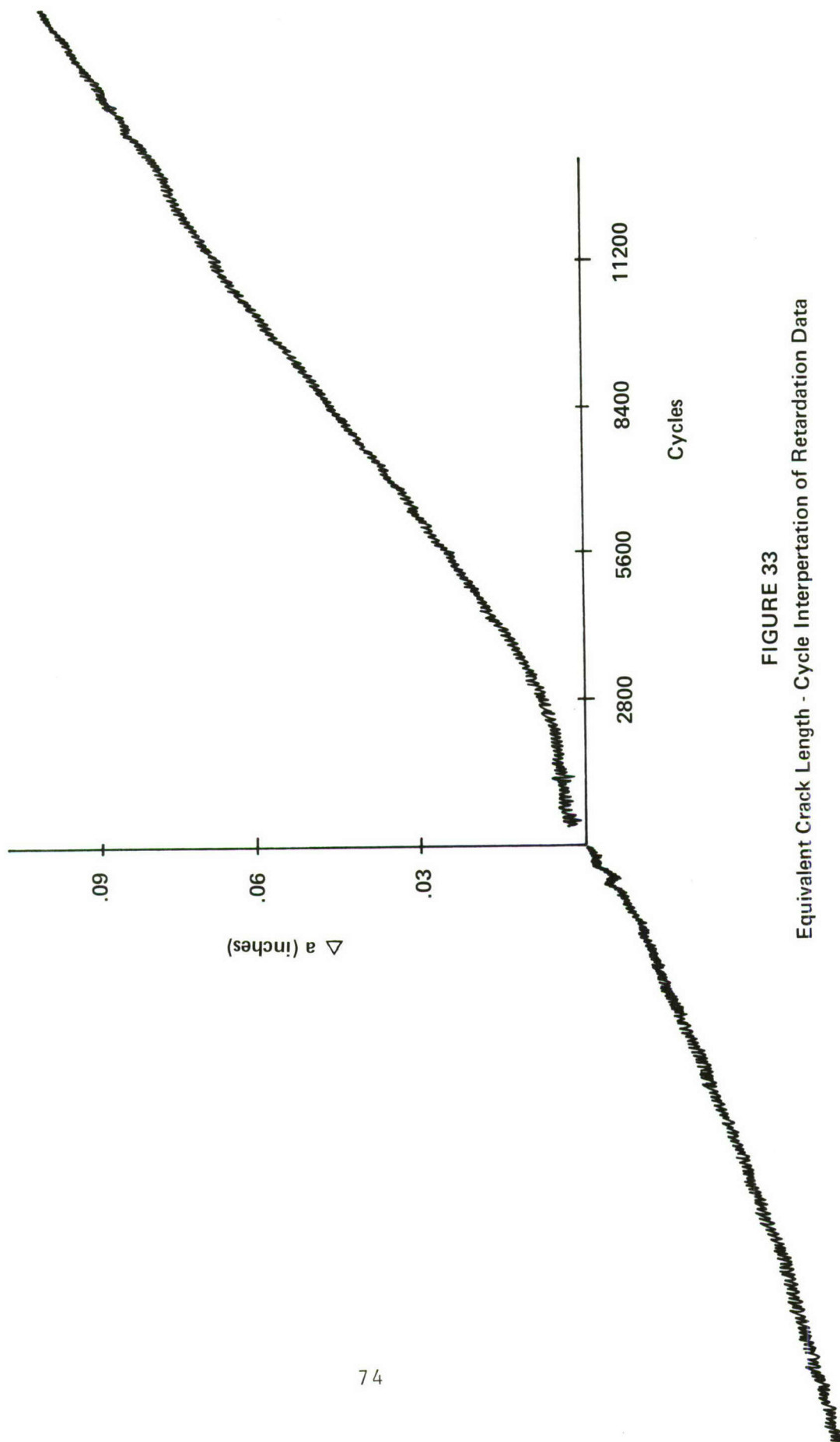


FIGURE 33
Equivalent Crack Length - Cycle Interpretation of Retardation Data

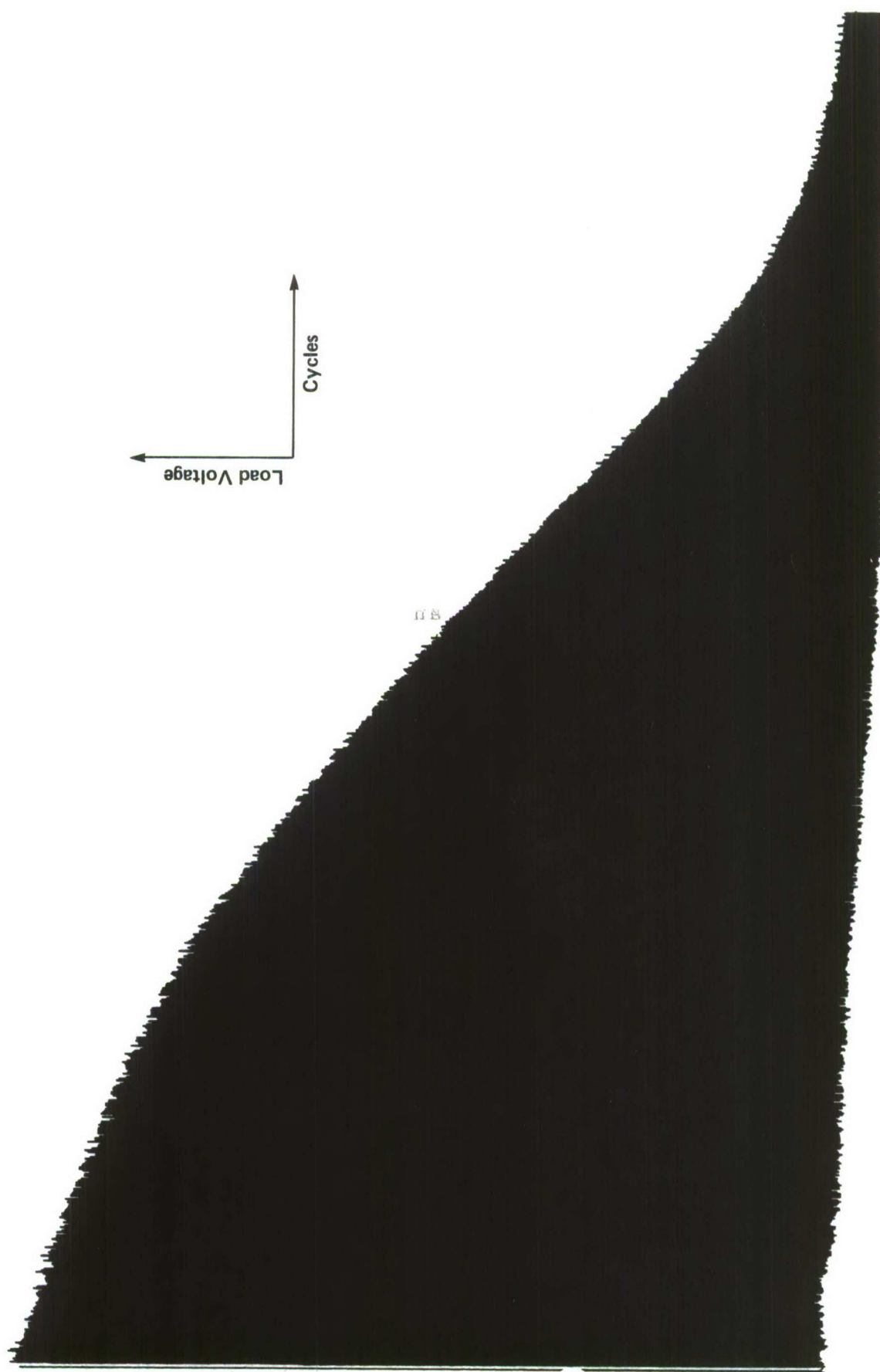


FIGURE 34
Low Frequency Crack Growth Rate Test

Investigation of Effects of Variables Other than ΔK

For the development of design data, that is da/dN versus ΔK , a specimen in which the stress intensity varies with crack length such as the compact specimen is appropriate. There, with a single test (plus replications), wide ranges of rate data can be developed. The only exception to this might be low frequency/low crack growth rate data where it would be cost effective to use the G-Rate Test at a number of stress intensity levels to establish a crack growth rate curve. However, for investigating variables other than stress intensity, the G-Rate Test is more efficient than a test such as the compact specimen test. Within the context of other programs we have used the G-Rate Test to investigate the effects of stress ratio, alloy chemistry, heat treatment, chemical environment, temperature, and frequency.

Statistical Variations in Crack Growth Rate

Although we have not attempted to develop any statistical information on crack growth rate it appears to us that for the first time a viable method of accomplishing this is available. The G-Rate Test eliminates many of the difficulties of using compact specimen data for statistical evaluation. Not the least of these is cost. Although the compact specimen can be used to generate a number of crack growth rate data points none of them are independent. Thus each compact specimen test has to be considered a single test. Alternative schemes may be possible (certain assumptions about dependence could be made) but in general the use of only a single point in the compact specimen in a statistical evaluation makes it prohibitively expensive to generate sufficient data to be useful for statistical evaluations. Additionally, the quantities measured in the compact specimen test are crack lengths and a scheme for differentiation must be established and accounted for in the statistical evaluation. Also the specific values of stress intensity for which the crack growth rate is established in one specimen will usually differ from that in another specimen and therefore some interpretation scheme to compare crack growth rates at common stress intensities would have to be used. Lastly we note that both the crack growth rate and stress intensity evaluation depend on the measurement of the crack length, thus errors in crack length

determined simultaneously affect dependent and independent variables (crack growth rate and stress intensity).

This coupling is not present in the G-Rate Test. A single specific ΔK and R can be chosen and each specimen can be tested at those input values. The crack growth rate is evaluated directly. No differentiation and no interpolation is required. Errors in the setting of ΔK and R are totally independent of the measurement of the crack growth rate. Above and beyond these advantages is, of course, the fact that the low cost of the G-Rate Test allows sufficient data for useful statistical information to be established economically.

SECTION V

SUMMARY

The test developed is an inexpensive reliable fatigue crack growth rate test that supplies the fatigue crack growth rate at a specific stress intensity level. The G-Rate Test has been shown to have potential as a quality control test for fatigue crack propagation and to have many other potential uses as well. It will not replace the compact specimen test for developing design data but can certainly be used to augment it.

APPENDIX A
ANALYSIS OF A REMOTE DISPLACEMENT
CONTROLLED CONSTANT K SPECIMEN

Consider the configuration shown in Figure 1, where a three point bend specimen with $S/B = 8$ is loaded by a controlled remote displacement. By remote we mean that interspersed in series with the test specimen is a compliant element. This compliant element could be a helical spring or another bend bar or the test system or any combination of these. In the ensuing discussion the specimen displacements, loads, compliance, etc. will be designated by the subscript 1. The physical quantities associated with the "spring" will be designated by the subscript 2. The controlling displacement Δ , and resulting load, P , will not be subscripted.

Since the spring and specimen are in series

$$\Delta = \Delta_1 + \Delta_2 \quad \text{A-1}$$

$$P = P_1 = P_2 \quad \text{A-2}$$

Also

$$\Delta_1 = C_1 P \quad \text{A-3}$$

$$\Delta_2 = C_2 P \quad \text{A-4}$$

where C_1 and C_2 are compliances and C_1 is a function of "a" the crack depth. Combining these equations gives

$$P = \Delta / (C_1 + C_2) \quad \text{A-5}$$

For the $S/W = 8$ three point bend specimen

$$K = 12P/Wt \sqrt{\pi a} F(a/W) \quad A-6$$

where*

$$F(a/W) = 1.107 - 1.552 (a/W) + 7.71 (a/W)^2 - 13.55 (a/W)^3 + 14.25 (a/W)^4 \quad A-7$$

This expression for $F(a/W)$ is thought to be within .2% for $a/W \leq .6$.

The compliance $C_1(a)$ can be generated using displacement equations given by Tada (Ref. A-1). Tada notes that the displacement relations for the $S/b = 8$ specimen are nearly the average of the $S/b = 4$ specimen expressions and the pure bending expressions. Using this and his expressions for the pure bending specimen and the $S/b = 4$ specimen we have

$$\Delta_{1 \text{ crack}} = 96P/Et V(a/W)$$

$$V\left(\frac{a}{W}\right) = \frac{1}{2} \left(\frac{a/W}{1-a/W} \right)^2 \left[11.51 - 39.26 \left(\frac{a}{W} \right) + 73.96 \left(\frac{a}{W} \right)^2 - 70.78 \left(\frac{a}{W} \right)^3 + 25.89 \left(\frac{a}{W} \right)^4 \right]^4 * \quad A-8$$

where $\Delta_{1 \text{ crack}}$ is the additional displacement due to the presence of the crack.

For a three point bend specimen, simple beam theory gives the displacement with no crack present as

$$\Delta_{1 \text{ no crack}} = 128P/Et \quad A-9$$

*Modified to correct typographical error in Ref. A-1

A-1 Tada, H. "The Stress Analysis of Cracks Handbook,"
Del Research Corporation, 1973

Thus

$$C_1(a) = 1/Et (128 + 96V(a/W)) \quad A-10$$

and

$$P = \Delta Et \left(C_2 + \frac{1}{(128 + 96V(a/W))} \right) \quad A-11$$

Equations A-6 and A-11 are the necessary relations to perform load/displacement/stress intensity analysis of the configuration of Figure 1. A series of numerical analysis were conducted in which load/displacement/stress intensity parameters as a function of crack length were evaluated for various values of the normalized compliance C_2Et . Results for four values of C_2Et are given in Tables A-I a, b, c, and d. Similar results for a test specimen with $S/W = 4$ are presented in Table A-II.

Although the maximum stress intensity factor is not always at $a = .25$, the second column which gives the ratio of K at each "a" to the K at $a = .25$ presents a picture of the variation in K occurring in the midrange of the three point bend specimen. Table A-Id ($C_2Et = .1$) presents results for what is essentially a direct displacement controlled test.

TABLE A-Ia
ANALYSIS OF REMOTE DISPLACEMENT CONTROLLED

THREE POINT BEND SPECIMEN

(S/W = 8, W = 1/2, C₂Et = 50)

a	$\frac{K(a)}{K(.25)}$	$\frac{K}{E\Delta}$	$\frac{K}{P}(t=.25)$	$\frac{K}{E\Delta}$
5.000E-02	5.613E-01	5.289E-02	3.869E+01	1.367E-03
5.500E-02	5.838E-01	5.501E-02	4.046E+01	1.360E-03
6.000E-02	6.050E-01	5.700E-02	4.216E+01	1.352E-03
6.500E-02	6.249E-01	5.889E-02	4.382E+01	1.344E-03
7.000E-02	6.439E-01	6.067E-02	4.544E+01	1.335E-03
7.500E-02	6.619E-01	6.237E-02	4.704E+01	1.326E-03
8.000E-02	6.792E-01	6.400E-02	4.862E+01	1.316E-03
8.500E-02	6.958E-01	6.556E-02	5.019E+01	1.306E-03
9.000E-02	7.117E-01	6.706E-02	5.175E+01	1.296E-03
9.500E-02	7.270E-01	6.850E-02	5.331E+01	1.285E-03
1.000E-01	7.418E-01	6.989E-02	5.487E+01	1.274E-03
1.050E-01	7.561E-01	7.124E-02	5.645E+01	1.262E-03
1.100E-01	7.699E-01	7.254E-02	5.803E+01	1.250E-03
1.150E-01	7.832E-01	7.380E-02	5.963E+01	1.238E-03
1.200E-01	7.961E-01	7.501E-02	6.125E+01	1.225E-03
1.250E-01	8.086E-01	7.619E-02	6.289E+01	1.212E-03
1.300E-01	8.207E-01	7.733E-02	6.455E+01	1.198E-03
1.350E-01	8.325E-01	7.844E-02	6.624E+01	1.184E-03
1.400E-01	8.438E-01	7.951E-02	6.797E+01	1.170E-03
1.450E-01	8.548E-01	8.054E-02	6.973E+01	1.155E-03
1.500E-01	8.654E-01	8.154E-02	7.153E+01	1.140E-03
1.550E-01	8.756E-01	8.250E-02	7.338E+01	1.124E-03
1.600E-01	8.855E-01	8.343E-02	7.527E+01	1.108E-03
1.650E-01	8.950E-01	8.433E-02	7.722E+01	1.092E-03
1.700E-01	9.042E-01	8.519E-02	7.922E+01	1.075E-03
1.750E-01	9.130E-01	8.602E-02	8.128E+01	1.058E-03
1.800E-01	9.214E-01	8.682E-02	8.341E+01	1.041E-03
1.850E-01	9.295E-01	8.758E-02	8.561E+01	1.023E-03
1.900E-01	9.372E-01	8.831E-02	8.789E+01	1.005E-03
1.950E-01	9.446E-01	8.900E-02	9.025E+01	9.862E-04
2.000E-01	9.515E-01	8.966E-02	9.270E+01	9.672E-04
2.050E-01	9.582E-01	9.028E-02	9.525E+01	9.479E-04
2.100E-01	9.644E-01	9.087E-02	9.790E+01	9.282E-04
2.150E-01	9.703E-01	9.143E-02	1.007E+02	9.082E-04
2.200E-01	9.758E-01	9.194E-02	1.036E+02	8.879E-04
2.250E-01	9.809E-01	9.242E-02	1.066E+02	8.672E-04
2.300E-01	9.856E-01	9.286E-02	1.097E+02	8.464E-04
2.350E-01	9.898E-01	9.327E-02	1.130E+02	8.252E-04
2.400E-01	9.937E-01	9.363E-02	1.165E+02	8.038E-04
2.450E-01	9.971E-01	9.395E-02	1.201E+02	7.822E-04
2.500E-01	1.000E+00	9.422E-02	1.239E+02	7.605E-04
2.550E-01	1.002E+00	9.446E-02	1.279E+02	7.385E-04
2.600E-01	1.004E+00	9.464E-02	1.321E+02	7.165E-04
2.650E-01	1.006E+00	9.477E-02	1.365E+02	6.943E-04
2.700E-01	1.007E+00	9.486E-02	1.411E+02	6.721E-04
2.750E-01	1.007E+00	9.488E-02	1.460E+02	6.498E-04
2.800E-01	1.007E+00	9.485E-02	1.511E+02	6.276E-04
2.850E-01	1.006E+00	9.476E-02	1.565E+02	6.053E-04
2.900E-01	1.004E+00	9.460E-02	1.622E+02	5.831E-04
2.950E-01	1.002E+00	9.437E-02	1.682E+02	5.610E-04
3.000E-01	9.983E-01	9.407E-02	1.745E+02	5.390E-04

TABLE A-1b
ANALYSIS OF REMOTE DISPLACEMENT CONTROLLED
THREE POINT BEND SPECIMEN
(S/W = 8, W = 1/2, C₂Et = 20)

a	$\frac{K(a)}{K(.25)}$	$\frac{K}{E\Delta}$	$\frac{K}{P} (t=.25)$	$\frac{K}{E\Delta}$
5.000E-02	6.102E-01	6.327E-02	3.869E+01	1.635E-03
5.500E-02	6.340E-01	6.574E-02	4.046E+01	1.625E-03
6.000E-02	6.562E-01	6.804E-02	4.216E+01	1.614E-03
6.500E-02	6.771E-01	7.020E-02	4.382E+01	1.602E-03
7.000E-02	6.967E-01	7.224E-02	4.544E+01	1.590E-03
7.500E-02	7.153E-01	7.417E-02	4.704E+01	1.577E-03
8.000E-02	7.330E-01	7.600E-02	4.862E+01	1.563E-03
8.500E-02	7.498E-01	7.774E-02	5.019E+01	1.549E-03
9.000E-02	7.658E-01	7.940E-02	5.175E+01	1.534E-03
9.500E-02	7.811E-01	8.099E-02	5.331E+01	1.519E-03
1.000E-01	7.957E-01	8.250E-02	5.487E+01	1.504E-03
1.050E-01	8.097E-01	8.395E-02	5.645E+01	1.487E-03
1.100E-01	8.231E-01	8.534E-02	5.803E+01	1.471E-03
1.150E-01	8.359E-01	8.667E-02	5.963E+01	1.453E-03
1.200E-01	8.481E-01	8.794E-02	6.125E+01	1.436E-03
1.250E-01	8.599E-01	8.916E-02	6.289E+01	1.418E-03
1.300E-01	8.711E-01	9.032E-02	6.455E+01	1.399E-03
1.350E-01	8.818E-01	9.143E-02	6.624E+01	1.380E-03
1.400E-01	8.920E-01	9.249E-02	6.797E+01	1.361E-03
1.450E-01	9.018E-01	9.350E-02	6.973E+01	1.341E-03
1.500E-01	9.110E-01	9.446E-02	7.153E+01	1.320E-03
1.550E-01	9.198E-01	9.537E-02	7.338E+01	1.300E-03
1.600E-01	9.281E-01	9.623E-02	7.527E+01	1.279E-03
1.650E-01	9.360E-01	9.705E-02	7.722E+01	1.257E-03
1.700E-01	9.434E-01	9.782E-02	7.922E+01	1.235E-03
1.750E-01	9.503E-01	9.854E-02	8.128E+01	1.212E-03
1.800E-01	9.568E-01	9.921E-02	8.341E+01	1.189E-03
1.850E-01	9.629E-01	9.984E-02	8.561E+01	1.166E-03
1.900E-01	9.684E-01	1.004E-01	8.789E+01	1.143E-03
1.950E-01	9.736E-01	1.009E-01	9.025E+01	1.119E-03
2.000E-01	9.783E-01	1.014E-01	9.270E+01	1.094E-03
2.050E-01	9.825E-01	1.019E-01	9.525E+01	1.070E-03
2.100E-01	9.863E-01	1.023E-01	9.790E+01	1.045E-03
2.150E-01	9.896E-01	1.026E-01	1.007E+02	1.019E-03
2.200E-01	9.925E-01	1.029E-01	1.036E+02	9.937E-04
2.250E-01	9.949E-01	1.032E-01	1.066E+02	9.680E-04
2.300E-01	9.969E-01	1.034E-01	1.097E+02	9.420E-04
2.350E-01	9.984E-01	1.035E-01	1.130E+02	9.159E-04
2.400E-01	9.994E-01	1.036E-01	1.165E+02	8.896E-04
2.450E-01	9.999E-01	1.037E-01	1.201E+02	8.633E-04
2.500E-01	1.000E+00	1.037E-01	1.239E+02	8.368E-04
2.550E-01	9.996E-01	1.036E-01	1.279E+02	8.103E-04
2.600E-01	9.986E-01	1.035E-01	1.321E+02	7.839E-04
2.650E-01	9.971E-01	1.034E-01	1.365E+02	7.574E-04
2.700E-01	9.951E-01	1.032E-01	1.411E+02	7.310E-04
2.750E-01	9.925E-01	1.029E-01	1.460E+02	7.048E-04
2.800E-01	9.893E-01	1.026E-01	1.511E+02	6.787E-04
2.850E-01	9.855E-01	1.022E-01	1.565E+02	6.527E-04
2.900E-01	9.810E-01	1.017E-01	1.622E+02	6.270E-04
2.950E-01	9.759E-01	1.012E-01	1.682E+02	6.015E-04
3.000E-01	9.700E-01	1.006E-01	1.745E+02	5.763E-04

TABLE A-Ic
ANALYSIS OF REMOTE DISPLACEMENT CONTROLLED
THREE POINT BEND SPECIMEN
(S/W = 8, W = 1/2, C₂Et = 10)

a	$\frac{K(a)}{K(.25)}$	$\frac{K}{E\Delta}$	$\frac{K}{P}(t=.25)$	$\frac{P}{E\Delta}$
5.000E-02	6.311E-01	6.770E-02	3.869E+01	1.750E-03
5.500E-02	6.554E-01	7.031E-02	4.046E+01	1.738E-03
6.000E-02	6.780E-01	7.273E-02	4.216E+01	1.725E-03
6.500E-02	6.992E-01	7.501E-02	4.382E+01	1.712E-03
7.000E-02	7.191E-01	7.715E-02	4.544E+01	1.698E-03
7.500E-02	7.379E-01	7.916E-02	4.704E+01	1.683E-03
8.000E-02	7.557E-01	8.107E-02	4.862E+01	1.667E-03
8.500E-02	7.726E-01	8.288E-02	5.019E+01	1.651E-03
9.000E-02	7.886E-01	8.460E-02	5.175E+01	1.635E-03
9.500E-02	8.038E-01	8.623E-02	5.331E+01	1.618E-03
1.000E-01	8.183E-01	8.778E-02	5.487E+01	1.600E-03
1.050E-01	8.321E-01	8.926E-02	5.645E+01	1.581E-03
1.100E-01	8.452E-01	9.067E-02	5.803E+01	1.563E-03
1.150E-01	8.578E-01	9.202E-02	5.963E+01	1.543E-03
1.200E-01	8.697E-01	9.330E-02	6.125E+01	1.523E-03
1.250E-01	8.811E-01	9.452E-02	6.289E+01	1.503E-03
1.300E-01	8.918E-01	9.567E-02	6.455E+01	1.482E-03
1.350E-01	9.021E-01	9.677E-02	6.624E+01	1.461E-03
1.400E-01	9.118E-01	9.781E-02	6.797E+01	1.439E-03
1.450E-01	9.210E-01	9.880E-02	6.973E+01	1.417E-03
1.500E-01	9.296E-01	9.973E-02	7.153E+01	1.394E-03
1.550E-01	9.378E-01	1.006E-01	7.338E+01	1.371E-03
1.600E-01	9.454E-01	1.014E-01	7.527E+01	1.347E-03
1.650E-01	9.526E-01	1.022E-01	7.722E+01	1.323E-03
1.700E-01	9.592E-01	1.029E-01	7.922E+01	1.299E-03
1.750E-01	9.653E-01	1.036E-01	8.128E+01	1.274E-03
1.800E-01	9.710E-01	1.042E-01	8.341E+01	1.249E-03
1.850E-01	9.762E-01	1.047E-01	8.561E+01	1.223E-03
1.900E-01	9.808E-01	1.052E-01	8.789E+01	1.197E-03
1.950E-01	9.851E-01	1.057E-01	9.025E+01	1.171E-03
2.000E-01	9.888E-01	1.061E-01	9.270E+01	1.144E-03
2.050E-01	9.920E-01	1.064E-01	9.525E+01	1.117E-03
2.100E-01	9.948E-01	1.067E-01	9.790E+01	1.090E-03
2.150E-01	9.971E-01	1.070E-01	1.007E+02	1.063E-03
2.200E-01	9.990E-01	1.072E-01	1.036E+02	1.035E-03
2.250E-01	1.000E+00	1.073E-01	1.066E+02	1.007E-03
2.300E-01	1.001E+00	1.074E-01	1.097E+02	9.789E-04
2.350E-01	1.002E+00	1.075E-01	1.130E+02	9.507E-04
2.400E-01	1.002E+00	1.074E-01	1.165E+02	9.225E-04
2.450E-01	1.001E+00	1.074E-01	1.201E+02	8.941E-04
2.500E-01	1.000E+00	1.073E-01	1.239E+02	8.658E-04
2.550E-01	9.985E-01	1.071E-01	1.279E+02	8.375E-04
2.600E-01	9.964E-01	1.069E-01	1.321E+02	8.092E-04
2.650E-01	9.939E-01	1.066E-01	1.365E+02	7.811E-04
2.700E-01	9.907E-01	1.063E-01	1.411E+02	7.531E-04
2.750E-01	9.871E-01	1.059E-01	1.460E+02	7.252E-04
2.800E-01	9.829E-01	1.054E-01	1.511E+02	6.976E-04
2.850E-01	9.780E-01	1.049E-01	1.565E+02	6.702E-04
2.900E-01	9.724E-01	1.043E-01	1.622E+02	6.431E-04
2.950E-01	9.664E-01	1.037E-01	1.682E+02	6.163E-04
3.000E-01	9.596E-01	1.029E-01	1.745E+02	5.899E-04

TABLE A-Id
ANALYSIS OF REMOTE DISPLACEMENT CONTROLLED
THREE POINT BEND SPECIMEN
(S/W = 8, W = 1/2, C₂Et = .1)

a	$\frac{K(a)}{K(.25)}$	$\frac{K}{E\Delta}$	$\frac{K}{P} (t=.25)$	$\frac{P}{E\Delta}$
5.000E-02	6.548E-01	7.274E-02	3.869E+01	1.880E-03
5.500E-02	6.797E-01	7.550E-02	4.046E+01	1.866E-03
6.000E-02	7.028E-01	7.807E-02	4.216E+01	1.852E-03
6.500E-02	7.243E-01	8.046E-02	4.382E+01	1.836E-03
7.000E-02	7.445E-01	8.271E-02	4.544E+01	1.820E-03
7.500E-02	7.635E-01	8.482E-02	4.704E+01	1.803E-03
8.000E-02	7.814E-01	8.680E-02	4.862E+01	1.785E-03
8.500E-02	7.983E-01	8.868E-02	5.019E+01	1.767E-03
9.000E-02	8.142E-01	9.045E-02	5.175E+01	1.748E-03
9.500E-02	8.294E-01	9.213E-02	5.331E+01	1.728E-03
1.000E-01	8.437E-01	9.372E-02	5.487E+01	1.708E-03
1.050E-01	8.572E-01	9.523E-02	5.645E+01	1.687E-03
1.100E-01	8.701E-01	9.666E-02	5.803E+01	1.666E-03
1.150E-01	8.823E-01	9.801E-02	5.963E+01	1.644E-03
1.200E-01	8.938E-01	9.929E-02	6.125E+01	1.621E-03
1.250E-01	9.047E-01	1.005E-01	6.289E+01	1.598E-03
1.300E-01	9.150E-01	1.016E-01	6.455E+01	1.575E-03
1.350E-01	9.246E-01	1.027E-01	6.624E+01	1.551E-03
1.400E-01	9.337E-01	1.037E-01	6.797E+01	1.526E-03
1.450E-01	9.423E-01	1.047E-01	6.973E+01	1.501E-03
1.500E-01	9.502E-01	1.056E-01	7.153E+01	1.476E-03
1.550E-01	9.576E-01	1.064E-01	7.338E+01	1.450E-03
1.600E-01	9.645E-01	1.071E-01	7.527E+01	1.423E-03
1.650E-01	9.708E-01	1.078E-01	7.722E+01	1.397E-03
1.700E-01	9.765E-01	1.085E-01	7.922E+01	1.369E-03
1.750E-01	9.818E-01	1.091E-01	8.128E+01	1.342E-03
1.800E-01	9.865E-01	1.096E-01	8.341E+01	1.314E-03
1.850E-01	9.907E-01	1.101E-01	8.561E+01	1.286E-03
1.900E-01	9.944E-01	1.105E-01	8.789E+01	1.257E-03
1.950E-01	9.975E-01	1.108E-01	9.025E+01	1.228E-03
2.000E-01	1.000E+00	1.111E-01	9.270E+01	1.199E-03
2.050E-01	1.002E+00	1.113E-01	9.525E+01	1.169E-03
2.100E-01	1.004E+00	1.115E-01	9.790E+01	1.139E-03
2.150E-01	1.005E+00	1.117E-01	1.007E+02	1.109E-03
2.200E-01	1.006E+00	1.117E-01	1.036E+02	1.079E-03
2.250E-01	1.006E+00	1.118E-01	1.066E+02	1.049E-03
2.300E-01	1.006E+00	1.117E-01	1.097E+02	1.018E-03
2.350E-01	1.005E+00	1.117E-01	1.130E+02	9.879E-04
2.400E-01	1.004E+00	1.115E-01	1.165E+02	9.574E-04
2.450E-01	1.002E+00	1.113E-01	1.201E+02	9.270E-04
2.500E-01	1.000E+00	1.111E-01	1.239E+02	8.965E-04
2.550E-01	9.973E-01	1.108E-01	1.279E+02	8.662E-04
2.600E-01	9.941E-01	1.104E-01	1.321E+02	8.360E-04
2.650E-01	9.904E-01	1.100E-01	1.365E+02	8.060E-04
2.700E-01	9.862E-01	1.096E-01	1.411E+02	7.762E-04
2.750E-01	9.814E-01	1.090E-01	1.460E+02	7.467E-04
2.800E-01	9.761E-01	1.084E-01	1.511E+02	7.174E-04
2.850E-01	9.702E-01	1.078E-01	1.565E+02	6.885E-04
2.900E-01	9.638E-01	1.071E-01	1.622E+02	6.599E-04
2.950E-01	9.567E-01	1.063E-01	1.682E+02	6.317E-04
3.000E-01	9.489E-01	1.054E-01	1.745E+02	6.040E-04

TABLE A-IIa
ANALYSIS OF REMOTE DISPLACEMENT CONTROLLED

THREE POINT BEND SPECIMEN

(S/W = 4, W = 1/2, C₂Et = 20)

a	$\frac{K(a)}{K(.25)}$	$\frac{K}{E\Delta}$	$\frac{K}{P}(t=.25)$	$\frac{K}{E\Delta}$
5.000E-02	5.913E-01	1.261E-01	1.875E+01	6.725E-03
5.500E-02	6.138E-01	1.309E-01	1.959E+01	6.684E-03
6.000E-02	6.347E-01	1.354E-01	2.039E+01	6.640E-03
6.500E-02	6.544E-01	1.396E-01	2.117E+01	6.593E-03
7.000E-02	6.729E-01	1.435E-01	2.194E+01	6.543E-03
7.500E-02	6.905E-01	1.473E-01	2.269E+01	6.491E-03
8.000E-02	7.072E-01	1.508E-01	2.343E+01	6.437E-03
8.500E-02	7.232E-01	1.542E-01	2.417E+01	6.381E-03
9.000E-02	7.385E-01	1.575E-01	2.491E+01	6.322E-03
9.500E-02	7.531E-01	1.606E-01	2.565E+01	6.263E-03
1.000E-01	7.672E-01	1.636E-01	2.639E+01	6.200E-03
1.050E-01	7.807E-01	1.665E-01	2.714E+01	6.136E-03
1.100E-01	7.937E-01	1.693E-01	2.789E+01	6.070E-03
1.150E-01	8.063E-01	1.720E-01	2.865E+01	6.003E-03
1.200E-01	8.184E-01	1.746E-01	2.942E+01	5.933E-03
1.250E-01	8.301E-01	1.771E-01	3.020E+01	5.862E-03
1.300E-01	8.414E-01	1.795E-01	3.100E+01	5.789E-03
1.350E-01	8.523E-01	1.818E-01	3.181E+01	5.714E-03
1.400E-01	8.628E-01	1.840E-01	3.264E+01	5.638E-03
1.450E-01	8.729E-01	1.862E-01	3.349E+01	5.560E-03
1.500E-01	8.827E-01	1.883E-01	3.436E+01	5.480E-03
1.550E-01	8.921E-01	1.903E-01	3.525E+01	5.398E-03
1.600E-01	9.011E-01	1.922E-01	3.616E+01	5.315E-03
1.650E-01	9.098E-01	1.940E-01	3.710E+01	5.230E-03
1.700E-01	9.181E-01	1.958E-01	3.807E+01	5.143E-03
1.750E-01	9.260E-01	1.975E-01	3.908E+01	5.054E-03
1.800E-01	9.336E-01	1.991E-01	4.011E+01	4.964E-03
1.850E-01	9.408E-01	2.007E-01	4.118E+01	4.872E-03
1.900E-01	9.477E-01	2.021E-01	4.229E+01	4.779E-03
1.950E-01	9.542E-01	2.035E-01	4.345E+01	4.684E-03
2.000E-01	9.603E-01	2.048E-01	4.465E+01	4.588E-03
2.050E-01	9.661E-01	2.061E-01	4.590E+01	4.490E-03
2.100E-01	9.715E-01	2.072E-01	4.720E+01	4.390E-03
2.150E-01	9.765E-01	2.083E-01	4.856E+01	4.289E-03
2.200E-01	9.811E-01	2.093E-01	4.997E+01	4.187E-03
2.250E-01	9.853E-01	2.102E-01	5.146E+01	4.084E-03
2.300E-01	9.891E-01	2.110E-01	5.301E+01	3.980E-03
2.350E-01	9.925E-01	2.117E-01	5.463E+01	3.875E-03
2.400E-01	9.955E-01	2.123E-01	5.634E+01	3.769E-03
2.450E-01	9.980E-01	2.129E-01	5.813E+01	3.662E-03
2.500E-01	1.000E+00	2.133E-01	6.001E+01	3.554E-03
2.550E-01	1.002E+00	2.136E-01	6.198E+01	3.447E-03
2.600E-01	1.003E+00	2.138E-01	6.406E+01	3.338E-03
2.650E-01	1.003E+00	2.140E-01	6.624E+01	3.230E-03
2.700E-01	1.003E+00	2.139E-01	6.853E+01	3.122E-03
2.750E-01	1.002E+00	2.138E-01	7.095E+01	3.013E-03
2.800E-01	1.001E+00	2.135E-01	7.350E+01	2.905E-03
2.850E-01	9.992E-01	2.131E-01	7.618E+01	2.798E-03
2.900E-01	9.966E-01	2.126E-01	7.900E+01	2.691E-03
2.950E-01	9.932E-01	2.118E-01	8.197E+01	2.584E-03
3.000E-01	9.890E-01	2.110E-01	8.511E+01	2.479E-03

TABLE A-IIb
ANALYSIS OF REMOTE DISPLACEMENT CONTROLLED
THREE POINT BEND SPECIMEN
(S/W = 4, W = 1/2, C₂Et = .1)

a	$\frac{K(a)}{K(.25)}$	$\frac{K}{E\Delta}$	$\frac{K}{P}(t=.25)$	$\frac{K}{E\Delta}$
5.000E-02	9.125E-01	2.714E-01	1.275E+01	1.447E-02
5.500E-02	9.405E-01	2.797E-01	1.959E+01	1.428E-02
6.000E-02	9.653E-01	2.871E-01	2.039E+01	1.408E-02
6.500E-02	9.874E-01	2.937E-01	2.117E+01	1.387E-02
7.000E-02	1.007E+00	2.995E-01	2.194E+01	1.366E-02
7.500E-02	1.025E+00	3.047E-01	2.269E+01	1.343E-02
8.000E-02	1.040E+00	3.094E-01	2.343E+01	1.320E-02
8.500E-02	1.054E+00	3.135E-01	2.417E+01	1.297E-02
9.000E-02	1.066E+00	3.171E-01	2.491E+01	1.273E-02
9.500E-02	1.077E+00	3.203E-01	2.565E+01	1.249E-02
1.000E-01	1.086E+00	3.231E-01	2.639E+01	1.224E-02
1.050E-01	1.094E+00	3.255E-01	2.714E+01	1.200E-02
1.100E-01	1.101E+00	3.276E-01	2.789E+01	1.175E-02
1.150E-01	1.107E+00	3.293E-01	2.865E+01	1.150E-02
1.200E-01	1.112E+00	3.308E-01	2.942E+01	1.124E-02
1.250E-01	1.116E+00	3.319E-01	3.020E+01	1.099E-02
1.300E-01	1.119E+00	3.328E-01	3.100E+01	1.074E-02
1.350E-01	1.121E+00	3.335E-01	3.181E+01	1.048E-02
1.400E-01	1.122E+00	3.338E-01	3.264E+01	1.023E-02
1.450E-01	1.123E+00	3.340E-01	3.349E+01	9.973E-03
1.500E-01	1.123E+00	3.339E-01	3.436E+01	9.719E-03
1.550E-01	1.122E+00	3.336E-01	3.525E+01	9.465E-03
1.600E-01	1.120E+00	3.331E-01	3.616E+01	9.212E-03
1.650E-01	1.118E+00	3.324E-01	3.710E+01	8.959E-03
1.700E-01	1.115E+00	3.315E-01	3.807E+01	8.708E-03
1.750E-01	1.111E+00	3.305E-01	3.908E+01	8.457E-03
1.800E-01	1.107E+00	3.292E-01	4.011E+01	8.208E-03
1.850E-01	1.102E+00	3.278E-01	4.118E+01	7.960E-03
1.900E-01	1.097E+00	3.262E-01	4.229E+01	7.713E-03
1.950E-01	1.091E+00	3.245E-01	4.345E+01	7.469E-03
2.000E-01	1.085E+00	3.226E-01	4.465E+01	7.226E-03
2.050E-01	1.078E+00	3.206E-01	4.590E+01	6.986E-03
2.100E-01	1.071E+00	3.185E-01	4.720E+01	6.748E-03
2.150E-01	1.063E+00	3.162E-01	4.856E+01	6.513E-03
2.200E-01	1.055E+00	3.139E-01	4.997E+01	6.281E-03
2.250E-01	1.047E+00	3.114E-01	5.146E+01	6.051E-03
2.300E-01	1.038E+00	3.088E-01	5.301E+01	5.825E-03
2.350E-01	1.029E+00	3.061E-01	5.462E+01	5.603E-03
2.400E-01	1.020E+00	3.033E-01	5.624E+01	5.384E-03
2.450E-01	1.010E+00	3.004E-01	5.813E+01	5.168E-03
2.500E-01	1.000E+00	2.974E-01	6.001E+01	4.957E-03
2.550E-01	9.897E-01	2.944E-01	6.198E+01	4.750E-03
2.600E-01	9.791E-01	2.912E-01	6.406E+01	4.547E-03
2.650E-01	9.682E-01	2.880E-01	6.624E+01	4.348E-03
2.700E-01	9.571E-01	2.847E-01	6.853E+01	4.154E-03
2.750E-01	9.456E-01	2.813E-01	7.095E+01	3.964E-03
2.800E-01	9.339E-01	2.778E-01	7.350E+01	3.779E-03
2.850E-01	9.218E-01	2.742E-01	7.618E+01	3.599E-03
2.900E-01	9.094E-01	2.705E-01	7.900E+01	3.424E-03
2.950E-01	8.966E-01	2.667E-01	8.197E+01	3.253E-03
3.000E-01	8.835E-01	2.628E-01	8.511E+01	3.088E-03

The above described analysis can easily be used to determine the constants D_1 and D_2 of Chapter II. Although our specimen initially has a .05 inch deep notch and not a .05 inch crack, the calculated compliance of the notched specimen using the crack equations is thought to be quite accurate. The compliance of an uncracked .5 inch deep, $S/W = 8$ beam is increased by less than 4% by the presence of a .05 inch crack. The additional compliance due to opening the crack to a 60° included angle notch would certainly be negligible. The constant $D_1 = K/P_o$, is determined simply by reviewing the analysis tables; finding the maximum value of $K/E\Delta$; and dividing this value by $P/E\Delta$ at $a = .05$ inches.

A plot of the result versus normalized spring compliance is given in Figure A-1. The result is almost but not quite linear in C_2Et . In Figure A-1, we have provided two ordinate scales, one for the test specimen used throughout most of this program ($S/W = 8$, $W = .5$ in., $t = .25$ in.) and a non-dimensional scale valid for all $S/W = 8$ specimens with a 60° notch extending to 10% of W .

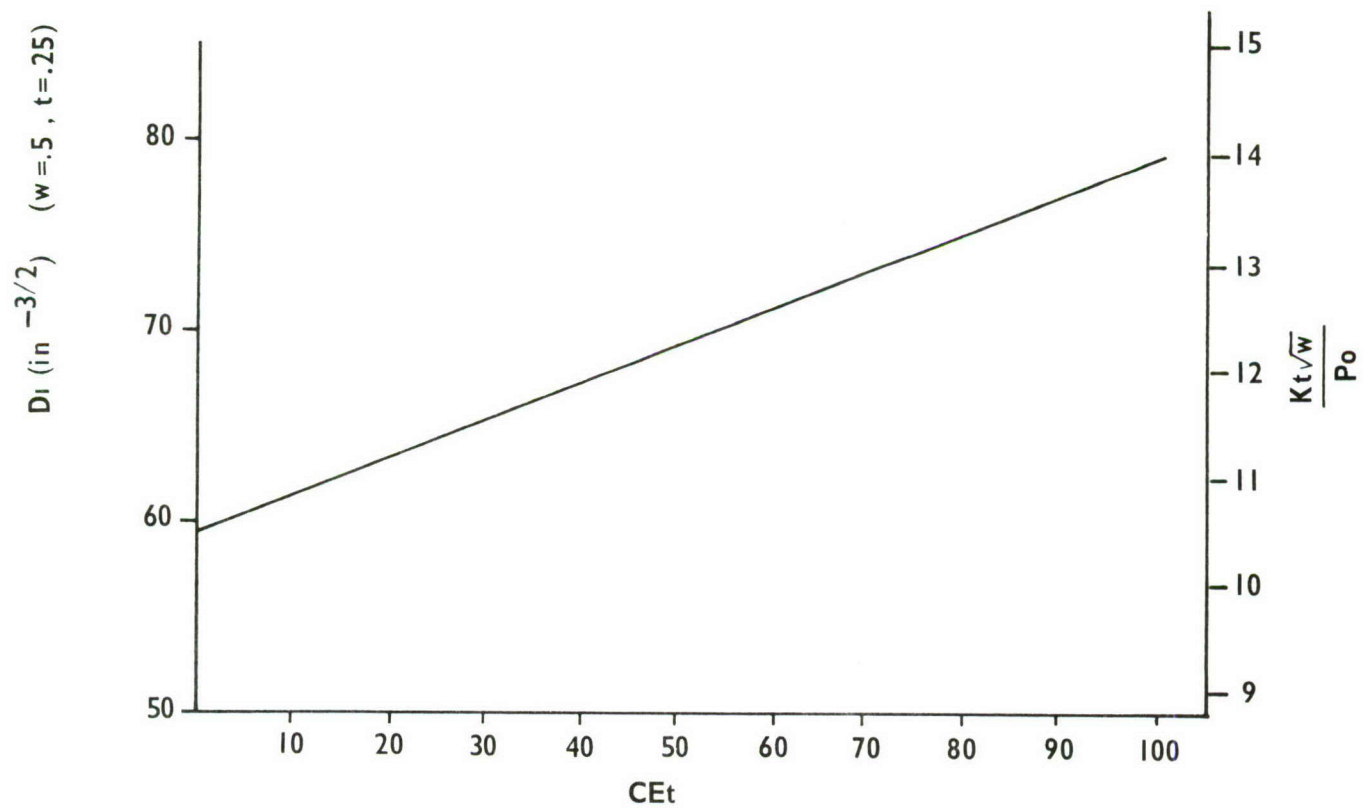


FIGURE A-1
Stress Intensity Evaluation Constant
($s/w = 8$)

The constant D_2 relating da/dN and dP/dN , i.e.

$$da/dN = D_2/P_o dP/dN \quad A-12$$

or

$$da = D_2/P_o dP \quad A-13$$

is also easily evaluated from the above described load/displacement/stress intensity analysis.

From equations 5 and 6 of the text we have

$$\mathcal{G} = K^2/E = -\Delta^2/2t \partial k/\partial a \quad A-14$$

where k is the overall specimen/spring stiffness. i.e

$$k = P/\Delta$$

for a constant Δ we have

$$dP/da = \Delta \partial k/\partial a \quad A-15$$

substituting this into A-14 and rearranging yields

$$da = \frac{1}{2t} \times \frac{(1/E\Delta)}{(K/E\Delta)^2} dP$$

multiplying and dividing by P_o yields

$$da = \frac{1}{2t} \frac{(P_o/E\Delta)}{(K/E\Delta)^2} \times \frac{1}{P_o} dP \quad A-16$$

and therefore

$$D_2 = \frac{1}{2t} \frac{P_o/E\Delta}{(K/E\Delta)^2} \quad A-17$$

Therefore, D_2 is generated for each value of C_2Et by reviewing the numerical results noting the maximum value of $K/E\Delta$; setting $P_0/E\Delta$ to $P/E\Delta$ for $a = .05$; and substituting into A-17. The results are presented in Table A-III. The constant D_2 is independent of specimen thickness, but will vary with the specimen width W . The non dimensional parameter $1/P_0 d(a/W)/dP$ is also presented in Table A-III. This non dimensional parameter is valid for all $S/W = 8$ specimens with 60° notch extending to 10% of W . Note that D_2 is constant over a wide range of spring stiffnesses.

The compliance of the test system used was measured by the simple expedient of setting a displacement on the control cam and measuring the displacement amplitude without a specimen present or the loading fixtures in contact (i.e., with zero load in the system). The loading fixtures were then placed in contact and the cyclic displacement applied. The maximum and minimum loads were recorded and the compliance evaluated by dividing the displacement range by the load range. The resulting measurements gave an average value of 1.05×10^{-5} in/lb. Using this value the values of D_1 and D_2 to be used in this program were generated using Figure A-1 and Table A-III and are shown in Table A-IV

TABLE A-III
CONSTANTS FOR EVALUATING CRACK GROWTH RATE

$C_2 Et$	D_2 ($W = .5$)	$P_o \frac{d \left(\frac{a}{W} \right)}{dP}$
.1	.300	.600
10.0	.302	.604
12.5	.304	.608
20.0	.304	.608
25.0	.304	.608
33.3	.304	.608
50	.304	.608
75	.300	.6
100	.298	.596
150	.282	.564
200	.286	.572
250	.280	.560
300	.278	.556
350	.274	.548
400	.272	.544

TABLE A-IV

CONSTANTS USED IN TEST PROGRAM

Material	Aluminum	Titanium	Steel
E	10.5×10^6 psi	17.0×10^6 psi	28.5×10^6 psi
C_2^{Et}	27.6	44.6	74.8
D_1	65	68.5	74
D_2	.304	.304	.300

APPENDIX B
PROGRAM MATERIAL SELECTION
PHILOSOPHY

The logic which governed our material choices derived from a need to obtain relatively small quantities of aluminum, titanium and steel alloys which span the extremes of specification requirements in order to validate the sensitivity of our newly developed fatigue crack growth quality control test. Additional factors considered in making our choice included extensiveness of alloy usage by the USAF on current and planned air vehicle systems as well as the breadth of current knowledge of the relationship between an alloy's fatigue crack growth rate and its alloy chemistry and thermomechanical working conditions. The latter involves a rather practical consideration in that we wish to span the specification extremes of any given alloy by purchasing small quantities from five distinct heats of each of the chosen alloys.

Aluminum

The two most prominently employed airframe alloy types are the 2000 and 7000 series. Primary aluminum suppliers refuse to sell their product if one attempts to specify an alloy chemistry range tighter than the range that the Aluminum Industries Association has decided will be associated with a given alloy designation. For example, if one wishes to purchase 2219 Al with a

restricted call out on copper, say 5.3% by wt. to 5.6% by wt. in place of the normal 5.1% - 6.1% range designated by the AIA, the various primary aluminum vendors will simply reject your purchase order on the basis that they do not make that modification of 2219 Al. In attempting to select a material system for this Program which would allow one to interrogate specification extremes with respect to their role in determining fatigue crack growth rate, one must take this problem into account. One means of accomplishing our "specification extremes interrogation" goal along with satisfying a desire to study an extensively used material can be obtained by selecting 7075/7475 as the alloy system of interest. Recognizing that all material purchased to the 7475 composition will satisfy the QQ - 250/12 plate product specification chemistry for 7075, one then has the opportunity here to study conventional 7075 along with a low silicon plus iron grade 7075, namely 7475. Alternatively one could have chosen 2024/2048 as the combination of interest since the latter composition provides us with a low tramp element version of the 2024 alloy along with a restricted copper range. The 7000 series pair was chosen on the basis that 7475 is currently used more extensively and is more easily obtained than 2048. The aluminum alloy heats which were employed in this Program are described in Tables B-I and B-II.

TABLE B-I

ALUMINUM

ALLOY LOT DESCRIPTION

Product Form 1/2" thick Plate

Del West Lot No.	Alloy Designation	Heat Treat* Temper	Materials Specification	Alloy Producer
A	7075	-T651	QQ 250/12	Kaiser
B	7075	-T651	QQ 250/12	Alcoa
C	7075	-T651	QQ 250/12	Reynolds
D	7475	-T7651	See Table No. B-II	Alcoa
E	7475	-T7351	See Table No. B-II	Alcoa

*As defined in Mil-H-6-88

TABLE B-II

ALLOY CHEMISTRY OF 7475
(Lots D and E in Wt%)

Si	Fe	Cu		Mn	Mo		Cr		Zn		Ti		Others	
		max	min		max	min	max	min	max	min	max	min	Each	Total
0.10	0.12	1.9	1.2	0.06	2.6	1.9	0.25	0.18	6.2	5.2	0.06	0.05	0.15	

Mechanical Properties

Del West Lot No.	Temper	F _{tu} (Ksi)	F _{ty} (Ksi)	Elongation in 2"		Electrical Conductivity	
				(%)		(% FCAS)	
D	T7651	79.25	72.4	14.6		38.5	
E	T7351	73	63	13.5		41.9	

Titanium

In this metallic system, the material choice is clear-cut and our selected alloy is 6Al-4V Ti in 1/2" thick plate product form. This alloy and product form are probably the most widely used of all titanium products on USAF emerging and operational systems. Small quantities from various heats are also available both from producers and warehouses. Extensive studies have been made in various laboratories on the role specification variables such as alloy chemistry, microstructure and heat treatment play in controlling its fatigue crack growth rate in dry air. For example, Harrigan, Kaplan and Summer (Ref. 1) have described the role these variables play in determining fatigue crack growth rate in dry air across the specification extremes permitted by Mil-T-9046 G.

Material lots of this alloy for the Program were produced by the Crucible Materials Research Center and are described in Tables B-III and B-IV.

Steel

Steel airframe materials selections for primary structure have been moving from the 4000 series of AISI compositions to such high nickel constituent steels as the 9Ni-4 Co series or HY 180. In the stainless steel category, the most often

1. Harrigan, M., M. Kaplan and A. W. Sommer, "Fracture Prevention and Control Symposium," D. Hoepfner, Editor, ASM, Metals Park, Ohio, 1974.

TABLE B-III
CHEMICAL ANALYSIS AND HEAT TREATMENT
PROCESSING OF TITANIUM HEATS

Product Form - 1/2" Plate									
Del West Heat No.	Crucible Heat No.	Al	V	N ₂	C	Fe	O ₂	Beta Transus	Heat Treatment
F	G99184	5.7	4.0	0.007	0.063	0.03	0.088	1790°F	1700°F/4 hrs. cool at 75°F/hr to 1400°F, air cool
G	G51963A	6.3	4.0	0.009	0.029	0.23	0.150	1830°F	1700°F/4 hrs. cool at 75°F to 1400°F, air cool
H	G99864	6.5	4.2	0.016	0.022	0.23	0.198	1860°F	1700°F/4 hrs. cool at 75°F to 1400°F, air cool
I	This Heat designation purposely left blank								
J	G51963A	6.3	4.0	0.009	0.029	0.23	0.150	1830°F	1900°F/0.5 hrs. air cool + 1350°F/1 hr.
K	G51963A	6.3	4.0	0.009	0.129	0.23	0.150	1830°F	1350°F/1 hr, air cool

TABLE B-IV

TENSILE PROPERTIES OF TI ALLOY HEATS

Del West	Direction	Tensile Properties			
		UTS (ksi)	YS (ksi)	EL (%)	RA (%)
F	T	126.0	110.8	15.0	38.7
	L	123.2	106.4	16.0	37.1
H	T	150.0	138.6	16.0	36.0
	L	139.6	123.5	16.0	33.1
G	T	141.6	126.5	16.0	41.2
	L	134.3	120.2	16.0	37.1
J	T	140.0	126.0	12.0	26.0
	L	139.3	125.7	13.0	27.8
K	T	148.7	138.6	14.0	34.7
	L	133.5	141.1	14.0	31.3

recent choice has been Ph 13 - 8Mo, with the exception of some currently unpublished data obtained by Rockwell International on the B-1 RDT-E program, there is little known concerning the dry air da/dN heat to heat variations to be expected in these newer high nickel and Ph stainless grade steels. B-1 data would indicate that the heat to heat variation of conventionally processed metal in dry air for 9Ni-4Co-0.20C steel forgings and Ph 13 - 8 Mo bar is minimal. Since stainless steel is melted in smaller ingots than 9Ni-4Co, obtaining lots from multiple heats will be easier. For this reason, Ph 13-Mo was selected as the steel alloy for this Program. The required alloy lots have been purchased from Armco Steel. They are described in Tables B-V and B-VI. In an attempt to force different da/dN vs. ΔK results among the five heats, three heats of identical chemistry were forged at distinctly different temperatures. The highest temperature forging should result in a substantial amount of residual delta ferrite and the lowest forge temperature should provide a tough finely divided austenite. In addition the role of aluminum chemistry in conventionally forged metal was also ascertained.

TABLE B-V

CHEMICAL ANALYSIS AND PROCESSING OF
PH 13-8MO STEEL FORGINGS

Product Form - 1 1/4" Thick Plate

Del West Heat No.	Armco Heat Heat No.	C	Mn	P	S	Si	Cr	Ni	Al	Mo	N ₂	Forge Temp	Temper Condition
L	3x0832	0.038	0.02	0.004	0.0009	0.10	12.84	8.04	1.01	2.10	N.D.	2150°F	H-1000
M	3x0829	0.043	0.01	0.002	0.004	0.002	12.79	8.30	1.23	2.16	0.0024	2150°F	H-1000
N	3x1086	0.034	0.020	0.002	0.004	0.02	12.85	8.25	1.13	2.08	0.0016	2150°F	H-1000
O	3x1086	0.034	0.020	0.002	0.004	0.02	12.85	8.25	1.13	2.08	0.0016	2350°F	H-1000
P	3x1086	0.034	0.020	0.002	0.004	0.02	12.85	8.25	1.13	2.08	0.0016	1800°F	H-1000

TABLE B-VI

MECHANICAL PROPERTIES OF PH 13-8 MO

STEEL FORGINGS

Del West Heat No.	F _{ty} (Ksi)	F _{tu} (Ksi)	Elong % in 2"	Red. in Area %	Condition
L	211	216	14	60	H-1000
M	208	215	15	59.5	H-1000
N	198	211	15	52.0	H-1000
O	201	205	15	54.2	H-1000
P	209	212	15	57.4	H-1000

APPENDIX C

CONSIDERATION OF CANDIDATE QUALITY CONTROL TEST SPECIMENS/PROCEDURES

A successful quality control test for fatigue crack propagation will have a number of characteristics. The criteria for success are simple: (a) the test will discern desirable material from undesirable material and (b) that the test will be inexpensive.

The test will have to:

1. Use a small amount of material. This will insure that specimens can be prepared from sources for which there is little material (e.g., small forgings).
2. Require the use of an inexpensive test machine. The test machine must be inexpensive to buy, run and maintain.
3. Be easily set up and run.
4. Run in a short time
5. Be relatively universal - that is, it must be applicable to a wide range of materials and forms and should probably be capable of being run in a variety of environments.
6. Be quantitatively related to an engineering design curve for da/dN versus ΔK . This quantitative relationship could be empirical but an analytic relationship which is universal would be preferred.
7. Provide highly reproducible results (very reliable).

In our review of the problem of developing a quality control fatigue crack propagation test, we have come to the conclusion that there are two distinct approaches which may be utilized. One involves testing over a wide range of stress intensities. Typical here is a determination of the cycles to failure of an initially cracked specimen of constant cross section subjected to constant amplitude cyclic load. The other approach involves testing over a narrow range of stress intensities. In this situation, ideally, one is running a test on a constant stress intensity specimen for a specific number of cycles and determining the change in crack length. Superficially, one might think these two approaches (tests over a wide variation in stress intensity versus tests at constant ΔK) are quite separate and offer various advantages and disadvantages with respect to one another when compared to the intended hardware use. This is, in fact, not the case because in a non spectrum load test it is only the low stress intensities a specimen sees during its life which govern its overall life. Thus, if a crack encounters stress intensities from 20 to 100 and corresponding rates of 10^{-6} to 10^{-3} in/cycle, variations in the rate at 20 $\text{Ksi}\sqrt{\text{in}}$ (10^{-6} in/cycle) will have a large impact on life and variations in the rate at 100 $\text{Ksi}\sqrt{\text{in}}$ (10^{-3} in/cycle) will have little effect on life. Thus testing

at either $20 \text{ Ksi}\sqrt{\text{in}}$ or through the whole range would produce essentially the same conclusions as to material acceptance or rejection. We believe that there is an increased ease of interpretation in a quality control test that tests at a single stress intensity level, but we recognize the fact that differences in test cost between a single K test and a range in K test could easily outweigh this advantage. We therefore considered both classes of tests.

The following is a summary of the candidate control tests which were considered.

Three Point Bend Tests.

Del West has evaluated four concepts utilizing a relatively small three point bend specimen in addition to the procedure we finally adopted. See Figure 1. Most prominently considered planform dimensions were 2 in. x 1/2 in. and 4 in. x 1/2 in. We had fixed on the .5 inch depth as a result of some preliminary tests performed on 2 x .35 inch planform specimens. This size was arbitrarily chosen, the primary purpose of the test was to check out our test fixture. In running these tests on .35 inch specimens we found that reasonably accurate crack length changes were difficult to measure in all cases. Once the starter notch and precrack are put into the specimen and a reasonable remaining ligament is left on the backside, less than .150 is left for a maximum crack

growth region. In the design of a rational quality test one would design a test in which the expected amount of crack growth was much less than the maximum allowable region. For the .35 inch specimen .1 inch would be a reasonable choice. This would imply crack growth as low as .05 inches in some tests. Our experience in measuring crack growth distances on these preliminary specimens indicate that this is too small a distance to measure reliably and easily. Part of the problem is the crack front curvature. In a .5 inch thick specimen, one can easily use .2 inches for a typical crack growth range and this results in a far more readily measured crack growth. The three point bend tests initially evaluated included:

- a) Constant Load (increasing K).
- b) Constant Displacement.
- c) Constant K using "Spring Loaded Specimen" with two crack length measurements.
- d) Constant K using "Spring Loaded Specimen" with two load measurements.

Note that we did not initially consider the measurement of the slope of a load-cycle plot to determine crack growth rate.

In the first three tests, the procedure would require crack length measurements. In the constant load test, it is possible to simply run the test to failure, then a measurement of only the initial crack length would be required. A number of ways of measuring crack length and crack length changes are available. We

assumed that scribe marks placed on the surface of the specimen at the crack tip before and after the test is run would be used for crack length and crack length change determination. Other techniques such as the changing of loads to mark the surface, or direct observation and recording of crack lengths could also be used.

Testing of the constant load specimen would entail:

- 1) precracking to a predetermined depth.

This depth will at some point have to be precisely known. Moreover, for the reasons to be described below little latitude in crack starting position would be acceptable.

- 2a) A predetermined number of cycles would be put on the specimen

or

- 2b) the specimen will be cycled to failure.

- 3a) The amount of growth is measured

or

- 3b) the number of cycles is counted.

- 4a) The amount of growth obtained is compared to the amount of growth acceptable for the specific initial crack length tested. If the growth is too large - the material is rejected.

4b) The number of cycles obtained is compared to the acceptable number of cycles for the specific initial crack length tested. If the number of cycles is too small the material is rejected.

Note the important role the initial crack length plays in material acceptance or rejection.

The constant load specimen has a large positive stress intensity variation with respect to crack length. In fact for the small specimens considered here the gradient is sufficiently large to cause major variations in stress intensity for relatively minor variations in geometry. For example, in a typical case considered, it was found that for each .001 error in initial crack length reading the amount of crack growth predicted would vary by approximately 2%. This combined with the relatively high cost of constant load (i.e., closed loop) test equipment led us to conclude that this test type was an unlikely candidate for a successful quality control test.

The constant displacement three point bend specimen has portions of increasing and decreasing stress intensity with changing crack length. This is shown schematically in Figure 2. In that Figure both a constant load and a constant displacement specimen is displayed. Note that for the constant displacement specimen at short crack lengths, changes in crack length do not

affect the specimen compliance and therefore the load remains essentially constant and the K versus " a " curve initially follows the constant load specimen curve. Eventually changes in crack length affect the specimen compliance significantly and the load begins to drop. As the crack continues to grow a point is reached where the load drop off is sufficiently fast to cause the stress intensity to decrease with increasing crack length. For most configurations of the three point bend specimen the peak stress intensity occurs in a location such that there is a relatively large negative gradient in stress intensity with respect to crack length throughout the major portion of the specimen. The test procedure would therefore have to correspond to the " a " procedure described above. The large negative gradient produces similar sources of error as do the large positive gradients in the load controlled specimen. However, the fact that displacement controlled test machines are less costly than load control test machines, makes this class of displacement control specimens more desirable than the load controlled specimens. In addition, there are configurations in which the peak stress intensity factor is more favorably located and stress intensity gradients in the specimen center remain low. These configurations fall within the general classification of the displacement controlled constant K test finally adopted.

The three point bend configuration for a test specimen is very appealing due to its small size, simple shape and the low bending load requirements. However, the sensitivity problems which may arise due to the large gradients in stress intensity under constant amplitude cyclic displacement in some specimens or under constant amplitude load could detract from its value for quality control. It is for this reason that we developed an approach which minimizes the otherwise large variation in stress intensity with crack length experienced with this simple geometry. This specimen is discussed in the main body of the text.

Throughout the initial studies both a 4 x .5 inch specimen and a 2 x .5 inch specimen with "spring loading" were considered as quality control test specimens. Note that for these specimens the test procedure would follow the "a" procedure described in conjunction with the constant load test; with one significant exception. When the amount of crack growth obtained at a specific number of cycles is compared to the allowable amount of crack growth, the initial crack length no longer plays a role. Thus the acceptance/rejection test is not only more accurate, but simpler as well. Moreover, due to the fact that the test is run for a specific well defined stress intensity the interpretation of the relevance of the quality control test is simpler also.

We will now discuss an early test concept for the three point bend specimen in which a technique to avoid crack length measurements had been developed. The motivation for this is that crack length measurements are time consuming, prone to error, and compared to other physical measurements (e.g., forces) less accurate. This approach depends on the fact that we can test a specimen (or specimen-spring combination) under constant displacement control and have the stress intensity (and hence the crack growth rate) remain constant.

In this early concept our approach was to measure loads, cycles and the applied displacement (not slopes and initial loads).

The resulting rate equation is

$$\frac{da}{dN} = \frac{1}{Q\Delta} \frac{P_i - P_f}{\Delta N}$$

where Q is a constant determined from analysis P_i and P_f are loads measured at intervals of ΔN cycles while the crack is in the constant K region, and Δ is the applied displacement.

Since Q can be determined by analysis, and Δ and ΔN are test input quantities, the crack growth rate is determined by the relatively simple measurement of the loads (at the beginning and end of the test that occur as result of imposing a displacement Δ .) Note that the loads and displacements used in this equation must be compatible. That is: if Δ is the range

in displacement applies, P_i and P_f must be load ranges, or if Δ is the maximum displacement P_i and P_f must be maximum loads. Measurement of the latter would be the more accurate procedure. It should be noted that the load change during a test is substantial and that over the .2 inches of growth discussed previously, the load decreases by over 70%.

The above procedure was appealing for a number of reasons: the load measurement is faster and more accurate than crack length measurements; a permanent test record in the form of an audiographic recording of data could be made available; the test and data recording has the possibility of being easily automated.

Note that this concept of measuring load at two points eventually led to the procedure of the test.

Similar approaches using constant K and varying K specimens under load control have been discussed in the literature and utilized in a number of laboratories. The compliance, however, is usually measured as opposed to simply measuring the displacement. To the best of our knowledge a constant K , displacement controlled specimen has not been considered for fatigue crack growth testing prior to this Program. Due to the facts that it is easy to control displacement amplitudes accurately but

difficult to measure displacements accurately and that loads may be evaluated very accurately, it appears that the use of a constant K displacement controlled specimen and load measurement will prove to be significantly more accurate than previous methods in which direct crack length measurements have been avoided.

An interesting alternative use of the above load monitoring concept is also possible. In many respects the value of ΔK at a specific crack growth is more useful than the value of the rate at a specific K. This is because the relative values of the K's at a common value of crack growth rate in two different materials indicate the increased loads (or decreased weight) that the higher K material can tolerate. Using the concept of measuring P to get the crack growth rate in a constant K specimen; a procedure which measures the crack growth rate and modifies the applied displacement until a desired rate is achieved will enable the K for a specific crack growth rate to be established as a material property and/or for use in a quality control test. The following describes such a test.

Test Scheme for Determining
K for a Specific Crack Growth Rate

Task

Starting with a properly fatigue precracked three point bend sample and a given $(da/dN)_o$, determine the associated ΔK at a specific stress ratio.

Method

For constant K, constant displacement specimen we have

$$\frac{P_i - P_f}{\Delta N} = Q \Delta \frac{da}{dN} \quad \text{at a given } da/dN$$

and for $(da/dN)_o$.

$$\Delta P_o = \left(P_i - P_f \right)_o = Q_1 \Delta (da/dN)_o \Delta N$$

The following test sequence where loads are sampled every ΔN cycles will yield ΔK .

1. Pick displacement such that da/dN will be less than $(da/dN)_o$ (to avoid retardation).
2. Measure P
3. Put ΔN cycles on specimen
4. Measure new P
5. Calculate ΔP . If $\Delta P = \Delta P_o$, by chance, then the K associated with the initial constant displacement can be found from the appropriate equations.

6. Should $\Delta P_o > \Delta P_{\text{measured}}$, then the entire test method (steps 1-5) is repeated using a new displacement which is obtained as follows:

$$\Delta_{\text{new}} = \Delta_{\text{old}} \times \left[\frac{\Delta P_o}{\Delta P_{\text{measured}}} \right]^{1/n}$$

where $n > \text{slope of } \log da/dN \text{ vs } \log \Delta K \text{ curve (e.g., } n = 10)$.

7. So long as each succeeding test yield a $\Delta P_{\text{measured}} < \Delta P_o$, one continues to reset displacements per step 6 and repeats the test.
8. When a displacement is found where $\Delta P_{\text{measured}} = \Delta P_o$, one can then use step 5 to determine the ΔK associated with the desired $(da/dN)_o$.

Notched Round Bar Tests

Other tests evaluated included the notched round bar under a variety of loading conditions. Under constant load conditions, the stress intensity gradients are more severe for the notched round bar than they are for the three point bend specimen, therefore most of our attention was focused on some form of displacement control. Bending (rotating beam), axial displacement, and a combination of both were considered. Preliminary analytic results indicated that the fact that practical limitations on load

requirements require reasonably small specimens and the fact that crack growth proceeds from all sides at once may cause relatively large errors in crack growth rate characterization due to relatively small errors in crack length measurement.

In addition to the high loads required, the tensile load notched round bar has significant technical and cost problems in terms of required alignment precision and uniform advance of the crack front. The rotating beam specimen overcomes these problems, but introduces the additional problem of loading at stress ratios of minus one. Stress ratios of minus one are undesirable in that they do not reproduce the normal condition of usage or da/dN determination. It is possible however to construct an apparatus that applies a static tensile axial displacement to a notched round bar and then allows the cyclic displacements to be applied in the manner of a rotating beam test by offsetting the bar at points along its length by a fixed amount. It is possible then to obtain a variation in stress intensity factor range that is low, but there would also be a variation in stress ratio. The stress ratio varies because the stress intensity due to the fixed axial tensile displacement and the stress intensity due to bending vary differently as the crack grows. However, it is possible to load such a specimen such that the a major portion of the crack depth, the stress ratio is close to zero. Since minor

variations in stress ratio will not have a major impact on crack growth rate, crack growth in this region will mime crack growth from a da/dN test, run at nominal stress ratios in the vicinity of zero.

Using a test specimen loaded in the above fashion, a test procedure in which the amount of crack growth for a specific number of cycles serves as the quality control parameter could be established. A procedure which had some potential to be inexpensive and reliable is the following: (1) A notched round bar is inserted in the test machine and precracked at a constant amplitude displacement in rotating bending to an approximate pre-determined depth. Since the crack depth cannot be seen, the depth will have to be approximately inferred by load drop off at the fixed offset. (2) A tensile deformation would then be placed on the specimen, the bending displacement adjusted, and the test run for a prescribed number of cycles. (3) The specimen would then be broken.

Since the precracking was done at a stress ratio of minus one and the test loading was performed at higher stress ratios, there should be a marking band at the crack length corresponding to the test initiation. The end of the fatigue cracking will also be readily apparent. For the specific number of cycles run there will be a specific allowable crack growth for each initial crack length. If the crack growth is exceeded, then the material would be rejected.

Although a test method using a notched round bar is reasonable, the following considerations made us focus most of our attention on the bend specimen configuration.

- (1) The notched round bar could not be used for sheet and light plate.
- (2) Alignment problems were expected to be significant.
- (3) Loads would have to be large.
- (4) Advance of crack from all sides would require a larger test specimen.
- (5) Control of stress ratio would be difficult.
- (6) Test apparatus would be more complex than that required for three point bend specimen.